MOLECULAR BEAM STUDIES

OF

SHORT-LIVED MOLECULES

MOLECULAR BEAM STUDIES
OF
SHORT-LIVED MOLECULES

By

JOHN GRAY, B.Sc.

A Thesis

Submitted to the Faculty of Graduate Studies

in Partial Fulfilment of the Requirements

for the Degree

Doctor of Philosophy

McMaster University

February 1970

DOCTOR OF PHILOSOPHY (1970)
(Chemistry)

McMASTER UNIVERSITY
Hamilton, Ontario

TITLE: Molecular Beam Studies of Short-Lived Molecules

AUTHOR: John Gray, B.Sc. (London University)

SUPERVISOR: Professor R. H. Tomlinson

NUMBER OF PAGES: (x); 148.

SCOPE AND CONTENTS:

A molecular beam apparatus has been designed and constructed for the purpose of studying gas phase interactions between ions and molecules. A neutralization-reionization technique has been developed which permits the lifetimes of some short lived molecules to be estimated. In this way the existence of He_2, HeH and HeD molecules has been demonstrated but similar experiments have produced no evidence for the existence of H_3, D_3 or D_2H molecules with the same order of lifetimes. A collisional dissociation technique has been devised which permits analysis of molecular ions in beams and demonstrated the existence of He_3^+ ions in low temperature helium discharges.

ACKNOWLEDGEMENTS

The author wishes to express his gratitude to Professor R.H. Tomlinson for his guidance throughout the course of this work. His faith in the outcome of the project was of considerable help in darker moments. Thanks are also due to members of the supervisory committee, Dr. A.J. Yarwood and Dr. J.A. Kuehner for their interest and helpful suggestions. Particular thanks are due to Dr. W.B. Clarke for his invaluable suggestions on the design of a number of mass spectrometer components and to the staff of the nuclear research workshop for their conscientious work in constructing the apparatus.

TABLE OF CONTENTS

LIST OF TABLES

LIST OF ILLUSTRATIONS

The atoms move in a void and catching each other up jostle together, and some recoil in any direction that may chance, and others become entangled with one another in various degrees according to the symmetry of their shapes and sizes and positions and order, and they remain together and thus the coming into being of composite things is effected.

SIMPLICIUS (6th Century A.D.)

CHAPTER 1

INTRODUCTION

Processes occurring via atomic or molecular collisions are fundamental to chemistry. The ideal experimental approach to the study of interactions in chemical systems lies in the molecular, rather than the macroscopic approach. The molecular beam technique permits direct investigation of molecular collision processes. A molecular beam to be used for the study of chemical interactions may be defined as a stream of molecules or atoms travelling in almost collision-free and unidirectional motion. To meet these requirements, the beam must traverse a region of sufficiently low pressure that the effects of unwanted molecular collisions may be ignored. This requires that the mean free path of the molecules in the beam exceed the path length of the apparatus.

In conventional studies of chemical reactions, a large number of processes occur simultaneously, involving molecules with wide distributions of quantum states and velocities. This necessitates the use of statistics to obtain molecular information from macroscopic data, since measurements are made of average properties over a wide distribution of incident energy and internal molecular states. On the other hand, molecular beam methods permit direct study of both energy and angular

dependence of chemical reactions over a large range of incident kinetic energies. Some additional advantages are:

(1) Beam experiments permit investigation of gas phase reactions without interference from possible surface reactions.

(2) Where a surface reaction is to be studied, the low density of particles within the beam eliminates the possibility of gas-phase reactions causing interference.

(3) Particles produced within the beam may retain their chemical and physical identities, since the low particle density in the beam precludes appreciable particle interactions. This permits study of free radicals and metastable atoms and molecules.

(4) In chemical reactions involving a sequence of steps, one step can be isolated and studied individually.

(5) Specific quantum states of reacting molecules can be selected for study. The most common method of accomplishing this involves the use of inhomogeneous magnetic fields to achieve spatial separation of components having different magnetic moment orientation.(1)

Molecular beams may be produced having widely differing kinetic energies. These beams may be conveniently divided into three groups: Thermal beams, having energies less than about 0.1 electron volts; chemical beams, with energies of about 0.1 to 10ev.; and high energy beams, with energies up to thousands of ev.

Molecular beams having thermal kinetic energies are usually produced from a small oven, maintained at a steady

temperature. The oven is provided with a narrow slit, through which the molecules can effuse, and, after suitable collimation, form a beam. The molecular velocities from such an oven have a Maxwell-Boltzmann distribution. It is therefore necessary to use a system of velocity selection in order to produce a beam having a narrow energy spread. This is usually accomplished using a series of rotating discs provided with slots,[2][3][4] so that molecular speeds may be selected on the basis of transit time through the discs.

Beams having high kinetic energy may be produced from electrostatically accelerated ion beams by charge transfer neutralization.[5][6] For example, a beam of Ar atoms may be produced by passing a beam of Ar^+ ions through a suitable pressure of Ar gas.[7] Since the cross-section for charge exchange is much greater than that for momentum transfer,[8] a considerable fraction of the ions may be neutralized without being deflected from the beam. The neutral beam is then obtained by removing the remaining ions with an electric field.

The intermediate energy range is that normally associated with chemical bond energies and hence is of most interest to chemists. Unfortunately it is also the most difficult to attain. Hasted[9] has reviewed some of the approaches used to overcome this problem. The use of a conventional oven source to produce beams in this energy range is impractical, due to the very high temperatures required. (The temperature associated with 1 ev. is 11,605° K). However, an approach which has had some success

employs high pressure oven sources.[10] The effusive flow of a conventional oven is then replaced by a supersonic jet. The effectiveness of this method was first demonstrated in 1954 by Becker and Bier,[11] who found that the major difficulty was the provision of sufficient pumping capacity to remove the gas admitted into the vacuum system. This approach has received considerable attention and useful beams of molecules have been obtained with kinetic energies up to 1 ev.[12-17]

Molecular beams with energies down to about 5 ev. have been produced from high energy ion beams, which have been slowed down with a retarding potential and subsequently neutralized.[18] This method has met with difficulties, since mutual repulsion between ions, after retardation, causes a loss of collimation of the beam, and results in beams of low intensity which are difficult to detect. One advantage, however, of this approach is that often no velocity selection is required since the energy spread of the neutrals is the same as that of the original ions, which can be controlled electrostatically.[19][20]

Another method recently demonstrated by Trujillo, et al.,[21] is the so-called "merging beam" technique. This involves directing beams of molecules, whose interaction is to be studied, at one another in such a way that the energy of interaction (i.e. relative energy in centre of mass co-ordinates) lies within the chemical energy range. This method has the advantage that high laboratory kinetic energies may be used for both beams, since the difference in the laboratory energies of the beams ΔE is

many times larger than the interaction energy I, which is given by:

$$I = \mu\left[\left(\frac{E_2}{m_2}\right)^{\frac{1}{2}} - \left(\frac{E_1}{m_1}\right)^{\frac{1}{2}}\right]^2$$

where m_1 and m_2 are the masses of molecules in the two beams and μ is the reduced mass. For the case $m_1 = m_2 = m$ and $\triangle E$ small compared with E_1 and E_2, then it can be shown that:

$$I = \triangle E^2 / 8E$$

where E is the average of the two beam energies.

For example, if two beams of atoms of the same mass, having 5000 ev. and 5100 ev. respectively, are made to travel in the same direction so as to interact, the energy of interaction between the atoms in the beams will be 0.25 ev. The use of high energy beams reduces experimental difficulties considerably.

Early studies involving atomic and molecular beams were primarily concerned with non-chemical phenomena. In 1911 Dunoyer[22] produced a beam of sodium atoms by heating sodium metal in an oven. This experiment demonstrated that atoms travel in a straight line through an evacuated region. The first quantitative studies with molecular beams were carried out by Stern, commencing in 1919. He measured the thermal velocities of molecules directly[23] and demonstrated the effects of space quantization and atomic magnetic moments[24, 25]. This work became known as the Stern-Gerlach experiment. In 1931 Stern verified the de Broglie equation $\lambda = \frac{h}{mv}$ for atoms by

diffracting beams of velocity selected helium atoms from the surface of a Li F crystal.[26] Since that time extensive research has been carried out in the field of physics using molecular beam methods. General surveys of the research carried out to the present time may be found in references[1][8][27-32].

Application of beam experiments to chemical problems is a more recent development, although early work included investigation of surface ionization, condensation, nucleation, evaporation and scattering. At the present time beam experiments with molecules and ions are being performed over a large energy range, to investigate the interactions between atoms, molecules, ions, electrons and photons.

The ideal way of studying a chemical reaction in the gas phase, whether molecule-molecule, ion-molecule or charge transfer, is to allow beams of the two reactants to collide with selected velocities and quantum states. The yield of products, their velocities, quantum states and angular distribution should then be measured. Conceptually such dynamic studies are not new since nuclear reactions have been studied in this way for fifty years.[33] The performing of such an experiment on a chemical reaction is still an ideal rather than a reality, but many investigations have yielded important data without fulfilling all the conditions of the ideal experiment. A number of reviews describing these investigations have been written.[12][31][34][35]

Present applications of molecular beam technology to chemical phenomena include studies of the mechanisms of organic

ion-molecule reactions,[36] studies of the energy dependence of energetic hydrogen atom reactions with cyclohexane[37] and n-butane,[38][39] together with investigation of the hydrogen iodide reactions,[40] and dissociation studies of H_2^+,[41] HeH^+,[42] and D_2^+[43] by collision with inert gas molecules. Extensive charge exchange studies are being carried out which include studies of $He^+ - He$[44] and $Ne^+ - Ne$[45] systems. Investigations are also being carried out on ion-molecule reactions of the type $Ar^+ + D_2 \longrightarrow ArD^+ + D$[46] and $Ar^+ + H_2 \longrightarrow ArH^+ + H$[47], together with measurements of van der Waals forces.[48] Reactive scattering of K atoms by HBr and DBr,[49] reaction of K atoms with oriented CF_3I molecules,[50] and crossed-beam studies of the ionization of Cs by Br_2[51] are also being carried out.

In summary, molecular beam scattering experiments have produced useful data on chemical reactions by allowing them to be studied without the inherent loss of detail and difficulties of interpretation associated with more conventional methods.

In the work described below, a molecular beam apparatus has been built to investigate charge transfer and ionization reactions with stable and short-lived molecules. The behaviour of H_2, D_2 and He Radio-Frequency discharges has been investigated with the apparatus and optimum conditions found for the operation and production of various atomic and molecular ion beams. Beams of neutral molecules and atoms have been produced from 5000 ev. ion beams by charge transfer reactions. The neutral products have been identified by reionization and mass analysis.

The experimental arrangement is such that molecules with lifetimes in excess of about 10^{-7} secs. may be detected as stable species.

The molecules which have been studied are HeH, HeD, He_2, H_3, D_2H and D_3. The behaviour of these molecules in the beam apparatus has been compared with that of stable molecules such as H_2, D_2 and HD, and atoms such as He, H, and D. Studies of the collisional dissociation of He_3^+ molecular ions have been carried out to demonstrate the existence of He_3^+ in low temperature Radio-Frequency discharges. Some of the results of this series of investigations have been reported in the literature.(52)(53)

CHAPTER 2

COLLISION PROCESSES

Collisions taking place between particles in the gas phase may be divided into three broad categories: 1. Elastic collisions; 2. inelastic collisions; and 3. reactive collisions. Elastic collisions are those in which the total kinetic energy, and consequently the internal energy of the collision partners, remains unchanged. Linear and angular momenta are conserved at all times throughout such a collision. Inelastic collisions are those in which the quantum states of the collision partners are changed and therefore involve energy transfer to and from the internal modes of the particles. Reactive collisions, with which this work is mainly concerned, comprise those in which a chemical reaction occurs, involving transfer of atoms, ions or electrons between the collision partners.

Some of the inelastic collisions which can occur between an ion A^+ and an atom B are shown in Table 1. The ion A^+ is regarded as the projectile, and the atom B at rest, although in the centre-of-mass coordinate system the distinction between projectile and target is lost. The numerical classification scheme is that suggested by Hasted[54], in which the integers

Table I

Classification of some Inelastic Reactions between Atomic Ion A^+ and Atom B

REACTION	NUMERICAL CLASSIFICATION	VERBAL DESIGNATION
$A^{+*} + B \longrightarrow A^{+} + B^{*}$	$(1^{*}0/10^{*})$	Excitation Transfer
$A^{+} + B \longrightarrow A + B^{+}$	(10/01)	Single Charge Transfer
$A^{+} + B \longrightarrow A^{-} + B^{2+}$	(10/-12)	Double Charge Transfer
$A^{+} + B \longrightarrow A^{+} + B^{+} + e$	(10/11e)	Ionization
$A^{+} + B \longrightarrow A + B^{2+} + e$	(10/02e)	Transfer Ionization
$A^{+} + B \longrightarrow A^{2+} + B + e$	(10/20e)	Stripping
$A^{+} + B \longrightarrow A^{*} + B^{+}$	$(10/0^{*}1)$	Charge Transfer to an excited level
$A^{+} + B \longrightarrow A + B^{+*}$	$(10/01^{*})$	

on the left denote the charge states of the reactants, while those on the right denote the charge states of the products. An asterisk is used to indicate an electronically excited state and the production of a free electron is denoted by the symbol e. Further reactions are possible if either of the reactants is molecular. These may involve rotational and vibrational excitation or collisional dissociation. A further series of reactions may occur in which an atom is transferred between the reactants. The simplest reaction of this type may be written

$$A^+ + BC \longrightarrow AB^+ + C$$

These reactions, together with many others involving ions, molecules, photons and electrons, have been reviewed by Hasted[55]. Reactions which are of particular relevance to this work include single charge transfer, ionization, collisional dissociation and atom transfer. These will be discussed in more detail.

1. Single Charge Transfer

Charge-transfer reactions involve the exchange of one or more electrons between the reactants. It is convenient to divide these reactions into two types:

Symmetric resonance reaction, represented by

$$A^+ + A \longrightarrow A + A^+$$

and Assymmetric reactions, represented by

$$A^+ + B \longrightarrow A + B^+$$

The energy dependence of the cross sections for these two processes is generally quite different. The reasons for this

may be discussed in terms of the "Adiabatic Hypothesis" due to Massey[8][56]. A quantity ΔE is defined as the difference between the ionization potentials of A and B in the assymmetric reaction. This is known as the energy defect of the reaction. Massey has shown that, in general, the cross section for charge transfer, at low relative velocity of approach, will be small unless ΔE is small. It can be shown that if

$$\frac{l\Delta E}{hv} \gg 1$$

the cross section for charge transfer will be small. (l represents the range of interaction between A^+ and B, and v their relative velocity of approach.) If v is increased to

$$v^* = \frac{l\Delta E}{h}$$

the cross section should attain its maximum value, which may be large. This condition corresponds to the collision time (l/v) being comparable with the transition time. The energy corresponding to maximum cross section may be written

$$E^* = 36(\Delta E)^2 m\, l^2 \text{ ev.}$$

when ΔE is expressed in ev., the mass of the incident particle m in atomic units and l in units of the Bohr radius. For the reaction

$$H^+ + H_2 \longrightarrow H + H_2^+$$

$\Delta E = 2.07$ ev., m = 1 a.m.u., and for the purpose of calculation l may be taken as approximately 5 Bohr radii. E^* then has a value of about 4300 ev. Experimentally, a value of about 4800 ev. has been obtained by Allison[57]. Since l, the so-

called "adiabatic parameter", is not well defined, the agreement is reasonable.

Thus, in general, the "adiabatic hypothesis" predicts that the cross section for assymetric charge transfer should be small at thermal energies, should rise to a maximum near the energy corresponding to E^* and should then decrease at higher energies, where the interaction time ultimately becomes too short for the transition to occur. With symmetrical resonance reactions ($\triangle E = 0$), it predicts that the cross section for charge transfer should increase monotonically as the impact energy decreases. These arguments account for the experimental observations. The cross section for the symmetric resonance reaction

$$H_2^+ + H_2 \longrightarrow H_2 + H_2^+$$

increases as the impact energy decreases and attains a maximum value at very low energies.[58] This compares with the assymmetric reaction between H^+ and H_2, mentioned above, where the maximum cross section occurs at about 4800 ev.

The theory of non-resonance assymmetric charge transfer has been reviewed by Massey and Burhop[8], Bates and Dalgarno[59], and Hasted[9]. The theory, although accounting qualitatively for experimental observations, makes no predictions as to the magnitude of the maximum cross section. Quantum mechanical calculations of symmetrical resonance cross sections by Firsov and Fetisov[81][82] have had some success, but the majority of cross-section values are experimental. Surveys of the litera-

ture values of experimental charge-transfer cross sections have been carried out by McDaniel[30], Allison and Garcia-Munoz[60] and Hasted[9].

Most measurements on charge-transfer cross sections have been made by passing beams of positive ions through a neutral gas target. The cross section for charge-changing collisions is greater than that for momentum-transferring collisions ("violent" collisions resulting in large angular scattering of the products), so that a large fraction of an ion beam may be neutralized without producing severe attenuation of the beam. The cross sections for competing reactions, such as ionization and stripping (Table 1), are also small compared with cross sections for charge transfer.

The factors governing the choice of charge transfer gases for production of neutral beams from ionic beams, have been reviewed by Whittkower et al.[61][62]. Allison[57] has measured the equilibrium concentrations of H^+, H, and H^- in a beam of H^+ ions passing through H_2 gas in such a way that a steady state equilibrium between the charged species was attained. A high proportion of H atoms was found ($>70\%$), so that it is apparent that a neutral beam of atoms or molecules may be produced from an ionic beam with high efficiency.

2. Ionization

The ionization of atoms and molecules in a beam was a necessary stage in the experiments being reported. Two methods were used:

a) Ionization by Electron Impact

$$A + e \longrightarrow e + A^{+} + \ddot{e}$$

The production of ions by electron impact has been investigated for many years. The literature on this topic is extensive[30]. Comprehensive reviews on the excitation and ionization of atoms by electron impact have been carried out by Massey[63], Burk and Smith[64] and Burk, Schey and Smith[65]. The majority of mass spectrometers and ion beam accelerators employ electron impact for the production of ions.

To produce ionization, the relative kinetic energy of atom A and the electron must be greater than the ionization potential of A when A is in the electronic ground state. Once this threshold is reached, the cross section increases rapidly to a peak value at about 100 ev. and then slowly decreases as the energy increases. This behaviour is typical of almost all atoms and molecules[66]. Normally, the gas to be ionized is at room temperature so that the kinetic energy of the molecules is negligible compared with that of the electrons. In the experiments to be described, the velocity of the neutral atoms is comparable with that of the electrons and must be taken into account when calculating the interaction energy.

b) Ionization by Heavy Particle Collision

$$A + B \longrightarrow A^{+} + B + e$$

The classical Thomson theory of ionization[67] predicts that electrons and protons with equal velocity, incident on a

given target should have the same cross section for ionization. Hooper et al.,[68] have confirmed this prediction experimentally for high energy protons. The same considerations apply to an atom incident on a target molecule. The behaviour of the cross section for ionization by heavy particle collision is basically the same as that for electrons. The relative energy threshold for ionization is usually a factor of two higher than the ionization potential of the colliding partner losing the electron. Above the threshold energy, the cross section increases rapidly to a maximum and then decreases as the energy is increased. The energy scale for this process, however, is quite different from that of ionization by electrons. The cross section reaches maximum value at a beam energy of about 10 - 50 kev. for H atoms, compared with about 70 ev. for electrons.[83]

At energies appreciably below that for maximum cross section, the relative velocity of the colliding particles is small compared with the velocity of the orbital electrons so that the interaction time is long. The cross section for ionization is then small because the electrons are able to adjust adiabatically to the slowly changing perturbation. On the other hand, high kinetic energies result in short interaction times making ejection of an electron improbable. From these considerations, a beam of H atoms with 5000 ev. energy, passing through H_2 gas, may be expected to have a relatively high cross section for the process

$$H + H_2 \longrightarrow H^+ + H_2 + e$$

However, ionization cross sections are generally smaller than charge transfer cross sections. This is illustrated by equilibrium fraction experiments,[57] in which a 5000 ev. H^+ ion beam is passed through H_2 gas so that charge transfer and ionization reactions occur.

$$H^+ + H_2 \longrightarrow H + H_2^+ \qquad {}_1q_0$$

$$H + H_2 \longrightarrow H^+ + H_2 + e \qquad {}_0q_1$$

When a steady-state equilibrium is attained, the ratio $H : H^+$ is found to be about 10 : 1. Experimental values of ${}_1q_0$ and ${}_0q_1$ at 5 kev. are 1×10^{-15} cm.^{2} and 0.8×10^{-16} cm.^{2} respectively.

3. Collisional Dissociation

A molecular ion undergoing charge transfer or ionization reactions may dissociate into constituent components. The energy required for this process is usually less than 10 ev. H_2^+ ions travelling through hydrogen gas may undergo single charge transfer to give H_2 molecules, but may also undergo dissociative reactions such as

$$H_2^+ + H_2 \longrightarrow H^+ + H + H_2$$

$$H_2^+ + H_2 \longrightarrow H^+ + H^+ + H_2 + e$$

$$H_2^+ + H_2 \longrightarrow H + H + H_2^+$$

Sweetman[69] has measured the cross sections for these reactions in the energy range 100 - 800 kev. Alternative dissociation reactions resulting in the production of negative ions, such as

$$H_2^+ + H_2 \longrightarrow H^- + H^+ + H_2^+$$

have been shown by Fodorenko et al., to have very small cross sections[70].

Collisional Dissociation reactions have been studied by Lindholm[71][72], Melton and Wells[73], and McGowan and Kerwin[74]. More recent investigations have been carried out on HeH^+[42] and D_2^+[43]. Purser[41] has studied the energetics of such reactions and reports that the spread in the kinetic energy of H^+ ions resulting from collisional dissociation of 5000 ev. H_2^+ ions, may be as high as 350 ev. in laboratory co-ordinates. Angular-distribution studies of the products of these reactions have been carried out by Sweetman[69], and the effects of vibrational excitation of the dissociating ion investigated by Riviere and Sweetman[75] and McClure[58]. The yields of the various dissociation fragments of H_2^+ and H_3^+ ions were found to vary by as much as 20% with changes in ion source conditions[58]. This was presumed to be due to changes in vibrational excitation of the primary ions.

4. Atom-Transfer Reactions

Reactions may occur between ions and molecules in which an atom is transfered from one reactant to the other. These are known generally as ion-molecule reactions. A typical reaction of this type, and one which has received considerable attention is

$$H_2^+ + H_2 \longrightarrow H_3^+ + H$$

Reactions of this type involve the breaking and forming of

chemical bonds. Experimental data have been obtained mainly from mass-spectrometric measurements[76-78], and discharge chambers[84]. These studies have shown that the cross section for an ion-atom interchange reaction may be large at low impact energies (0.1 to 10 ev.), but decreases steadily as the energy increases and is virtually zero at energies in the kev. region.

The polarization theory[77] predicts a collision cross section between ions and molecules given by

$$\sigma_c = e\left|\frac{2\alpha m\pi^2}{\mu E}\right|^{\frac{1}{2}}$$

where α is the polarizability of the molecule, μ the reduced mass, e, m and E the charge, mass and kinetic energy of the ion. Proportionality between σ_c and $E^{-\frac{1}{2}}$ has been observed for some ion-molecule reactions. For example:

$$Ar^+ + H_2 \longrightarrow ArH^+ + H$$

However the electrical interaction between the charge on an ion, and the induced dipole of a molecule is negligible above an energy of about 1 ev. Henglein[79] has postulated that at energies above 1 ev., "stripping" or "pick-up" processes occur. However, in general, cross sections for atom-transfer reactions are found to be vanishingly small at relative interaction energies above about 10 ev. Futtrell and Abramson[80] have reviewed the kinetic energy dependence of ion-molecule reactions from both experimental and theoretical viewpoints.

Summary

The reactions discussed above are only a few of the many possible reactions which may take place in a molecular

beam apparatus. They are of particular relevance to the experiments to be described. Further discussion on the applicability of these reactions to the production of neutral beams will be found in Ch.5.

CHAPTER 3

APPARATUS

General Description

The apparatus used in this work was designed and built so that the positions of many of the components were interchangeable. This provided maximum versatility and scope for a variety of experiments to be carried out. The apparatus is shown schematically in Fig.1.

A Radio-Frequency discharge ion source was used to produce beams of atomic and molecular ions such as H^+, H_2^+, He^+ and HeH^+. The ion beam was extracted from the source electrostatically, and accelerated through 5000 volts. The beam was focused at the entrance to the first mass analyser by a gap lens followed by a quadrupole lens. A beam of the ions of interest was mass selected and passed through aligning plates, a second quadrupole lens, and subsequently through a charge exchange cell containing either lithium vapour or a gas such as hydrogen or helium.

The neutral atoms or molecules formed were permitted to continue undeflected, while the remaining ions were removed by electrostatic deflector plates. A fraction of the neutral beam was reionized by electron bombardment and the ions formed were mass analysed and collected in a Faraday cup. The geometry

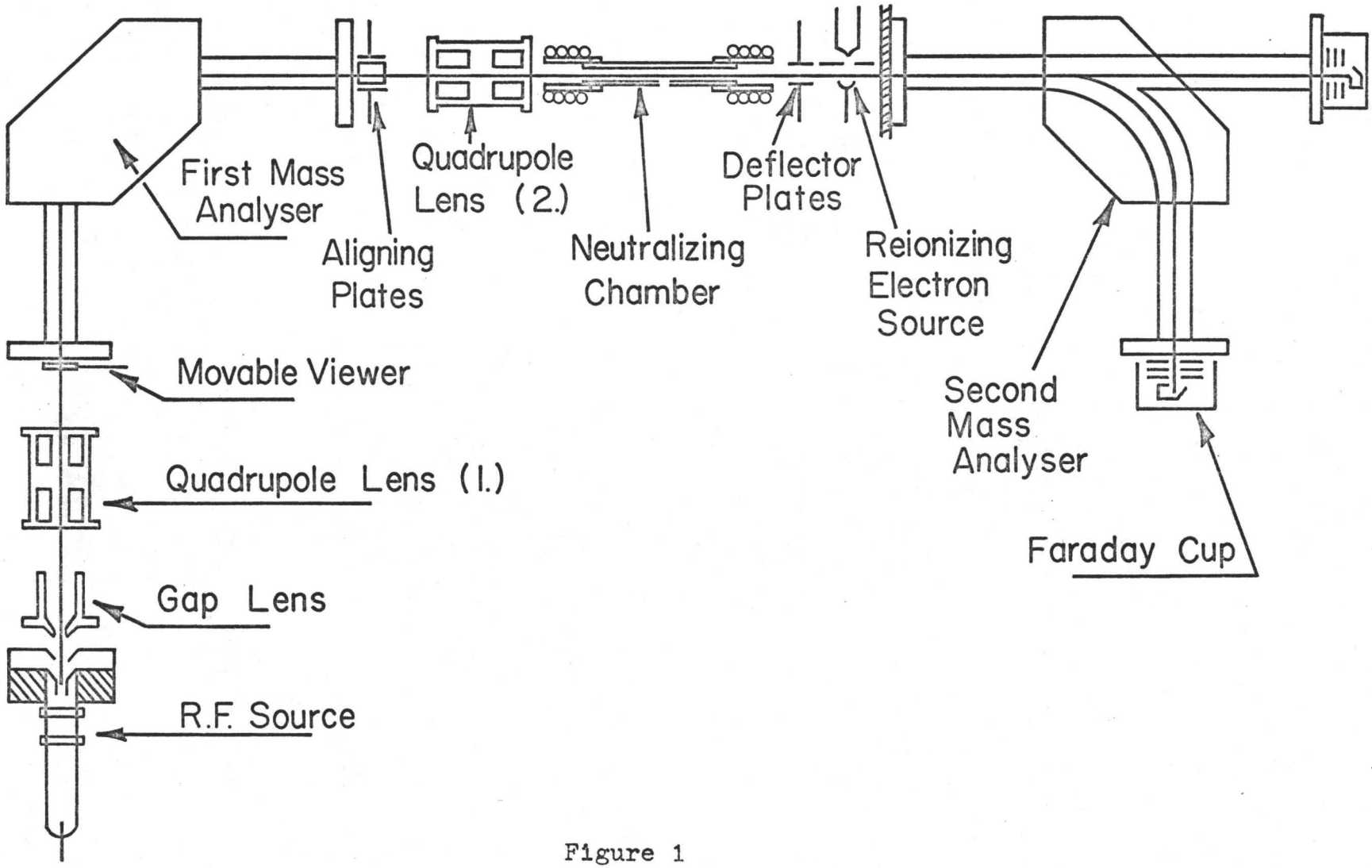

Figure 1

Schematic of the molecular beam apparatus

of the apparatus was such that only atoms or molecules with high translational kinetic energy were focused by the magnetic field. Low energy products formed in the background gas, and products formed from momentum-transferring collisions were not focused at the detector.

For descriptive purposes the apparatus may be divided into the following sections:

1) Ion Source
2) Gas Handling and Vacuum Systems
3) Focusing, Mass Analysis and Alignment Systems
4) Charge Transfer Cell
5) Ionization, Mass Analysis and Detection Systems
6) Electronics

1) Ion Source

An ion source is a device which produces atoms or molecules with a net positive or negative charge. The molecules of interest are admitted into the ion source and ionized near an aperture, through which the ions can be extracted. The ion beam extracted from such a source often contains a substantial fraction of atomic, as well as molecular ions. Although other techniques are occasionally used, electron bombardment is the most common method of producing ions. The electrons are normally accelerated by an electric field to an energy somewhat higher than the ionization potential of the molecules to be ionized.

The sources which are most commonly used for the produc-

tion of intense beams of ions depend upon the ionization produced in gaseous discharges. However, the means of producing this ionization and of concentrating the beam vary considerably. Several types of ion sources may be mentioned.

1. Cold-cathode canal-ray tube
2. Spark discharge
3. Hot-cathode arc
4. Low voltage capillary arc
5. Discharge in an axial magnetic field
6. Electron oscillation discharge
7. Radio-Frequency discharge

Livingstone and Blewett[97] have reviewed the characteristics of these ion sources, and Rose[98] has presented the basic concepts underlying the production of ion beams. At the present time two sources are most commonly used:

(a) Duoplasmatron

Developed first by von Ardenne[99], the duoplasmatron is a hot-cathode magnetic ion source. This source has been used extensively at Oak Ridge[100] and is now available commercially. A survey of plasmatron sources has been carried out by Morgan et al.[101]

(b) Radio-Frequency Discharge

The application of Radio-Frequency discharges to ion beam production was first investigated by Thoneman[102] and Rutherglen et al.,[103] in England, and Bayly et al.,[104] in Canada. This was the type of ion source selected for the

present work. It was an adaptation of the Oak Ridge source described by Moak et al.,[105] which was itself based on the earlier work of Rutherglen[103], Bayly[104], Thoneman[106] and Hall[107].

The construction of the ion source is shown in Fig.2. It consisted of a Pyrex ion bottle mounted on an aluminum base plate. A solenoid coil surrounded the base of the ion bottle and a quartz sleeve fitted around the exit canal of the base plate. A radio-frequency oscillator produced the discharge, and a high voltage probe permitted extraction of a beam. The gas to be ionized was fed into the ion bottle through a hole in the base plate.

The radio-frequency field applied to the excitor rings was approximately 60 Mc./s. frequency. A stable discharge was formed, in which electrons and positive ions were in equilibrium. A free electron in such a discharge may have a mean free path of about 1 cm., depending on the pressure, so that, as it is accelerated by the R.F. field, ion pairs are produced by collision with gas molecules. The solenoid coil produced a magnetic field with lines of force in the direction of the long axis of the bottle. This restricted the electrons to the centre of the discharge and caused them to spiral. This increased the density of ions in the region of the exit canal. The Pyrex shield protected the extraction probe from electron bombardment.

The extraction system consisted of a small tungsten probe (anode), hidden from the discharge by a short capillary,

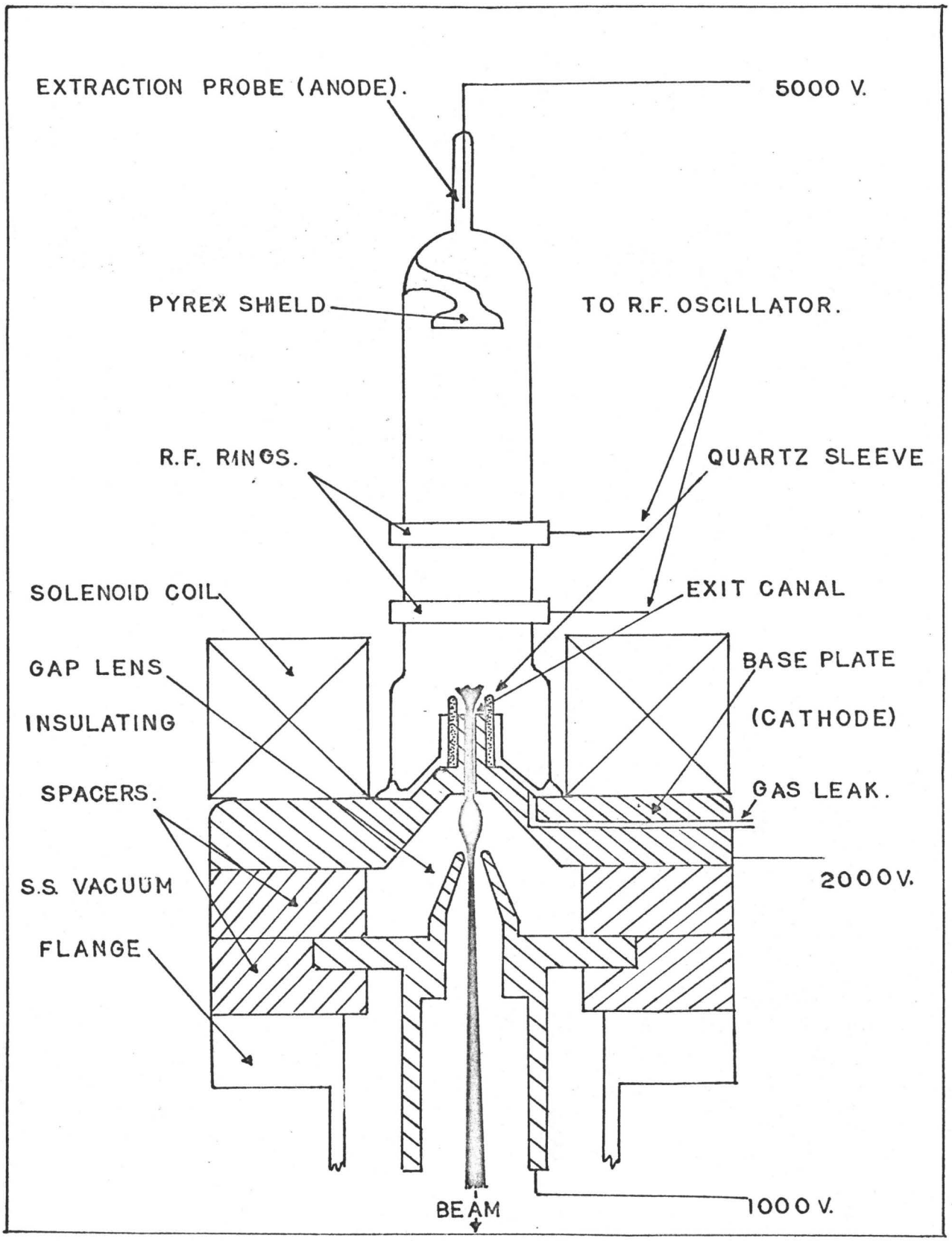

Figure 2

Radio-frequency ion source and gap lens

and a cathode, consisting of a cylindrical aluminum tip protruding into the discharge from the base plate. A canal, 0.5 mm. in diameter, permitted the ions to enter the high vacuum region. A beam was obtained by applying a potential of 3000 volts between the anode and cathode. Being a good conductor, the discharge was essentially at the anode potential, and almost all the applied potential was across the cathode dark space, which developed at the canal tip as the extraction voltage was increased. The quartz sleeve prevented surface recombination of the ions on the metallic cathode and functioned as a virtual anode with respect to the exit canal. This resulted in a focusing effect (Fig.2), which allowed the ions to traverse the exit canal without striking the walls.

On entering the high vacuum region the ions travelled in all directions and had to be focused to form a beam. This was done with the gap lens. The focal length and spot size of the beam were controlled by the voltage on the gap lens, which was made negative with respect to the base plate. The gap lens was insulated from the aluminum base plate by two Bakelite spacers. When insulators are "visible" to an ion beam, electrostatic charges may build up which affect the beam trajectory. For this reason the gap lens was shaped so as to shield the beam from the spacers.

The ion source thus produced a collimated beam of ions with kinetic energy equal to the anode potential.

2) Gas Handling and Vacuum Systems

a) Leak Systems

To operate the ion source efficiently it was necessary to maintain a controlled flow of gas into the ion bottle. Two methods were used

(i) Palladium Leak

(ii) Mechanical double needle valve

The palladium leak device served as a selective valve for admitting hydrogen or deuterium gas into the ion bottle, since when heated, palladium becomes porous to hydrogen-like gases. The flow of gas was controlled by varying the temperature of the palladium. The leak assembly consisted of a palladium tube surrounded by a Pyrex sleeve, around which was wound a heating coil. The tube and coil were contained in a brass cylinder into which hydrogen flowed. The hydrogen passed into the heated palladium tube and through to the ion bottle. The connection between the output from the tube and the ion bottle was made through a polyethylene tube. This served to insulate the leak assembly (ground) from the ion source (+ 3000 v.).

The palladium leak also effectively purified the hydrogen entering the discharge. The disadvantages however were: 1) Contamination of the palladium occurred if air was admitted to the leak while the tube was hot, and 2) only hydrogen or deuterium gas could be used. To overcome these difficulties a mechanical double-needle valve, manufactured by "Nupro", was

used. This valve was capable of leak rates of 0.5 to 100 atm. cm^3. $hr.^{-1}$ and could be used with any gas.

The gas handling system, incorporating the leak devices, is shown in Fig.3. The gas lines were made from $\frac{1}{4}$" copper tubing. Joints were made with "Swagelock" couplings on the high pressure side and silver solder on the vacuum side. A switching device permitted either leak to be used. Discharges from mixed gases were obtained by mixing the gases in the high pressure line and passing the mixture through the mechanical leak. Before running an experiment, the whole gas line was evacuated with a mechanical pump and repeatedly flushed with the gas to be used in the discharge. Finally, the high pressure line was filled with the gas to a pressure of about 30 $lb.in.^{-2}$.

b) Vacuum System

It was essential that a good vacuum be maintained in the apparatus so as to minimize attenuation of the beam caused by scattering from background gas molecules. The gas effusing from the ion source was removed by two 3-stage mercury diffusion pumps, manufactured by "Consolidated Electrodynamic Corporation". Both pumps were incorporated into the apparatus as close as possible to the exit canal of the ion source, to provide maximum pumping efficiency. The pumps had 4" diameter entrance apertures and were equipped with liquid nitrogen traps. A low backing pressure for the diffusion pumps was provided by a 450 $l.min.^{-1}$ mechanical pump, manufactured by "Edwards High Vacuum Corporation".

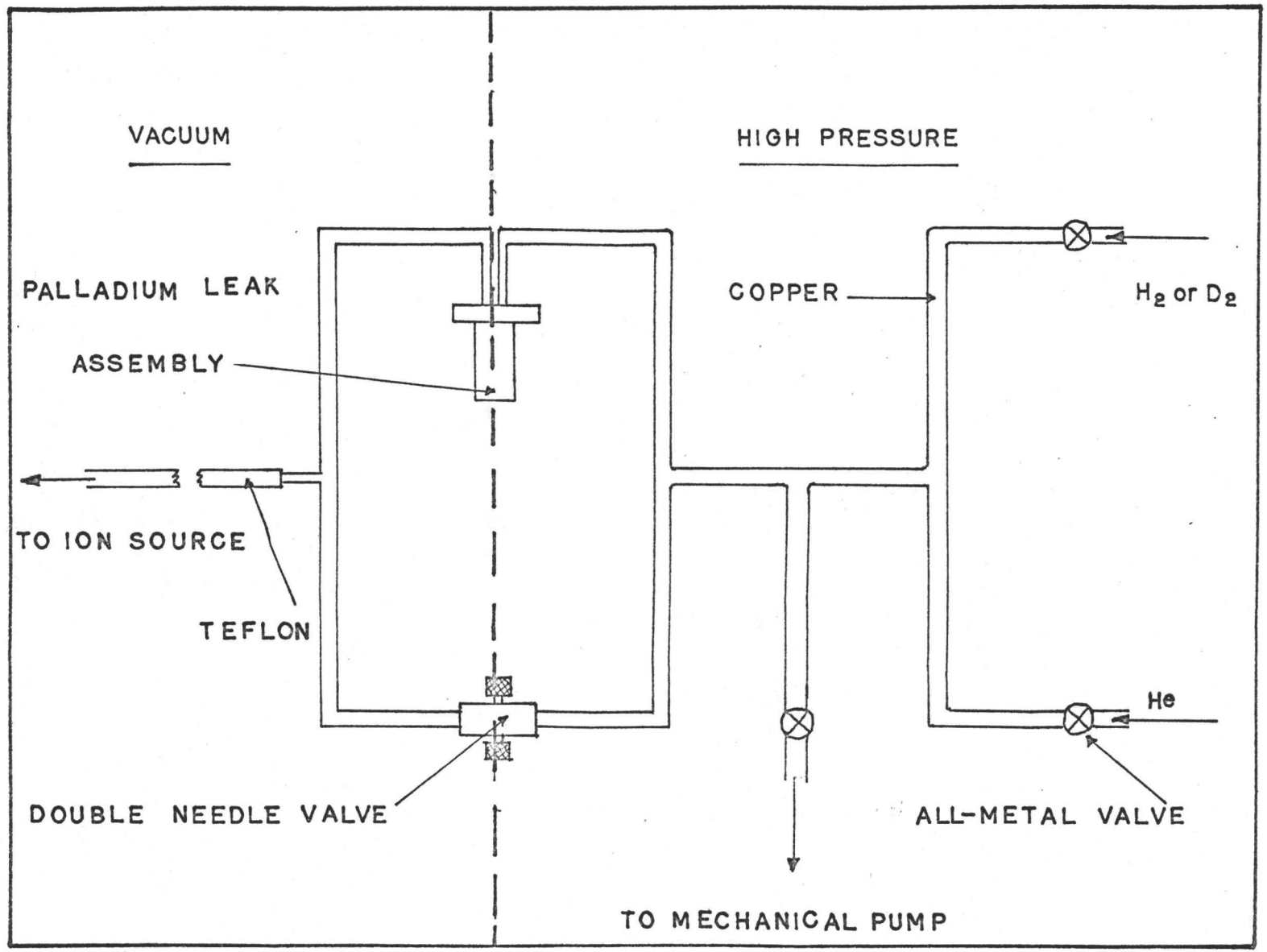

Figure 3

Gas handling system

A static pressure of 5×10^{-7} mm. Hg. was obtained, whereas during operation the pressure rose to 1×10^{-5} mm. Hg. At this pressure the mean free path of ions in the beam was of the order of a few metres. A low vacuum was maintained in the region of the charge transfer canal by a third diffusion pump. This was a 3-stage mercury diffusion pump, manufactured by "Edwards High Vacuum Corporation", and was backed by a mechanical pump rated at 150 $l.min.^{-1}$. Mercury diffusion pumps were used throughout the apparatus because of the problem of carbon deposition associated with oil diffusion pumps. The vibrations produced by the mechanical pumps were insulated from the beam apparatus by bellows couplings, and the diffusion pumps and beam tubes mounted on a heavy chassis to further reduce vibrations.

Pressure in the apparatus was monitored with Pirani and ion gauges, manufactured by "Edwards High Vacuum Corporation". Liquid nitrogen levels were maintained in the vapour traps with an automatic filling device employing thermocouples placed in the liquid nitrogen. The apparatus was leak-checked periodically using a helium mass spectrometer leak detector.

A series of vacuum-tight flange couplings were designed so that all the components could be interchanged when necessary. Fig.4 shows a typical 'o' ring vacuum seal between two flanges. Flange A was equipped with a $2\frac{7}{8}$" i.d. circular channel which accommodated a rubber 'o' ring. Flange B was machined flat so that when the flanges were drawn together the 'o' ring formed

a vacuum tight seal between the components. In this way a variety of components could be attached to the apparatus while still maintaining a good vacuum.

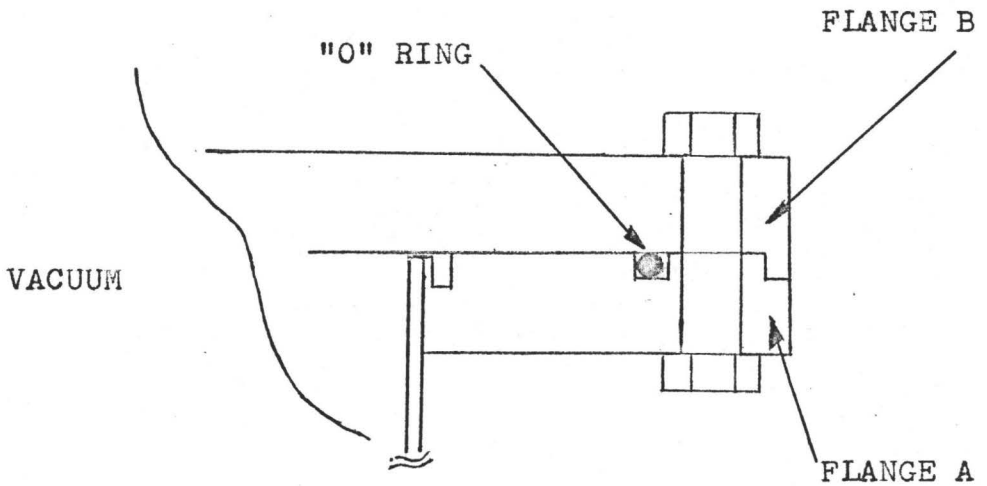

Figure 4

Vacuum flange coupling system

Where low temperatures were involved, as with the liquid nitrogen traps, silver 'o' rings were used rather than rubber. Unfortunately the silver 'o' rings became permanently deformed on compression, and had to be replaced if the vacuum seal was broken for any reason. Electrical connections into the vacuum were made using high vacuum electrical feed-throughs obtained from a number of manufacturers. Water connections were made with 'o' ring seals.

3) Focusing, Mass Analysis and Alignment Systems

a) Lens System

A lens system was used to increase the transmission of the ion beam through the apparatus. Mass analysis was carried out using a sector shaped magnetic field, with the ions entering and leaving normal to the field edges. Such an analyser focuses to first order in angle, for displacements in the plane normal to the field, but has negligible focusing properties for displacements parallel to the field. Thus for maximum transmission, the beam should ideally be in the form of a narrow ribbon or wedge. This enables the entrance slit of the mass analyser to be made narrow, which results in good mass resolution[108] while permitting high beam intensities to be transmitted.

An ideal means of attaining this desired beam shape is to pass the beam through an electrostatic quadrupole lens (Fig.5) The potential distribution in this lens is given by

$$V = \pm V_o \, (r^2 / R_o^2) \cos 2\theta$$

and the equipotentials for such a field are rectangular hyperbolas. This field may be well approximated by the use of circular cylinders with considerable simplification in construction. Fig.5 shows the mode of action of such a lens pair. The positive potentials on the cylinders lying in the x - y plane of the first lens cause a convergence of the beam, while the negative potentials on the corresponding cylinders of the second lens cause a divergence. The divergence is weaker than

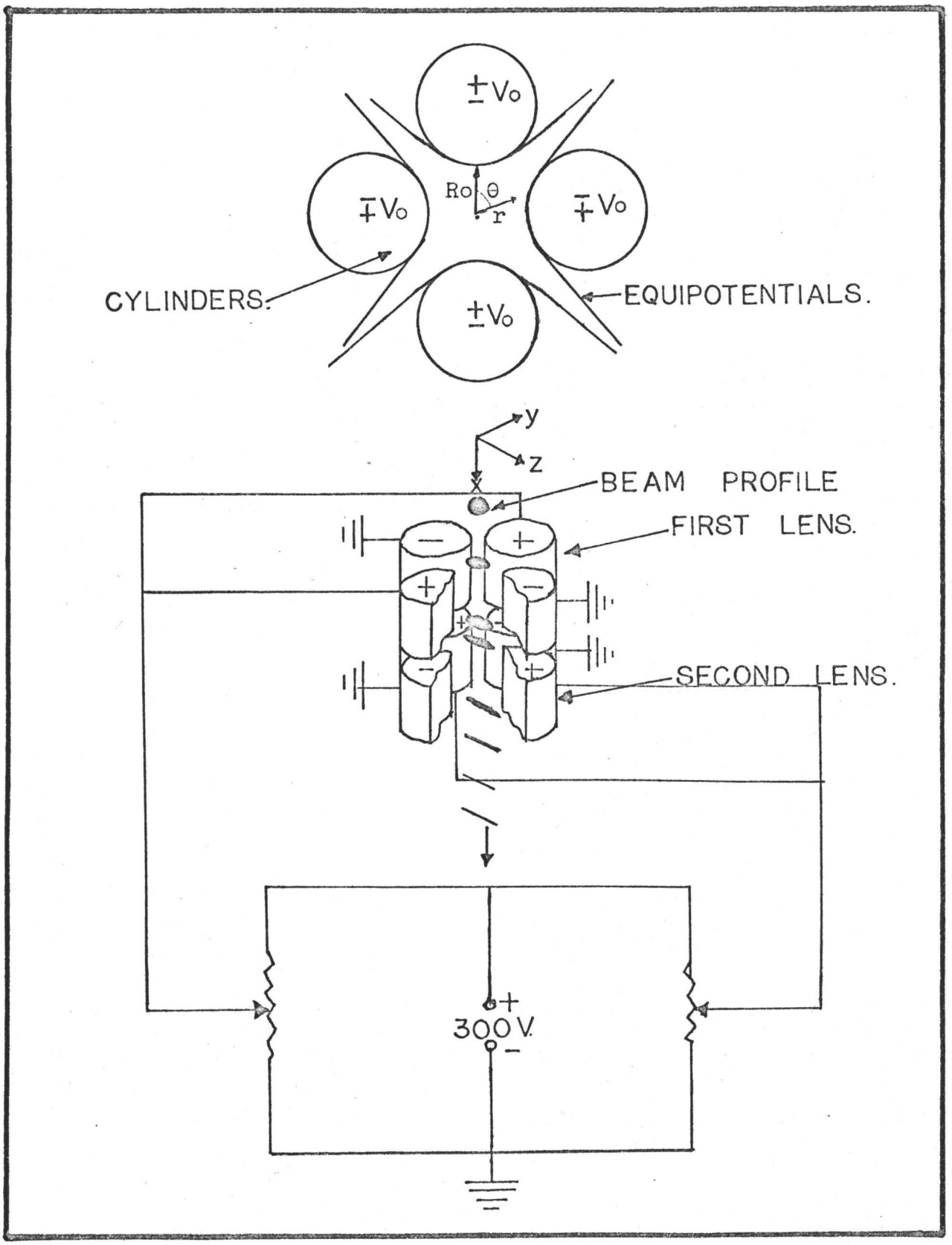

Figure 5

Mode of action of the quadrupole lens pair

the convergence, since potentials on the second lens are made smaller than on the first. In the x - z plane, the first lens causes a divergence, whereas the second lens causes a weaker convergence. This results in a wedge-shaped beam at the point of cross over. In this way, the quadrupole lens pair converts a circular beam into a line-focused beam, ideal for mass spectrometers[109][110] and particle accelerators[111][112][113].

The physical construction of the lens is shown in Fig.6. The lens elements were made from highly polished stainless steel tube 0.5" O.D. by 1" long. They were mounted inside a stainless steel cylinder so that R_o was 0.2" and the separation of the two lenses 0.5". The whole lens assembly was fitted inside a vacuum chamber equipped with vacuum flanges at both ends. Electrical connections were made through low current vacuum feed-throughs mounted around the vacuum chamber, and brass adaptors made to permit B.N.C. high voltage coaxial connectors to be used.

In summary, some of the advantages gained by the use of quadrupole lenses in this experiment are:

(i) The lens permitted the production of a ribbon-shaped beam having maximum transmission through the mass analyser.

(ii) The lens elements required relatively low potentials (0 to 300 v.) in contrast to other lenses in common use.

(iii) The lenses served the dual function of focusing and centring the beam.

(iv) The lens could accept large entering beams (up to

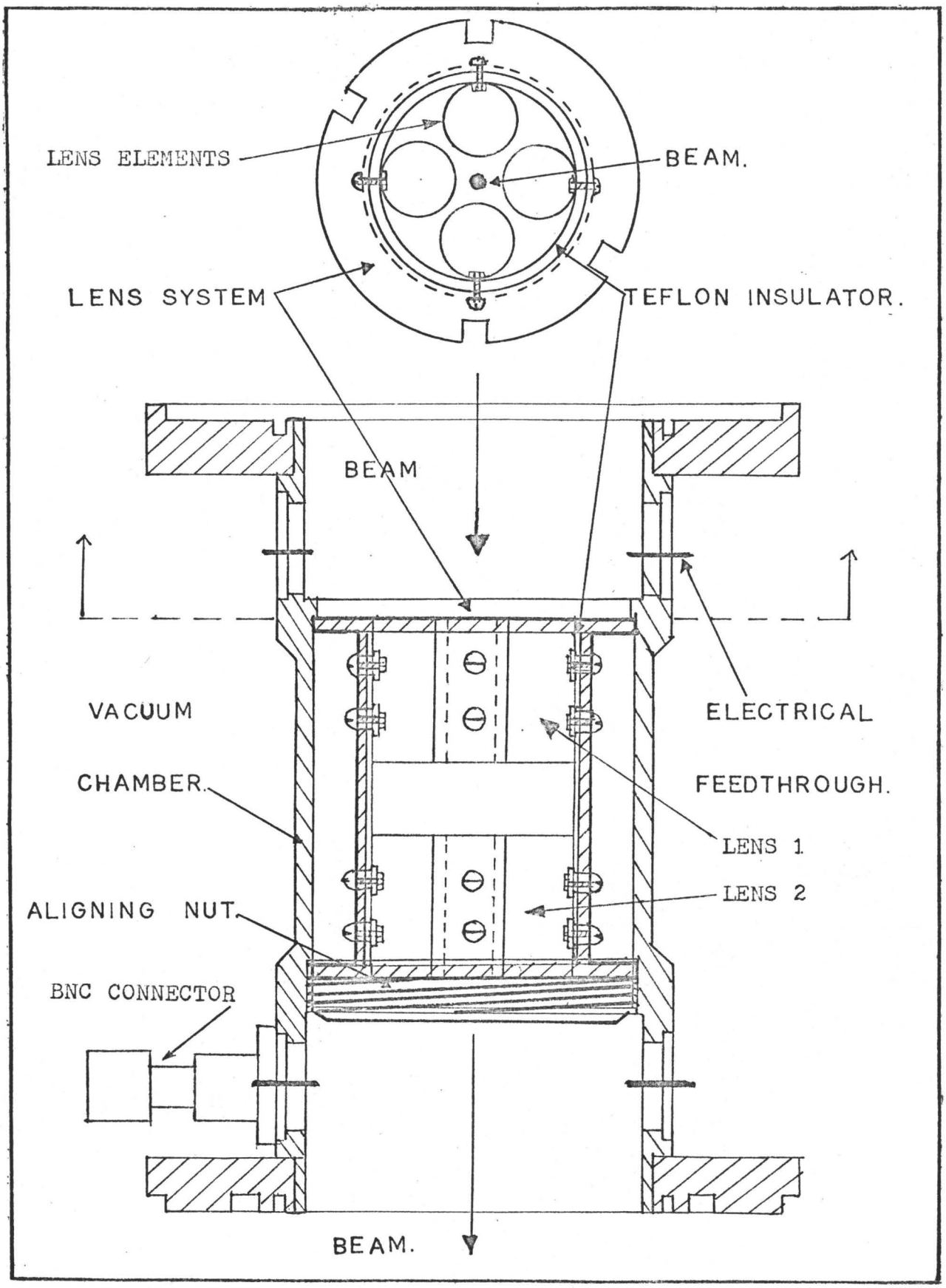

Figure 6

Construction of the quadrupole lens pair

0.25" radius) and still produce a sharp line-focus.

(v) The construction was relatively simple and inexpensive since accurately machined plates were not required.

(vi) The potentials required for a given focal length were calculable. Shun Lu[114] has derived equations relating the design parameters of the lens, and plotted nomographs which allow focal length calculations to be made.

b) Mass Analysis and Alignment

The beam produced from the R.F. hydrogen discharge contained a number of atomic and molecular ions such as H^+, H_2^+, H_3^+, OH^+, and H_3O^+. It was usually necessary to select a beam of the ions of interest and exclude all others. This was done by mass analysis. Three methods of mass analysis are commonly used:

1. Velocity selection
2. Energy selection
3. Momentum selection

Velocity selection may be achieved by applying mutually perpendicular electrostatic and magnetic fields to the ion beam. The forces acting on an ion in the beam are:

$$F = H.q.v$$

and $$F = E.q.$$

where H and E are the magnetic and electric fields, q the charge on the ion, and v the velocity. When the forces balance, the beam travels in a straight line and mass selection is achieved, since ions with different masses, when accelerated through a

given potential, acquire different velocities.

Electrostatic fields may be used to separate beam components having different energies, and magnetic fields to separate components with different momenta. Both these methods involve a change in axis of the beam. Magnetic analysis was used in the apparatus described here. The ion beam was passed through a 4" radius of curvature, 90° sector, mass analyser employing magnetic field scanning. The magnet, manufactured by "Alpha Scientific Laboratories", had a variable pole gap and was water cooled. With a pole gap of 1 cm. the field was variable from zero to 15,000 gauss. Current for the magnet was provided by a 1 kw. current regulated power supply, manufactured by "Alpha Scientific Laboratories". The current stability of the supply was 0.1% of maximum output. The high current stability resulted in high magnetic field stability, which was essential since the beam emerging from the magnetic field was required to travel a distance of about 2 metres before being detected. This meant that any change in magnetic field would result in a pronounced drift of the beam at the detector. The current to the magnet was controlled by a 10-turn potentiometer.

The magnet was mounted on a movable base equipped with levelling screws to permit alignment of the magnetic field. The pole pieces were accurately machined from Armco magnet iron and cadmium plated to prevent corrosion. The beam tube was machined from 1" thick stainless steel plate, and a .062"

stainless steel cover was cut to the shape of the channel and welded on to form the tube. Vacuum flanges were welded at either end and the whole beam tube aligned.

Barber[115] and Stephens et al.,[116][117] have shown that if a slightly divergent beam of ions with the same momentum is passed perpendicularly into a homogeneous magnetic field, between two V-shaped poles, and is bent through such an angle as to leave the field perpendicularly, then the ions will be refocused at a point such that the incident focal point, the apex of the V and the emergent focal point all lie on a straight line. After passing through the emergent focal point, however, the beam again diverges. To prevent this divergence a second quadrupole lens was situated after the mass analyser to refocus the ions to a parallel beam. The lens was also used to convert the ribbon-like beam back to one of circular cross-section. Horizontal and vertical deflector plates were positioned before the lens to correct any misalignment of the beam. The focal length of the quadrupole lens was adjusted to give maximum beam transmission through the charge transfer cell.

4) Charge Transfer Cell

The ion beam entered the charge transfer cell and passed through a region containing a relatively high pressure of either gas (hydrogen or helium), or lithium vapour. The use of a metallic vapour as a charge transfer agent was first suggested by Donnally, who considered the use of cesium vapour for the production of H(2s) atoms from H^+ ions.[118][119]

Charge transfer with lithium vapour was attractive in the present work because its use precluded the need for large capacity diffusion pumps which would be necessary with gases such as hydrogen and helium.

The rudiments of the design of the charge transfer cell were obtained from a publication by Middleton and Adams.(120) Considerable modifications were made to overcome some of the problems found by these workers. The physical arrangement is shown in Fig.7. The ion beam was passed through a canal, 150 mm. long and 5 mm. in diameter, into which the charge exchanging molecules were fed. The canal was held in position by two lava insulators which were machined from Grade A lava, and fired at 2000° F. for 24 hours. The lava was supplied by the "American Lava Corporation". The insulators were designed to allow for expansion of the canal on heating.

A stainless steel oven chamber was attached beneath the canal, and about 10 grams of lithium metal placed in it. This was done in an atmosphere of helium to prevent oxidation of the lithium metal. The vapour produced by heating the chamber passed through a 1/16" diameter hole into the canal. This was performed by radiant heat produced from a coil wrapped around lava insulators which were mounted on the inside of a heat reflector, enclosing the canal and oven assembly. The heat reflector was made from a highly polished stainless steel cylinder cut along the long edge to produce two halves. These halves were removable to permit access to the canal and oven

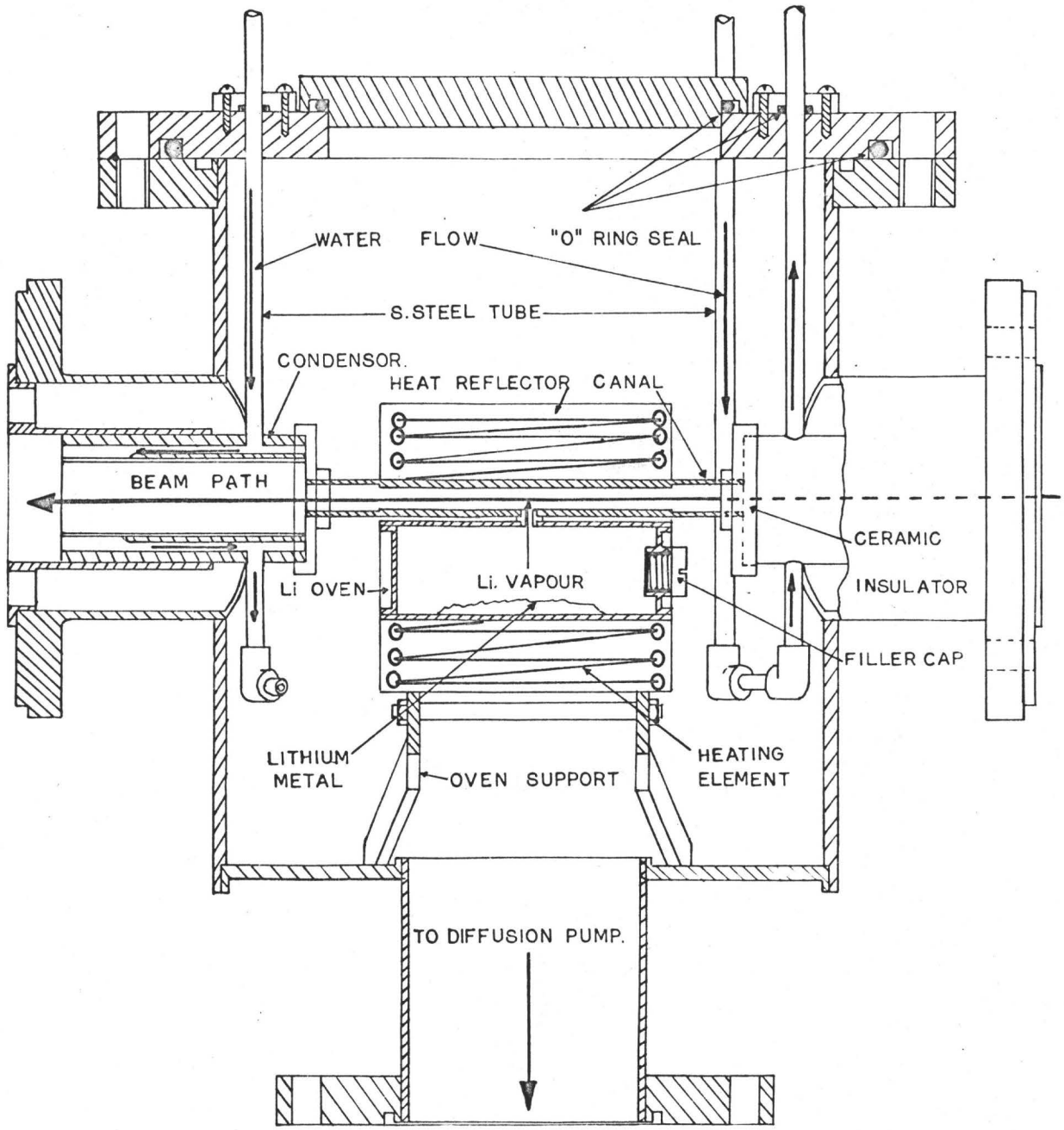

Figure 7

Construction of the charge transfer cell

sections. This allowed replacement of the lithium charge and inspection of the canal.

Water cooled condensors were attached to both ends of the canal to minimize the diffusion of lithium vapour into the rest of the apparatus. They were made by welding together two concentric stainless steel cylinders. Water was carried to and from the condensors by 3/16" stainless steel tubing. Baffles were situated along the length of the cylinders to improve the water circulation. The condensors, together with the canal and oven assembly, were fitted into accurately machined positioning flanges on which the alignment of the canal depended. The rim of each positioning flange was drilled with holes to increase the pumping rate of non-condensible gases.

The whole assembly was placed inside a 6" radius stainless steel vacuum chamber mounted upon a mercury diffusion pump. The pump was used to remove excess gas when non-condensible gases were used for charge transfer. No pumping was required when lithium vapour was used. The top of the chamber was constructed in two parts. The outer ring contained the electrical and water feedthroughs. The inner cap was removable to permit easy access to the canal assembly. The outer ring could be removed if necessary, by disconnecting the electrical and water feedthroughs. High current "Ceramaseal" electrical feedthroughs carried the heater coil current. The water pipes were equipped with 'o' ring vacuum seals.

The beam emerging from the charge transfer cell contained both ions and neutrals. The ions were removed from the beam by applying a -5000 volt potential across the electrostatic deflector plates (Fig.8). The plates were machined from Nichrome steel plate, 1" long by 0.75" wide, and positioned 0.5" apart. They were mounted directly onto low current vacuum feedthroughs welded into a stainless steel ring. The neutral atoms and molecules were naturally unaffected by the electric field and continued undeflected. Rather than attempt to detect and analyse neutrals, it was decided to reionize a fraction of them and study the ions formed by mass analysis.

5) Ionization, Mass Analysis and Detection Systems

a) Ionization

A fraction of the neutral beam was ionized by electron bombardment. Fig.9 shows the arrangement used. The electron source was based on the early design of Bleakney[121][122] and Nier[123-126]. A thoriated tungsten filament, 1 cm. long, was used to produce a stream of electrons across the path of the molecular beam. The ribbon was spot-welded, using nickel sleeves, across two high current vacuum feedthroughs situated in a removable cap. This enabled the assembly to be taken apart and the filament replaced, without disturbing the rest of the apparatus. A plate, equipped with a hole 1 mm. x 10 mm., was positioned 2 mm. from the filament and insulated from the stainless steel ring by alumina spacers. This provided acceleration and collimation of the electron beam.

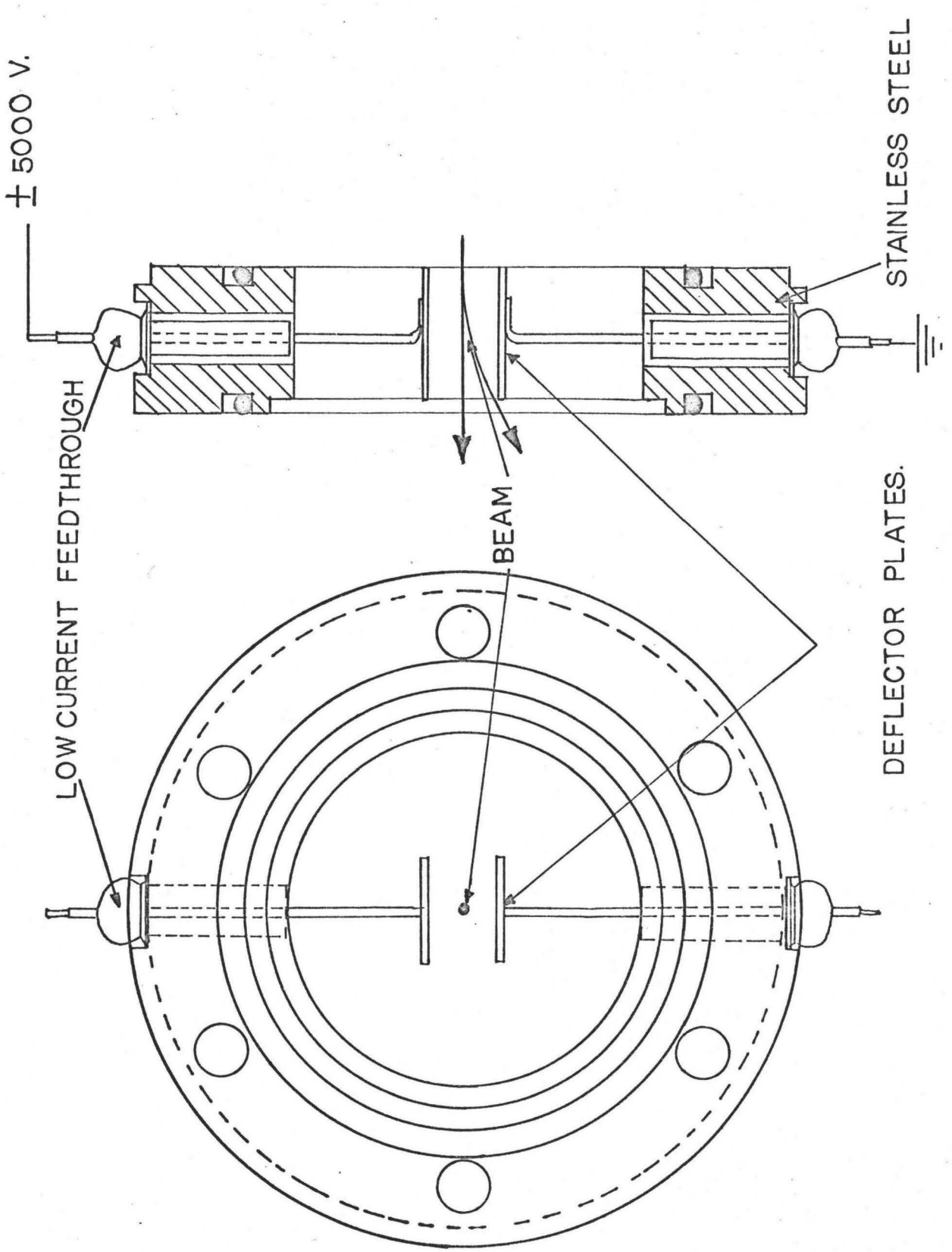

Figure 8

Electrostatic deflector plates

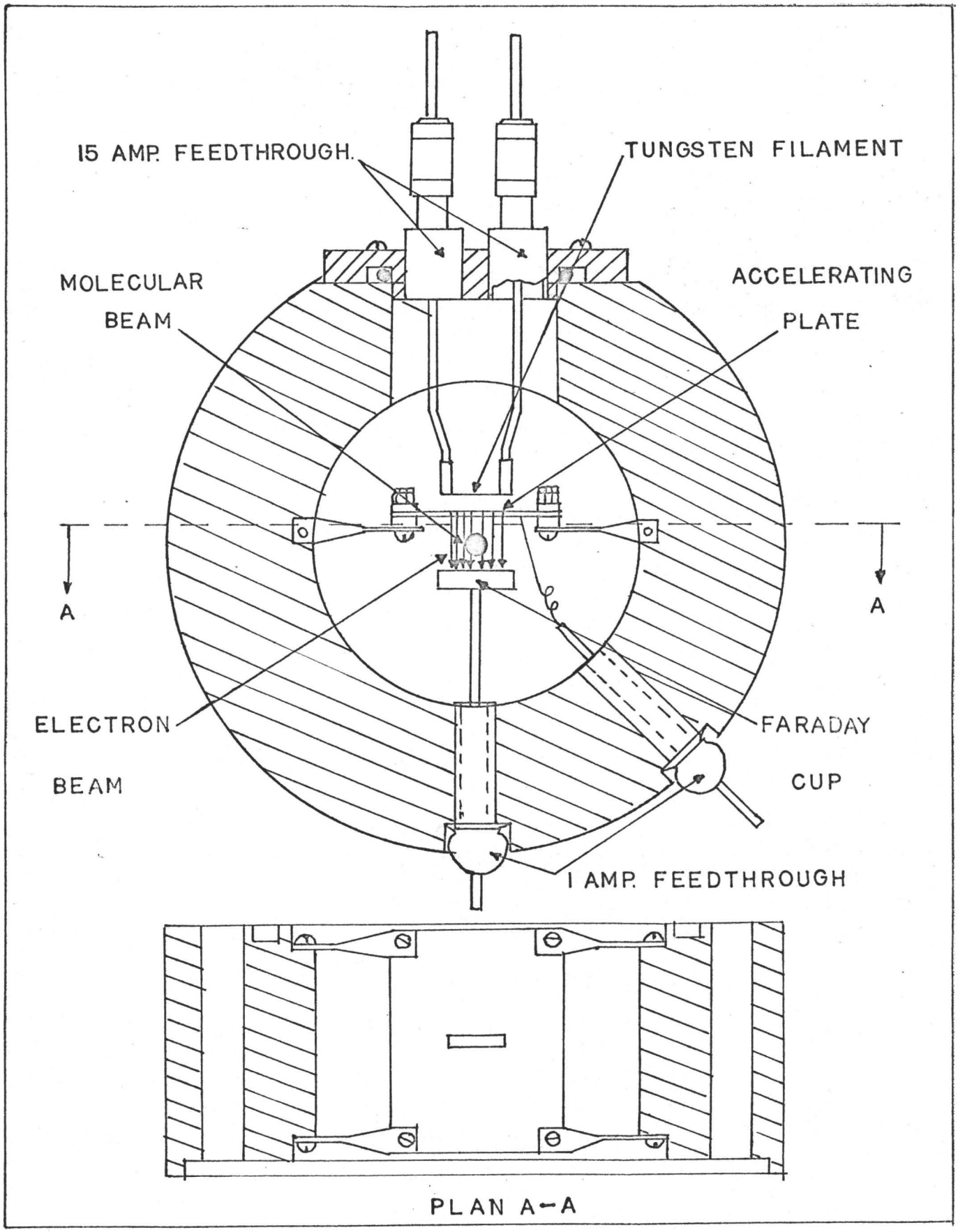

Figure 9

Electron bombardment reionizer

The size of the electron beam ensured that all the neutral beam passed through it. The electrons were collected on a Faraday cup and the trap current measured. The Faraday cup was operated at ground potential and the filament and plate at approximately -100 v. and -70 v. respectively. The small potential difference between the plate and the filament caused the electrons to accelerate through the collimating aperture. Electrical connections for the accelerating plate and Faraday cup were made through terminals in the stainless steel ring. Trap current was measured with a 0 to 1 D.C. milliammeter. Filament currents of 3 to 5 amperes were used to produce trap currents up to 1 ma.

b) Mass Analysis

Analysis of the ions produced was carried out using a 4" radius of curvature, 90^{o} sector, magnetic mass analyser, similar to the first mass analyser. The power supply used was not so highly regulated as was the first, since it was necessary only to scan the beam across a detector. In earlier work, no slit system was used on either mass analyser. Later, however, the introduction of a relatively crude slit system into the second analyser was found to improve the peak shapes. The slits had a calculated resolving power of 50. The resolving power d_m of the analyser is defined by $d_m = m_o/\triangle m_o$ for just resolvable peaks of masses m_o and $m_o + \triangle m_o$. In this mass analyser, d_m is given by $d_m = r/(S_o + S_c)$, where r is the radius of curvature and S_o and S_c are the object and image

slit widths. In this case, r = 10 cm. and $S_o = S_c =$ 1 mm., giving a resolving power of 50.

The beam tube in the second analyser was similar to that in the first, but was designed to permit beams to be detected in the straight-through position in the absence of a magnetic field. This arrangement permitted alignment of the beam selected by the first mass analyser.

c) Detection Systems

Three types of detectors have been used to monitor neutral and ion beams in this apparatus. The earliest was an adapted cathode ray tube, shown in Fig.12. The soda glass of the tube was cemented to a 2" diameter Pyrex-Kovar graded seal using "Armstrong" epoxy resin. This resulted in a strong vacuum-tight seal. A vacuum flange was then welded to the Kovar metal. The Pyrex tube was equipped with a ground glass joint containing an electrical feedthrough. Connected to the inside of the feedthrough was a metal disc which allowed approximate measurement of the beam intensity to be made. The disc could be removed from the beam path by rotating the lower part of the joint. This allowed visual inspection of the beam profile on the cathode ray screen. It was possible to observe the beam shape continuously while focusing adjustments were carried out. Eventually, however, the cathode ray screen darkened and had to be replaced by a second viewing system, shown in Fig.10.

Scintillator discs, manufactured by "Phillips Corporation" for use with an X-ray diffraction apparatus, were used in place

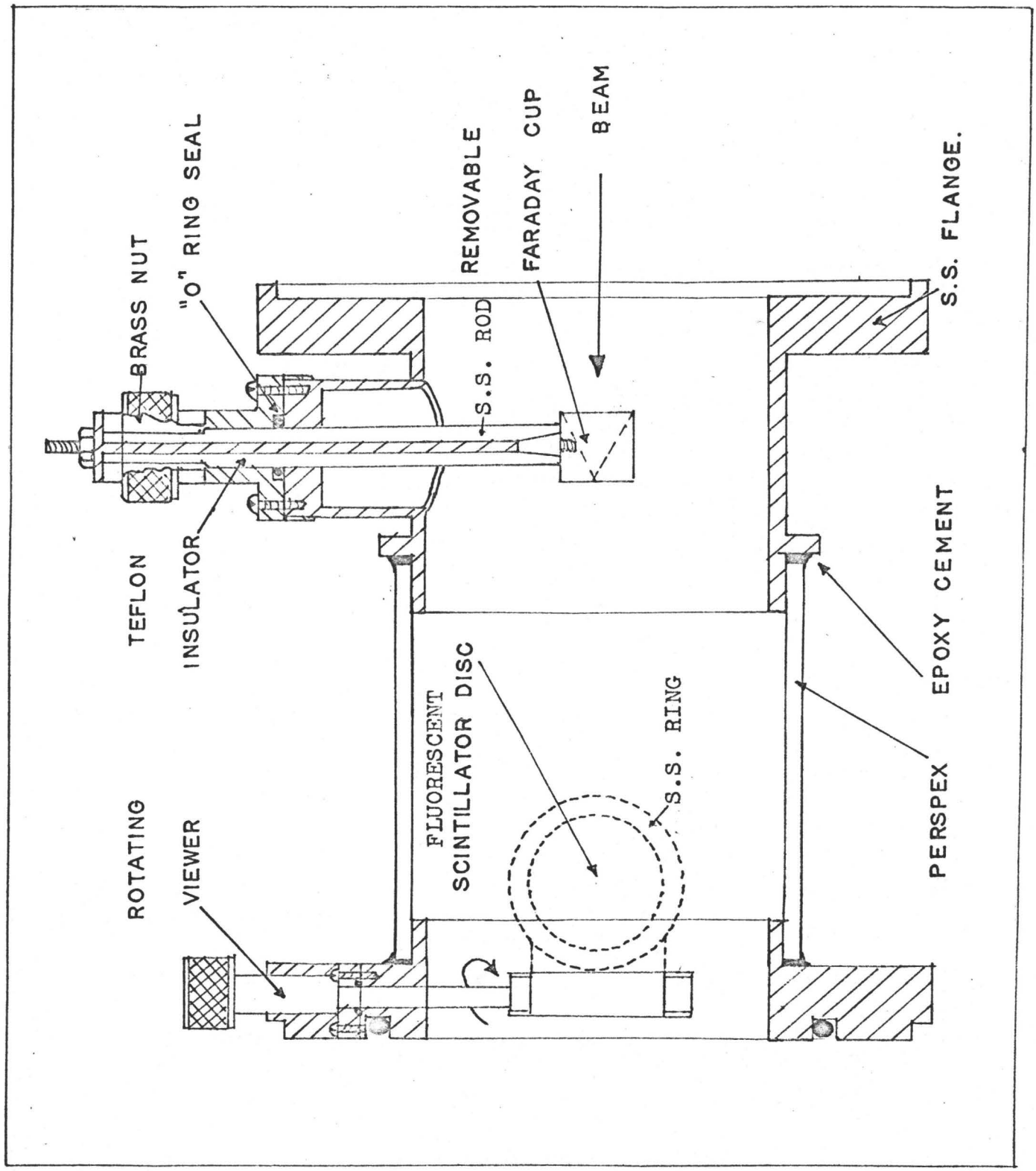

Figure 10

Beam detector unit employing a scintillator disc and a Faraday cup

of the cathode ray screen. The fluorescence produced by the impact of the beam was clearly visible in a darkened laboratory and the lifetime of the discs was much longer than that of the cathode ray screen, so that replacement was very infrequent. The 1" diameter discs were mounted between two stainless steel rings attached to one end of a movable rod. The other end of the rod emerged from the vacuum system through an 'o' ring seal. By means of this rod it was possible to rotate the fluorescent target through 90° and thus remove it from the beam path when required. To allow observation of the target, a Perspex tube, 2½" in diameter and 3" long, was bonded to the flange with epoxy cement. As the beam travelled the length of the perspex cylinder, the path followed was clearly visible due to the light emitted during collisions with background molecules.

At the other end of the viewing tube, a vacuum flange, containing a removable Faraday cup, was attached. The cup was cut from a stainless steel rod ½" long by ½" in diameter. A 45° cone was drilled in the end to form a cup and thus reduce the loss of secondary electrons emitted by the target on ion impact. The cup was mounted on a tapered stainless steel rod which was insulated from the metal flange by a Teflon sleeve. A tightening nut, outside the vacuum, was used to draw the rod into the Teflon sleeve and form a vacuum-tight seal. The cup-holder emerged from the vacuum through an 'o' ring seal, which permitted the cup to be withdrawn from the beam path. The

flanges on the detector unit permitted it to be placed in various positions in the apparatus. This enabled the beam to be focused and aligned at a number of different points along the beam path. By removing the viewer and cup, the beam was allowed to continue through the rest of the apparatus.

Quantitative measurements of beam intensity were made with the Faraday Cup, shown in Fig.11. Two detectors of this type were used on the final apparatus, shown in Fig.1. The cup was made from a single sheet of Nichrome metal and shaped so as to minimize electron loss. It was spot-welded onto a Nichrome disc so that the entrance to the cup lay in the beam path. Immediately in front of the cup, a bias plate with a 5 mm. entrance aperture was attached. Secondary electron emission was suppressed by placing a negative potential on this plate. Two further plates were used to collimate the beam. The plates were held in position by four support rods screwed into the base flange. Insulation between the discs and the support rods was provided by alumina sleeves. Sleeves of larger diameter fitted around the inner sleeves and served to accurately align the plate system.

Electrical terminals were soldered into the base flange to carry voltage to the repeller plate and measure the beam current from the cup. B.N.C. coaxial connectors were attached to the terminals. Electrical connections inside the vacuum were made with Nichrome wire surrounded by glass sleeves to prevent accidental grounding. Beam currents were measured with

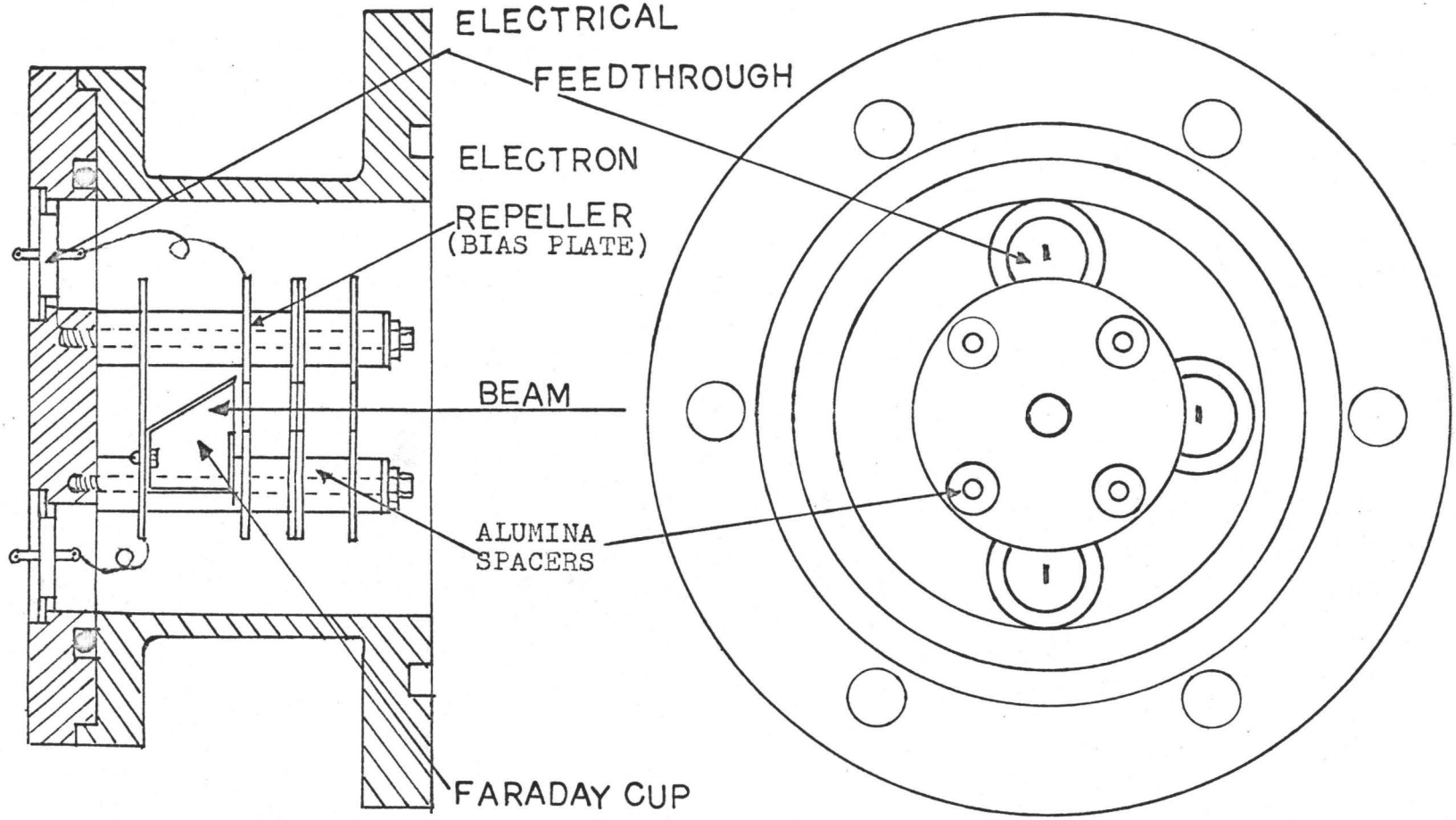

Figure 11

Faraday cup detector

a "Keithley" electrometer, capable of measuring currents down to 10^{-14} amp. A permanent record of beam intensities was obtained with a "Mosely" strip-chart recorder. A switching device permitted currents from both Faraday cups to be measured.

6) Electronics

The problems associated with background currents produced by the Radio-Frequency oscillator, caused considerable difficulty in the early work. In particular, circuitry used to measure beam intensity, picked up R.F. induced currents which were greater than the beam currents to be measured. A number of steps were taken to alleviate this problem. (1) The R.F. oscillator and ion source were enclosed in a grounded Faraday cage. (2) Coaxially shielded cable was used for all connections to the apparatus. (3) The cables connecting the detectors to the electrometer were made as short as possible to minimize the induced currents. (4) All ground connections were made at the same point to eliminate "ground-loops". These precautions reduced the problems to a manageable level.

Much of the electronic circuitry used with this apparatus was designed and built in the laboratory, exceptions being the Radio-Frequency oscillator and the 10 K.V. high voltage supply. The electronics which were built followed standard circuit designs[127] and, in general, circuit diagrams are not shown. A brief description of the electronic circuitry used is as follows.

(a) Radio-Frequency Oscillator and Power Supply

The push-pull R.F. oscillator consisted of two 829 B power tubes. The plates of the two oscillator tubes were capacitatively coupled to the ion bottle by the two excitor rings. The power delivered to the ion bottle was approximately 120 watts, and the frequency of the oscillator approximately 60 megacycles $sec.^{-1}$. The oscillator power supply employed full wave rectification using solid state rectifiers. The power supply had a choke input filter and the output voltage was variable up to 900 v.

(b) High Voltage Supply

High voltage for the acceleration of the ion beam was provided by a high voltage (10,000 v. D.C.) supply, manufactured by "The John Fluke Manufacturing Company". It was capable of providing an output of 0 to 10,000 volts D.C. at 0 to 10 milliamperes. The output was fed through two parallel series of resistors to ground. Variable high voltage was taken from these potential dividers to operate the extraction and focusing devices. 10-turn potentiometers provided continuously variable voltages. All potentials in the ion source were made positive with respect to ground.

(c) Solenoid Power Supply

The solenoid power supply employed a full-wave rectifier circuit. The output was adjustable from 0 to 35 volts at approximately 3 amp.

(d) Palladium Leak Supply

The palladium leak supply consisted of a simple step-down filament transformer which provided an output voltage variable from 0 to 6.3 volts A.C. at 1 amp.

(e) Quadrupole Lens Supply

Voltage for the lens elements of each quadrupole lens was provided by a D.C. power supply, manufactured by "The Hewlett Packard Company". The output was variable from 0 to 320 volts at 0.1 amp. The output was passed through two 10-turn potentiometers in parallel to provide voltages for the elements of each lens.

(f) Lithium Oven

The supply for the heater coil of the lithium oven consisted of a step-down filament transformer which provided an output voltage variable from 0 to 50 volts A.C.

(g) Deflector Plates

Voltages for the deflector plates were provided by a 0 to $\pm$ 5,000 volt full-wave rectified high voltage supply.

(h) Reionizer

The filament supply was a 0 to 12 volt - 0 to 10 amp. full-wave rectified D.C. supply. Accelerating potentials were provided by a 0 to 100 volt half-wave rectified D.C. supply.

CHAPTER 4

OPERATION AND PERFORMANCE OF THE APPARATUS

During construction of the apparatus, a number of different experimental arrangements were used to investigate the behaviour of the various components. Two of these are shown in Fig. 12. In all experiments, the procedure for obtaining an ion beam from the source was the same. The apparatus was pumped down to a static pressure of 1×10^{-6} mm. Hg. The gas to be ionized was slowly fed into the ion bottle until the pressure in the beam tube was about 2×10^{-5} mm. Hg. The pressure in the ion bottle was then estimated to be about 20 microns. A radio-frequency discharge was produced and left running for two hours to permit out-gassing from the walls of the ion bottle. A beam of ions was then produced from the discharge by slowly increasing the voltages on the extractor plate, base plate and gap lens simultaneously.

Fig. 13 shows the arrangement used to determine the optimum source-operating conditions. The intensity of the ion beam striking the gap lens was measured with a 0 to 1 D.C. milli-ammeter. The flow of gas into the discharge was varied until maximum beam current was obtained. This pressure was then maintained while the solenoid current and r.f. ring spacing were adjusted for maximum beam current. Once this operation

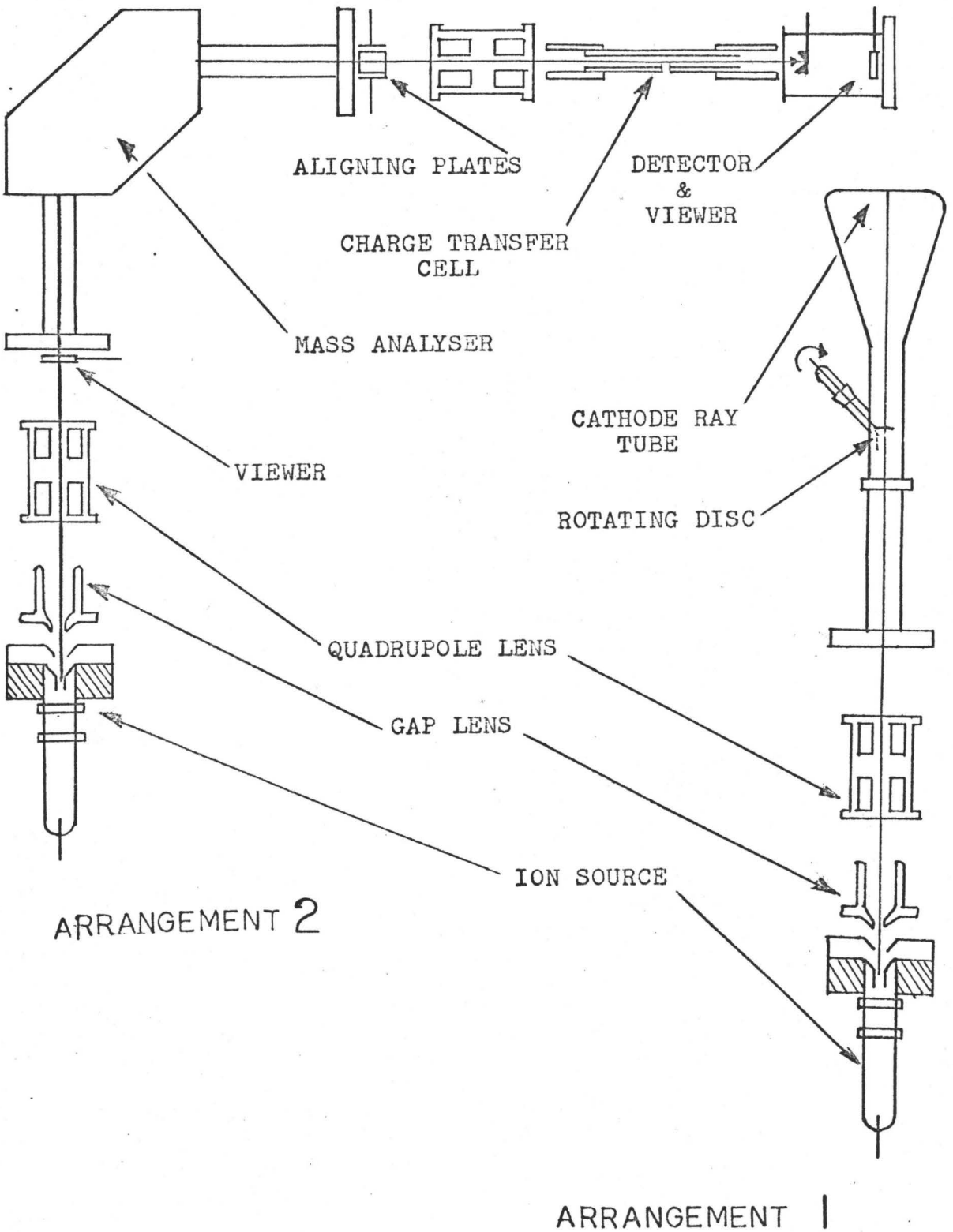

Figure 12

Experimental arrangements to investigate beam characteristics

had been carried out, the ring spacing was maintained throughout all further adjustments.

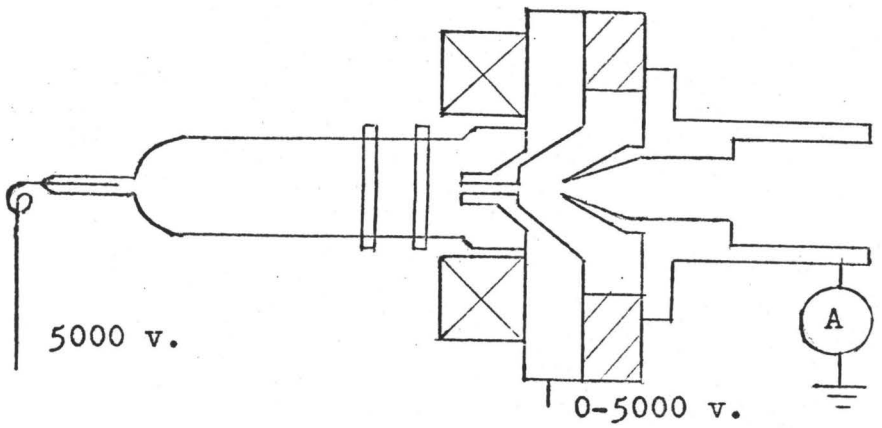

Experimental arrangement to investigate optimum source-operating conditions

Figure 13

The total beam current was found to depend on a number of variable parameters including gas pressure in the source, extraction potential, focusing potential, r.f. power, quadrupole lens potentials, and gas pressure in the charge-transfer cell. Table II shows typical operating conditions for the production of an ion beam from a hydrogen discharge.

The effects of various parameters on the beam will be discussed individually. All data shown are for beams produced from a hydrogen discharge.

1) Pressure Dependence.

The variation of the total beam intensity as a function of gas pressure in the ion source, was investigated with the apparatus in arrangement 2 as shown in Fig. 12. The pressure in the discharge was not measured directly but was estimated from measurement of the pressure in the beam tube. The pressure

Table II

Optimum Operating Conditions

Total beam energy	5000 ev.
Extraction potential	2800-3000 v.
Gap lens potential	1300 v.
Ion source pressure	10-30 microns
Pressure in beam tube	$1\text{-}3 \times 10^{-5}$ mm. Hg
Solenoid voltage	10 v.
R.f. ring spacing	22mm.
Oscillator power	100 watts
Gas leak rate	20 atm. $cm.^3$ $hour^{-1}$
H^+ beam current	22.5×10^{-6} amp.
H_2^+ beam current	39.0×10^{-6} amp.
H_3^+ beam current	14.0×10^{-6} amp.
Total hydrogen beam	75.5×10^{-6} amp.

was controlled by varying the gas flow into the ion bottle and the resulting beam detected at the Faraday cup and measured with an electrometer. Table III shows the data obtained with 4 kev. and 5 kev. energy hydrogen beams. These data are plotted in Figures 14 and 15.

As may be seen, maximum beam intensities were obtained at higher gas pressures. This may be due to the increased probability of collision between ions and molecules at higher pressures, resulting in higher ionization efficiency. At a pressure of about 3.5×10^{-5} mm.Hg. the discharge became unstable, thus imposing a limit on the pressure at which the source could be operated. The generally higher beam intensities at 5 kev. energies may be due to more efficient extraction at higher voltages and to increased scattering of the 4 kev. beam caused by space-charge effects and collisions with background gas. Beams produced with 6 kev. energy were more intense than with 5 kev., but insulation problems in the source precluded the regular use of voltages higher than 5000v.

2) Dependence on Extraction Potential

Optimum extraction conditions were determined with the experimental arrangement shown in Fig. 13. The extraction potential was varied from 0 to 5000 volts by maintaining a potential of 5000 volts on the extractor probe and varying the base-plate potential from 5000 to 0 volts. The beam current was maximized at each extraction potential and subsequently collected on the gap lens and measured with an electrometer. The results obtained with a 5000 ev. beam from a hydrogen

Table III

Variation of beam intensity with pressure.

5 kev.		4 kev.	
Pressure (10^{-5}mm.Hg.)	Total beam current (10^{-6} amp.)	Pressure (10^{-5}mm. Hg.)	Total beam current (10^{-6} amp.)
1.3	8	1.3	20
1.4	9	1.4	26
1.5	11	1.5	30
1.6	15	1.65	34
1.8	21	1.8	37
2.0	32	2.0	40
2.4	60	2.4	43
3.0	74	2.8	44
3.3	75	3.0	44
		3.3	44

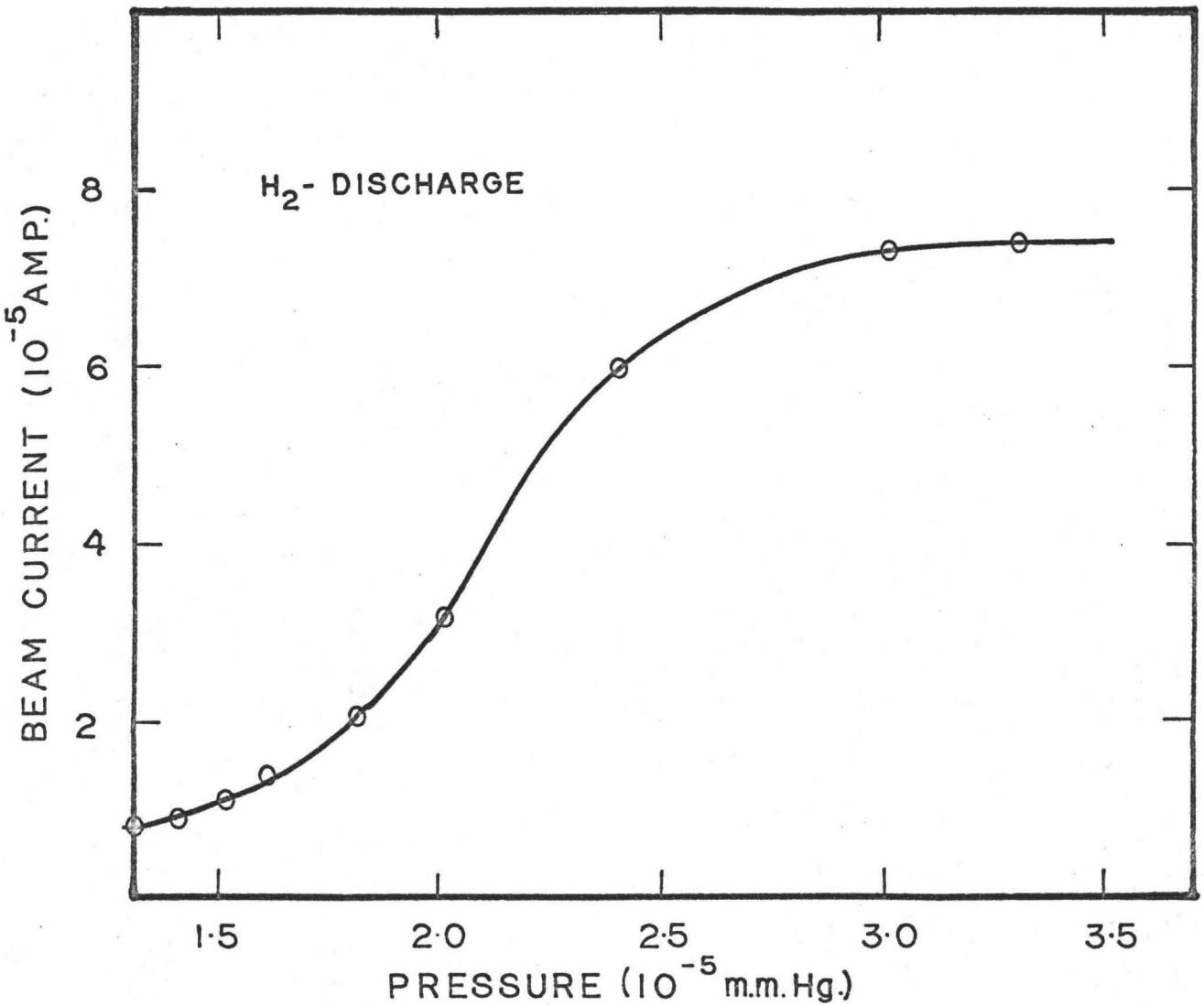

Figure 14

Variation of 5 kev. beam current with pressure

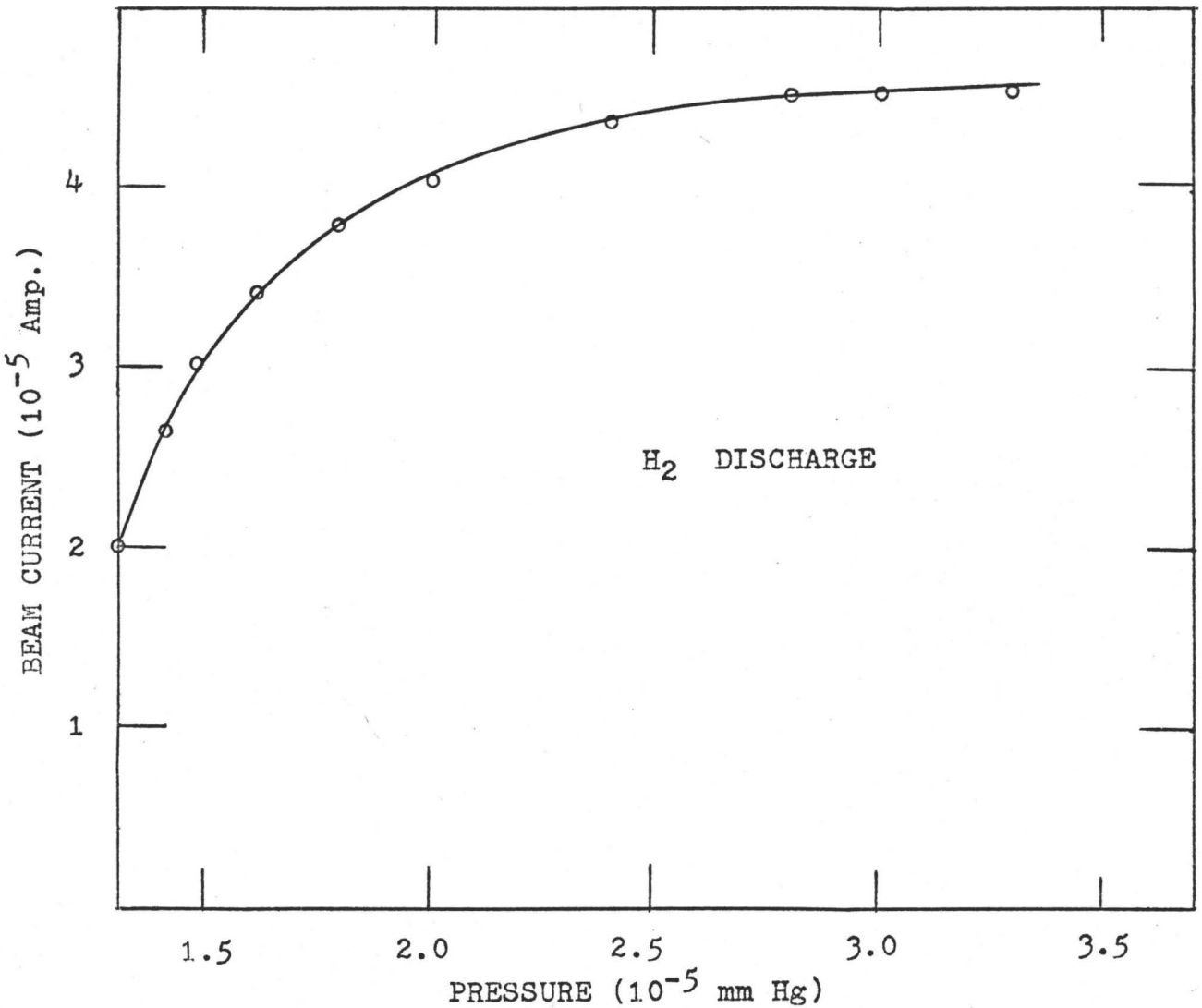

Figure 15

Variation of 4 kev. beam current with pressure

discharge are shown in Table IV. The data are plotted in Fig.16 where it may be seen that maximum beam current was obtained with an extraction potential of about 2800 to 3000 volts. During normal operation of the apparatus, a potentiometer device in the high-voltage divider system permitted fine adjustment of the extraction potential to obtain maximum beam intensity.

3) Variation in Beam Composition with Pressure.

The pressure of hydrogen gas in the discharge was varied by changing the leak rate and an indication of the source pressure obtained by measuring the pressure in the beam tube. The composition of the beam was found by mass analysis using arrangement 2 shown in Fig.12. The intensity of each component of the beam was maximized at each pressure setting and the current measured at the Faraday cup. The data obtained with 4 kev. and 5 kev. beams are shown in Table V, and plotted in Figs. 17 and 18.

Using these data it was possible to select the optimum pressure for the production of a particular ion. Generally, the beam intensities increase with pressure with the exception of the H_2^+ ion beam, whose intensity reaches a maximum and then decreases. This may be due to H_2^+ ions reacting to form H_3^+ ions in the discharge:

$$H_2^+ + H_2 \longrightarrow H_3^+ + H$$

Varney[85] has measured the rate constant for this reaction and found it to be high. Hasted[55] has reported that hydrogen glow-discharges at very high pressure (500 microns) contain

Table IV

Variation of beam intensity with extraction potential

Extraction potential (volts)	Beam current (10^{-6} amp)
0	0
350	0
600	0
850	1
1100	1
1325	2
1600	4
1800	10
2050	40
2325	75
2550	100
2800	125
3025	135
3250	125
3425	100
3650	100
3875	85
4100	80
4325	75
4500	75
4750	70

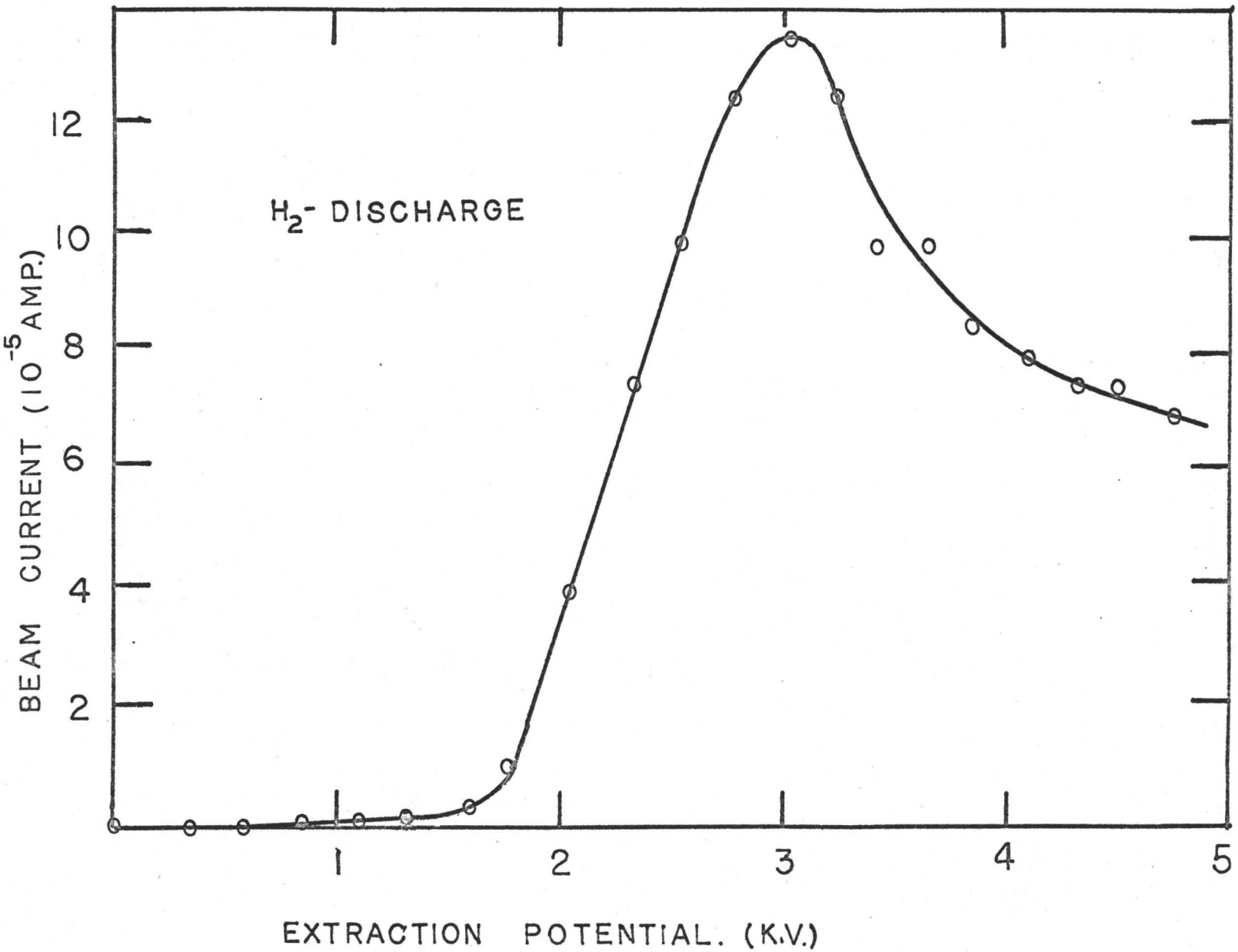

Figure 16

Variation of beam current with extraction potential

Table V

Variation of beam composition with pressure

Pressure (10^{-5}mm.Hg.)	Beam intensity (10^{-6} amp.)			Pressure (10^{-5}mm.Hg.)	Beam intensity (10^{-6} amp.)		
	H^+	H_2^+	H_3^+		H^+	H_2^+	H_3^+
1.3	3	16	1	1.0	2	6	1
1.4	4	21	2	1.3	3	10	1
1.6	5	24	3	1.5	4	12	2
2.0	9	25	6	1.6	4	14	2
2.4	12	22	8	2.0	6	22	4
2.95	14	18	10	2.5	16	34	7
3.3	15	17	11	2.7	24	38	9
				2.8	25	39	12
				3.3	31	29	16
	4 kev.				5 kev.		

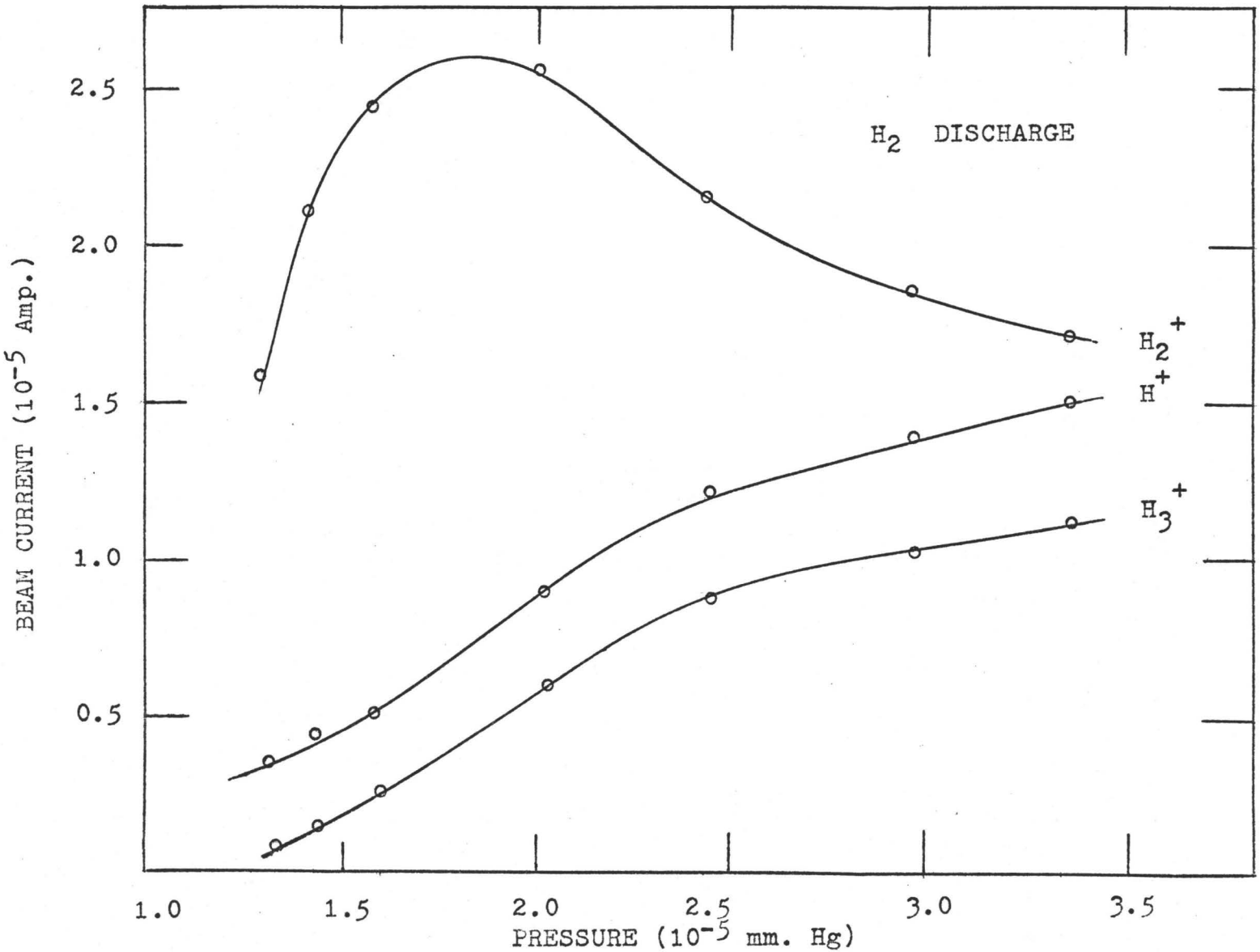

Figure 17

Variation of beam composition with pressure (4 kev.)

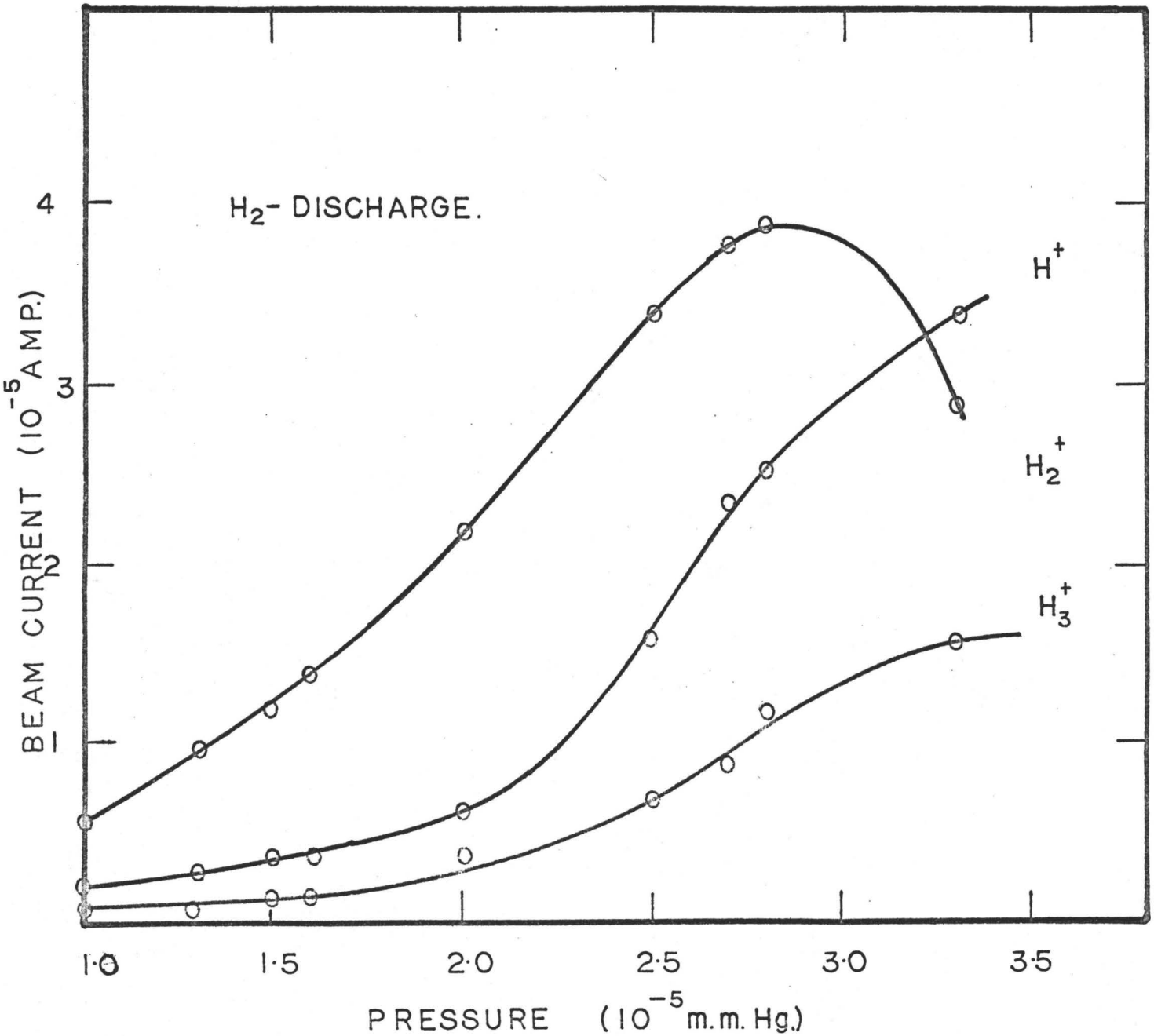

Figure 18
Variation of beam composition with pressure (5 kev.)

about 80% H_3^+ ions. It seems reasonable, therefore, that the increase in H_3^+ and the decrease in H_2^+, with increased pressure, may be understood in terms of this reaction. H^+ ions may be produced by ionization of H atoms produced by this reaction, and also by dissociative ionization of H_2.

$$H_2 + e \longrightarrow H^+ + H + 2e$$

Both mechanisms would be expected to have increased rates with an increase in H_2 pressure, as was found.

4) Quadrupole lenses

The focusing action of the quadrupole lens was first investigated using the cathode ray screen shown in arrangement 1 Fig 12. It was found that a 10 mm. diameter beam entering the lens, could be focused to a 1mm. by 2mm. rectangle at a distance of 60cm. Similar results were obtained when X-ray target discs replaced the cathode ray screen. With the apparatus set up as in Fig 1, the potentials on the two quadrupole lens pairs were adjusted to give maximum beam intensity at the detector. The focal lengths from the first lens to the mass analyser and from the second lens to the charge transfer cell were then 4" and 15" respectively. Using these values the lens potentials were calculated using the matrix formulation of Teng[113]. Good agreement was obtained as shown in Table VI. The discrepancies are easily understood in terms of the uncertainty in the fringing fields of the magnets and quadrupole lenses.

Table VI

Calculated and experimental quadrupole lens voltages

First lens pair	Focal length 4".	
	Experimental	Calculated
lens 1	54 v.	51 v.
lens 2	42 v.	39 v.
Second lens pair	**Focal length 15".**	
	Experimental	Calculated
lens 1	38 v.	34 v.
lens 2	27 v.	24 v.

5) Mass Analysis of the Discharges.

In order to calibrate the first mass analyser, a number of mass spectra were obtained from discharges containing hydrogen, helium, and deuterium, with the apparatus in arrangement 2 shown in Fig. 12.By allowing traces of air to enter the discharge, it was possible to produce beams of molecules having molecular weights up to about 50.By comparing the positions and intensities of peaks from different discharges, it was possible to build up a mass-calibration curve which allowed unknown peaks to be identified. The mass spectrum obtained from a hydrogen discharge together with air impurities is shown in Fig. 19. The identification and typical intensities are shown in Table VII. The intensities of impurity peaks depend on the pressure of air in the discharge and may vary considerably. Molecules with molecular weights above 20 have been identified but are not shown in Fig. 19.

Because of the nature of the radio-frequency discharge, a number of molecular ions are produced by ion-molecule reactions in the discharge which are not normally found in ordinary mass-spectra. For example, relatively intense beams of H_3^+, CH^+, NH^+, and H_3O^+ are found.

The mass spectrum of a deuterium discharge was obtained in the same way and is shown in Fig. 20. Table VIII shows the assignments and relative intensities of the peaks. Peaks corresponding to deuterium-containing ions show the appropriate shift in the spectrum when compared with hydrogen-containing

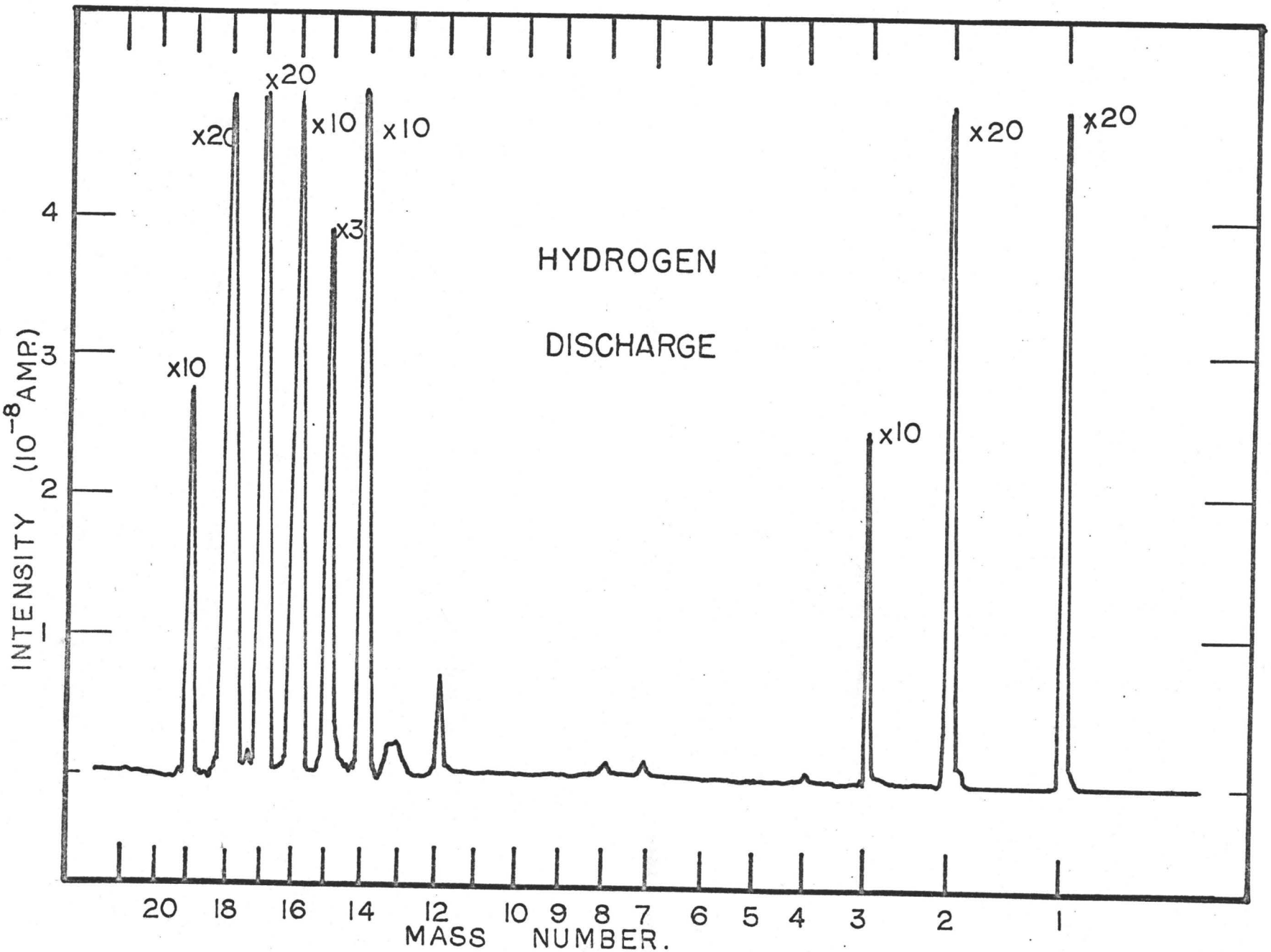

Figure 19
Mass spectrum of a hydrogen discharge

Table VII

Mass spectrum of a hydrogen discharge

Mass	Identity	Typical Intensity (10^{-7} amp.)
1	H^+	2
2	H_2^+	2
3	H_3^+	1
4	D_2^+	0.005
7	N^{2+}	0.01
8	O^{2+}	0.01
12	C^+	0.1
13	CH^+	0.05
14	N^+	1.0
15	NH^+	0.3
16	O^+	1.0
17	OH^+	2.0
18	H_2O^+	2.0
19	H_3O^+	1.0
28	N_2^+	1.0
29	$^{15}NN^+$	0.01
30	NO^+	0.1
31	$^{15}NO^+$	0.01
32	O_2^+	0.1
44	CO_2^+	0.1

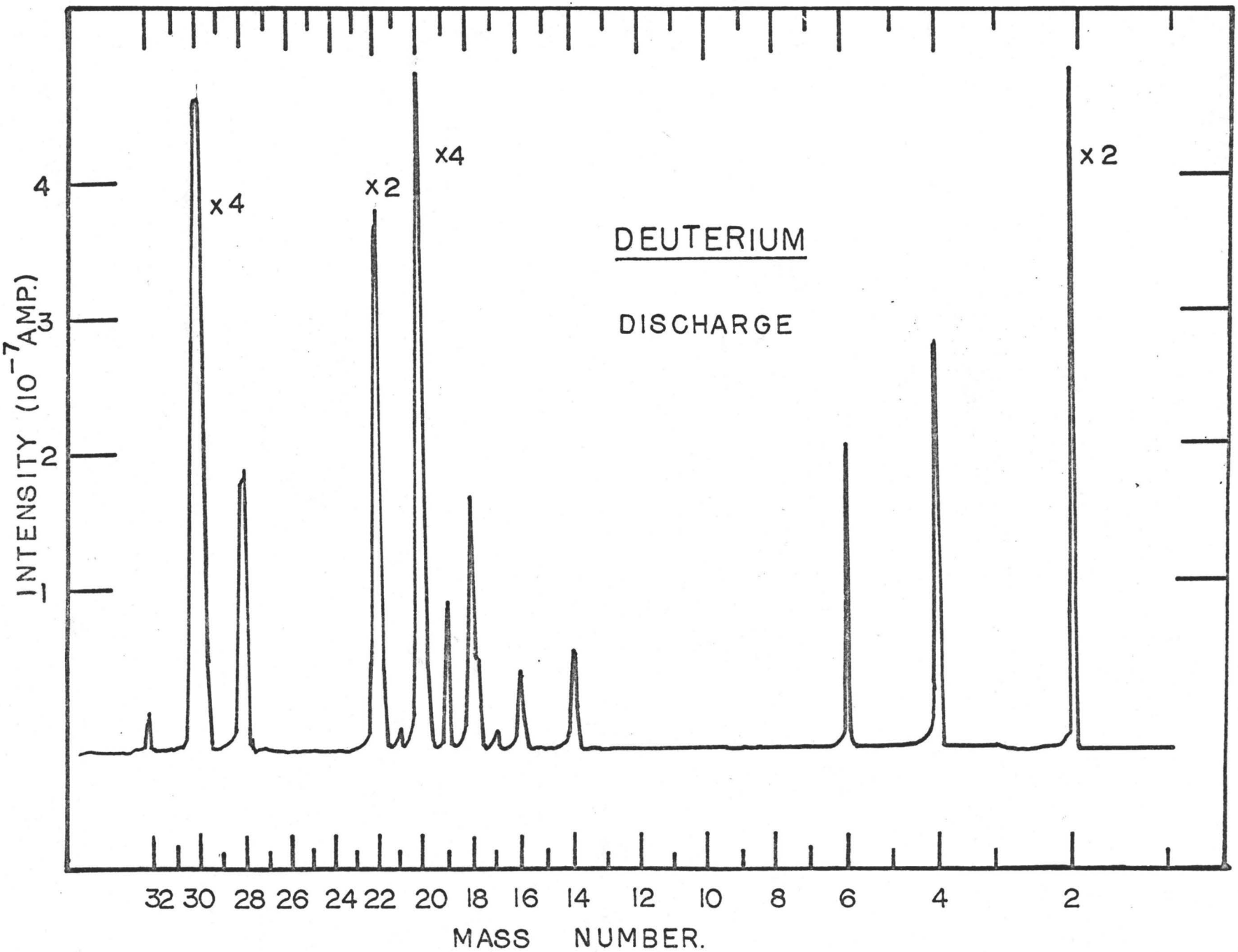

Figure 20 Mass spectrum of a deuterium discharge

Table VIII

Mass spectrum of a deuterium discharge

Mass	Identity	Typical Intensity (10^{-7} amp.)
1	H^+	0.05
2	D^+	10.0
3	HD^+	0.05
4	D_2^+	3.0
5	D_2H^+	0.05
6	D_3^+	2.5
7	N^{2+}	0.01
8	O^{2+}	0.01
12	C^+	0.01
14	$N^+(CD^+)$	1.0
16	$O^+(ND^+)$	1.0
17	OH^+	0.2
18	OD^+	2.0
19	HDO^+	1.0
20	D_2O^+	20.0
21	D_2HO^+	0.2
22	D_3O^+	8.0
28	N_2^+	2.0
30	NO^+	20.0
32	O_2^+	0.2
44	CO_2^+	0.2

ions. This enabled positive identification to be made of these peaks. For example, the peak at mass 17, representing OH^+ in the hydrogen spectrum, corresponds to mass 18 (OD^+) in the deuterium spectrum. Similarly, H_2O^+ (mass 18) corresponds to D_2O^+ (mass 20), and H_3O^+ (mass 19) corresponds to D_3O^+ (mass 22). In addition, "mixed" water molecule ions such as HDO^+ and D_2HO^+ are produced in the deuterium discharge.

Figure 21 shows the mass spectrum obtained from a helium discharge containing traces of hydrogen and air. Table IX shows the identification and relative abundances of each ion. The peaks corresponding to air impurities (N^+, O^+, N_2^+ and O_2^+ e.g.) are of the same order as those found in the hydrogen discharges, whereas the peaks corresponding to OH^+, H_2O^+, and H_3O^+ are a factor of 10 lower. This suggests that the water molecule ions may be produced by ion-molecule reactions in the hydrogen discharges, since the intensities would be expected to be approximately constant in both the hydrogen and helium discharges. Similarly, large amounts of OD^+, D_2O^+, and D_3O^+ are produced in the deuterium discharge, which suggests that these ions are formed by ion-molecule reactions rather than by direct ionization of water molecules, in which D_2O is present in only trace quantities.

The peak at mass 20 in the helium discharge has been assigned to $^{40}Ar^{2+}$ rather than $^{20}Ne^+$ because, if ^{20}Ne were present, a peak corresponding to $^{22}Ne^+$ would also be expected. The natural abundances are 8% (^{22}Ne) and 90% (^{20}Ne). Further

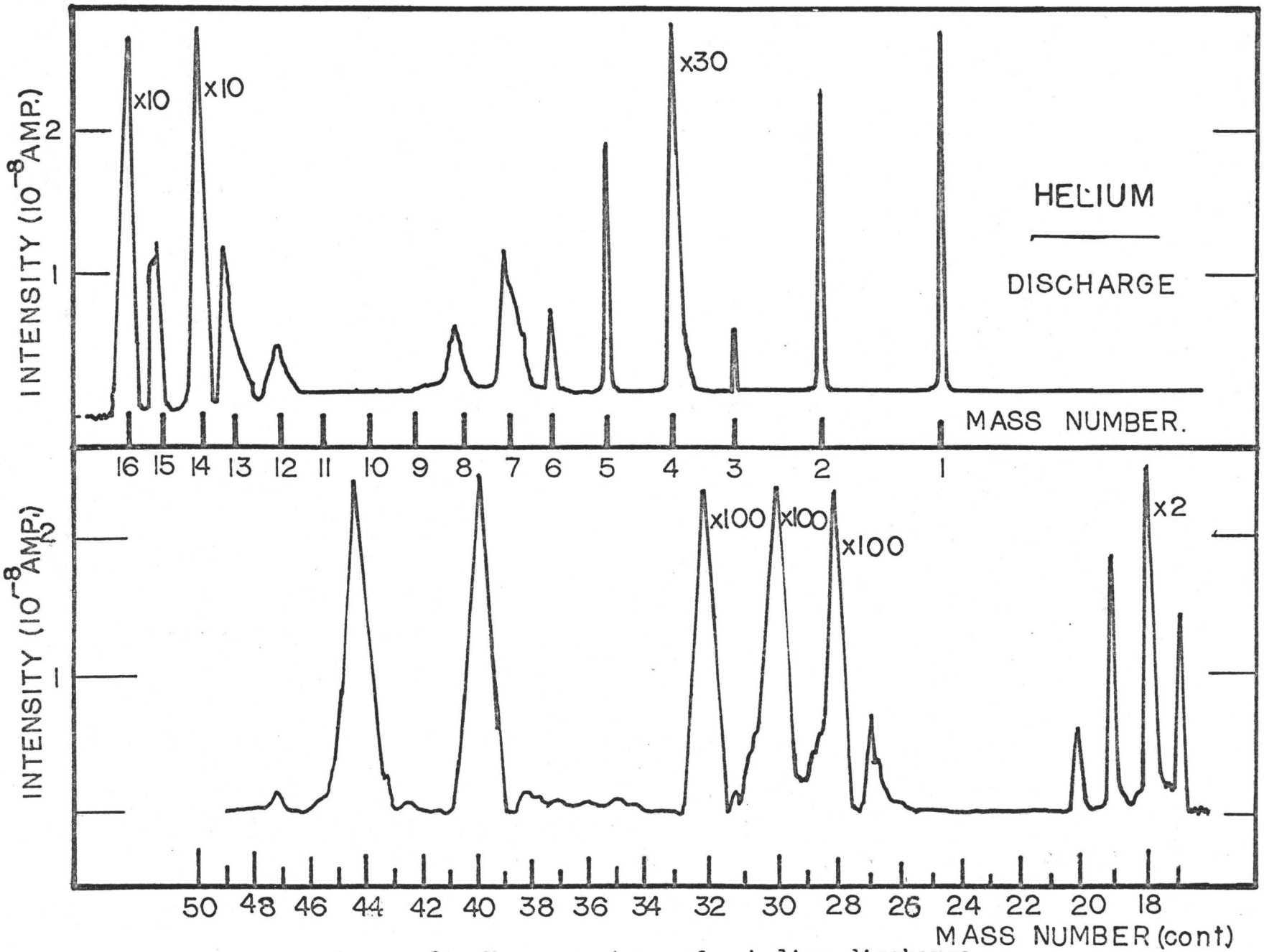

Figure 21 Mass spectrum of a helium discharge

Table IX

Mass spectrum of a helium discharge

Mass	Identity	Typical Intensity (10^{-7} amp.)
1	H^+	0.3
2	H_2^+	0.3
3	H_3^+	0.05
4	He^+	3.0
5	HeH^+	0.2
6	C^{2+}	0.05
7	N^{2+}	0.1
8	O^{2+}, He_2^+	0.05
12	C^+	0.03
13	CH^+	0.1
14	N^+	3.0
15	$^{15}N^+, NH^+$	0.1
16	O^+	3.0
17	OH^+	0.15
18	H_2O^+	0.5
19	H_3O^+	0.2
20	Ar^{2+}	0.05
28	N_2^+, CO^+	30.0
30	NO^+	30.0
32	O_2^+	30.0
40	Ar^+	0.3
44	CO_2^+	0.3

evidence for the $^{40}Ar^{2+}$ assignment is the presence of a peak at mass 40 in the helium spectrum which is not present in the hydrogen or deuterium spectra. This is attributable to $^{40}Ar^{+}$. The peak at mass 27 has not been identified.

The production of beams of ions having relatively high molecular weights may be of importance in future work. In the present work however, the ions of primary importance were H^+, H_2^+, H_3^+, D^+, D_2^+, D_3^+, D_2H^+, He^+, HeH^+, and He_2^+. All of which are low molecular weight ions so that impurity ions caused no interference.

Using data collected from these three spectra, the mass-calibration curve shown in Figure 22 was plotted. Table X shows the magnet current potentiometer settings associated with each mass found in the spectra. The calibration curve permitted the identification of unknown species produced in the discharge.

6) Charge-Transfer Cell

The pressure of lithium vapour in the charge-transfer cell was not measured directly, so that an alternative method of determining the efficiency of neutralization was required. This was done by observing the attenuation of the ion beam as a function of the heater-coil current using the apparatus shown in Figure 1. The heater current was increased in steps, and after allowing sufficient time for equilibration, the ion-beam intensity was measured. Typical data obtained with 5000 ev. H_2^+ ions are shown in Table XI. The attenuation of the beam

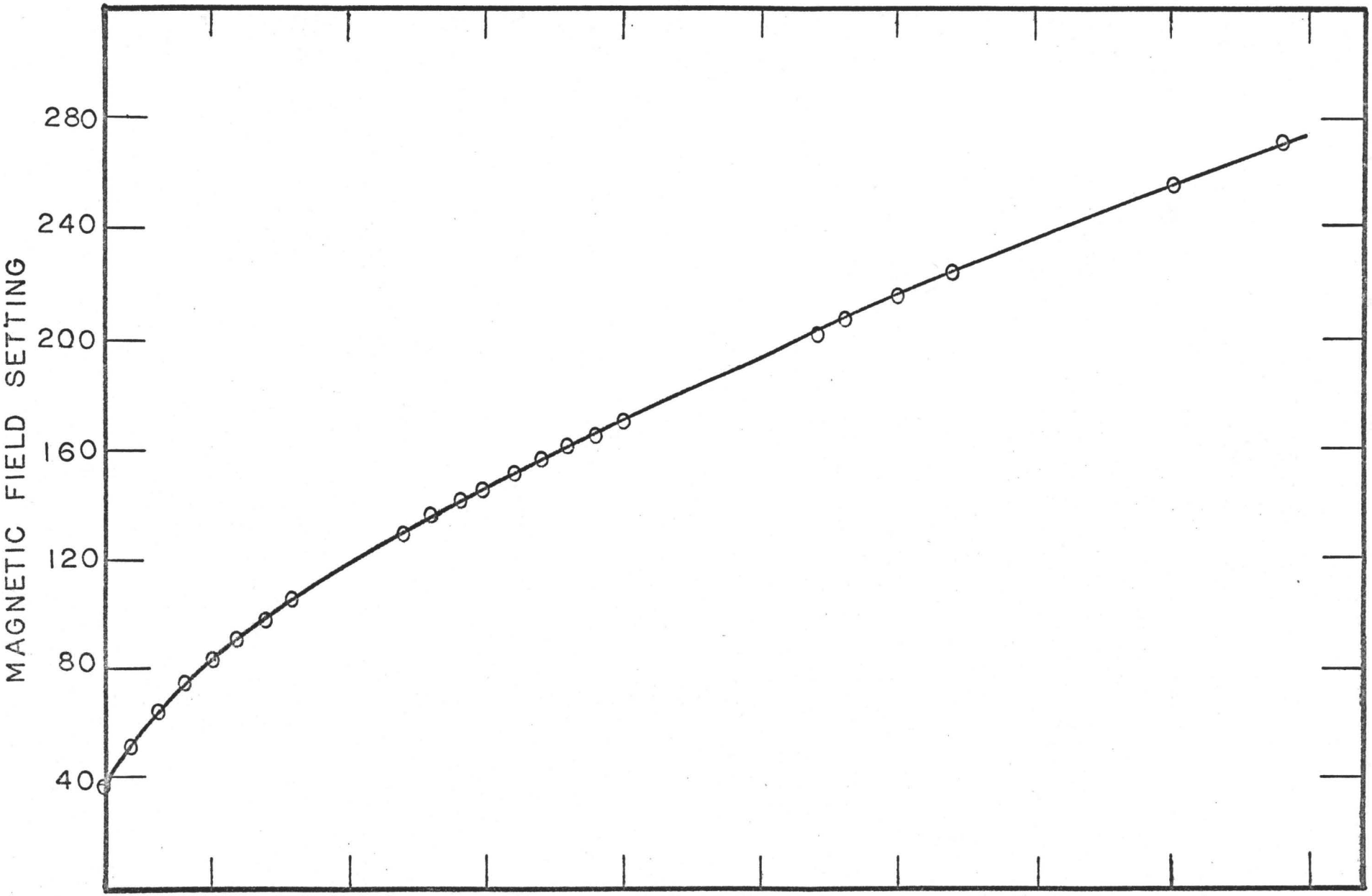

Figure 22 Mass calibration curve

Table X

Variation of magnet current with mass

Potentiometer Setting	Mass Assigned
37	1
53	2
67	3
75	4
83.5	5
92	6
97	7
105.5	8
131	12
138	13
141.5	14
147	15
152	16
158	17
162	18
167	19
172.5	20
202	27
207.5	28
216	30
224.5	32
255.5	40
272	44

Table XI

Beam attenuation in the charge-transfer cell

Beam current (10^{-6} amp.)	Heater coil current (amp.)
9.4	0.0
9.4	0.5
9.4	1.0
9.4	1.5
9.4	2.0
9.2	2.5
8.5	3.0
7.5	3.5
6.9	4.0
6.6	4.5
6.5	5.0
6.5	5.5

as the current increases, corresponds to the loss of ions from the beam by neutralization and by scattering. The cross section for neutralization however, is considerably greater than that for collisional scattering, so that much of the attenuation corresponds to the production of a neutral beam. A less likely possibility is the production of negatively charged ions as a result of ions undergoing two charge-changing collisions. This would require a higher pressure of lithium vapour than is normally used in this apparatus. These data are plotted in Figure 23, where it is apparent that a heater coil current of about 4.5 amperes is sufficient to produce an optimum number of neutral molecules.

7) Reionization of the Neutral Beam.

Reionization of the neutral beam was carried out using a stream of electrons produced from a heated filament. The performance of this reionizer was investigated in two ways, both using the apparatus shown in Figure 1. Firstly, the intensity of the electron beam crossing the molecular beam was kept constant and the electron kinetic energy varied from 10 to 100 ev. A beam of neutral H_2 molecules was passed through the electron beam and the H_2^+ ions produced were mass analysed and their intensity measured. It was found that variation in the kinetic energy of the electrons had little or no effect on the number of secondary H_2^+ ions produced. This may be understood in terms of the relative kinetic energy involved in a collision between a hydrogen molecule and an electron.

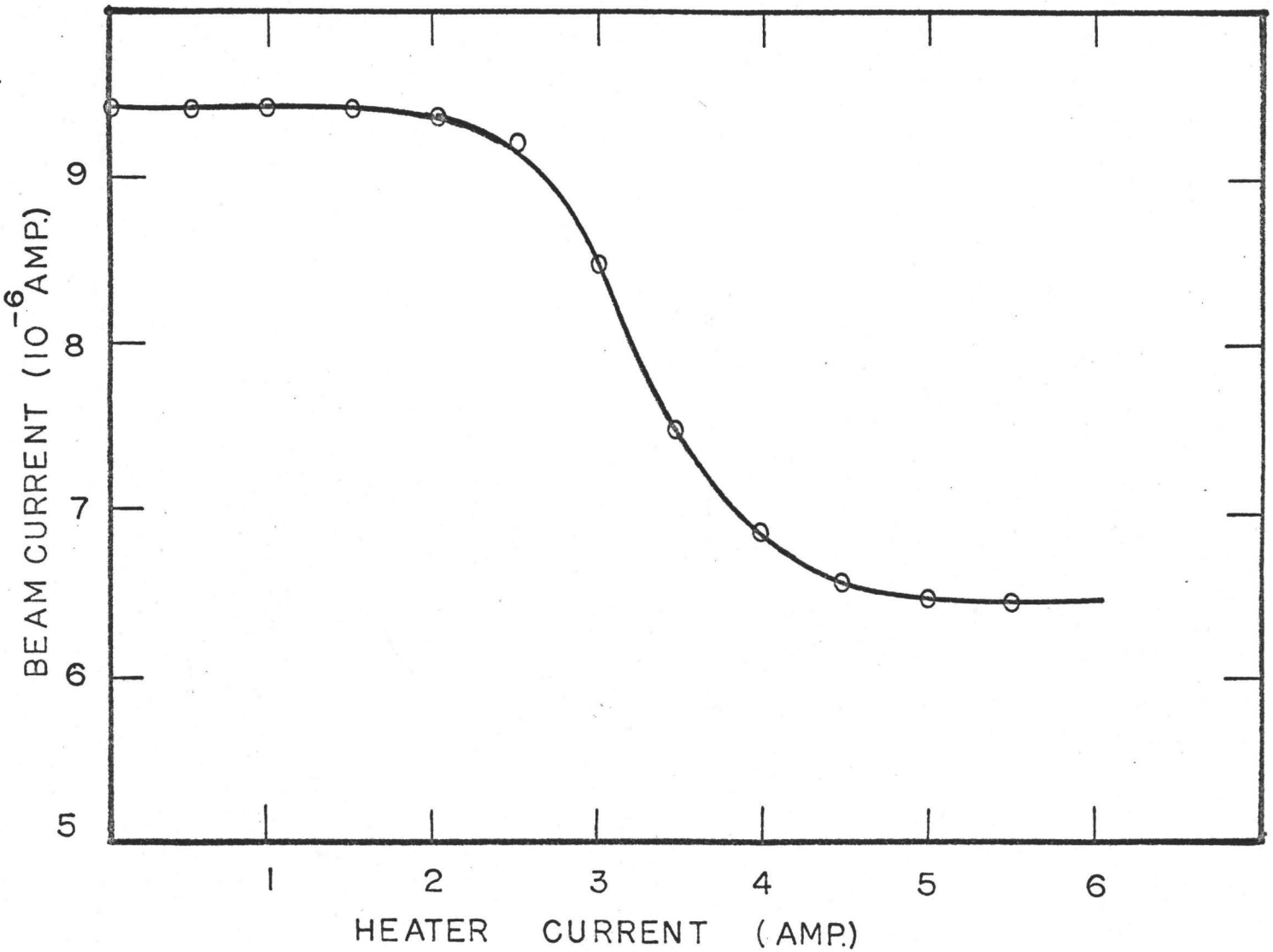

Figure 23

Beam attenuation in the charge-transfer cell

The cross section for ionization by collision with electrons has been shown to be maximum at a relative kinetic energy of about 100 ev. In this experiment, the hydrogen beam possesses 5000 ev. kinetic energy, so that the additional relative energy due to the approach of the electron is small. Thus it appears reasonable that the cross section for ionization should remain virtually constant.

In the second experiment, the kinetic energy of the electrons was kept constant while the electron current was varied by changing the filament current. The data obtained are shown in Table XII and plotted in Figure 24. As may be seen the intensity of reionized H_2^+ ions increased as the number of electrons was increased, although not linearly. The background pressure along the beam path was maintained at less than 1×10^{-5} mm.Hg. However, Figure 24 shows that when the electron current is zero, there are still about 1×10^{-11} amperes of reionized H_2^+. This is due to the high efficiency of ionization by collision with background gas, as discussed in Chapter 2. When the pressure was increased, the number of ions produced in this way became approximately equal to the number produced by electron bombardment.

8) Detector System

The Faraday cup assemblies were designed to minimize the loss of secondary electrons from the metal surface of the target. A bias plate was positioned in front of the cup,

Table XII

Reionization efficiency

Electron Current (10^{-3} amp.)	Reionized H_2^+ current (10^{-11} amp)
0.0	1.0
0.1	6.0
0.2	9.5
0.3	12.0
0.4	14.0
0.55	16.0
0.75	18.5
0.95	21.0

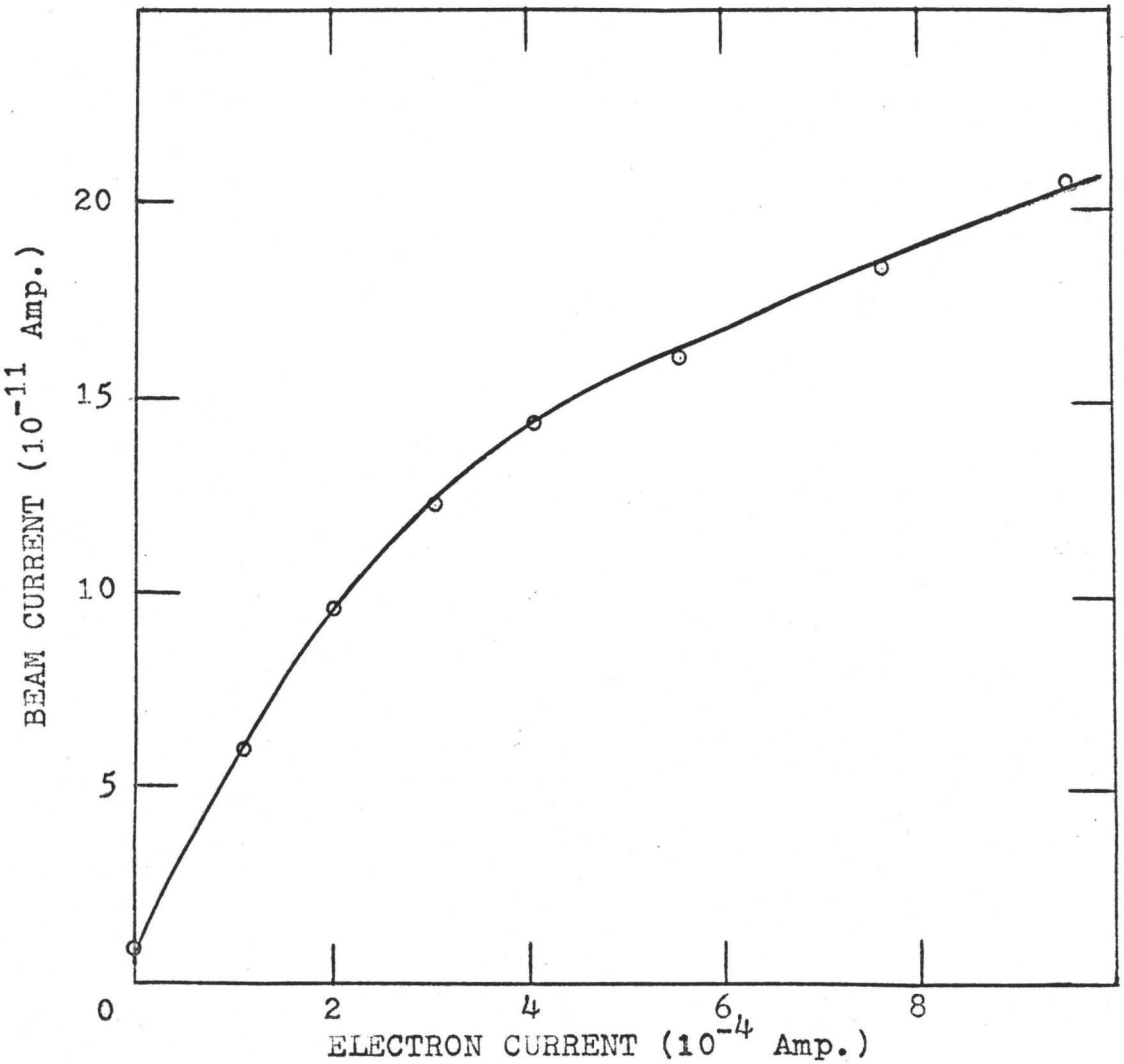

Figure 24

Variation of reionized H_2^+ beam current with electron bombardment current

to which a positive or negative potential could be applied. A positive potential enhanced the loss of electrons, resulting in an erroneously high beam current reading. A negative potential suppressed the electron emission and resulted in a true indication of the number of ions striking the cup. With a 5 kev. beam of H_2^+ ions striking the Faraday cup, the potential on the bias plate was varied from -100v. to +100v. and the beam-current reading taken. The data obtained are shown in Table XIII and plotted in Figure 25.

A positive bias of 40 volts resulted in a beam-current reading which was 2.4 times the reading at zero bias potential. A negative bias of 40 volts reduced the current reading by about 20% from the zero bias reading. In most experiments the detector was operated with a negative bias of 40 volts but in a few cases the bias was made zero or even positive to detect very low intensity beams.

Summary

The experimental data described in this chapter demonstrated the way in which the beams were affected by the various components in the apparatus. These data permitted calibration of the various components and indicated optimum operating conditions.

Table XIII

Variation of Faraday cup current with bias voltage

Bias voltage (volts)	Current (10^{-6}amp.)
-100	2.4
-80	2.4
-60	2.4
-40	2.4
-30	2.5
-20	2.5
-10	2.6
0	3.0
+5	4.2
+10	5.0
+20	6.2
+40	7.0
+60	7.0
+80	7.1
+100	7.1

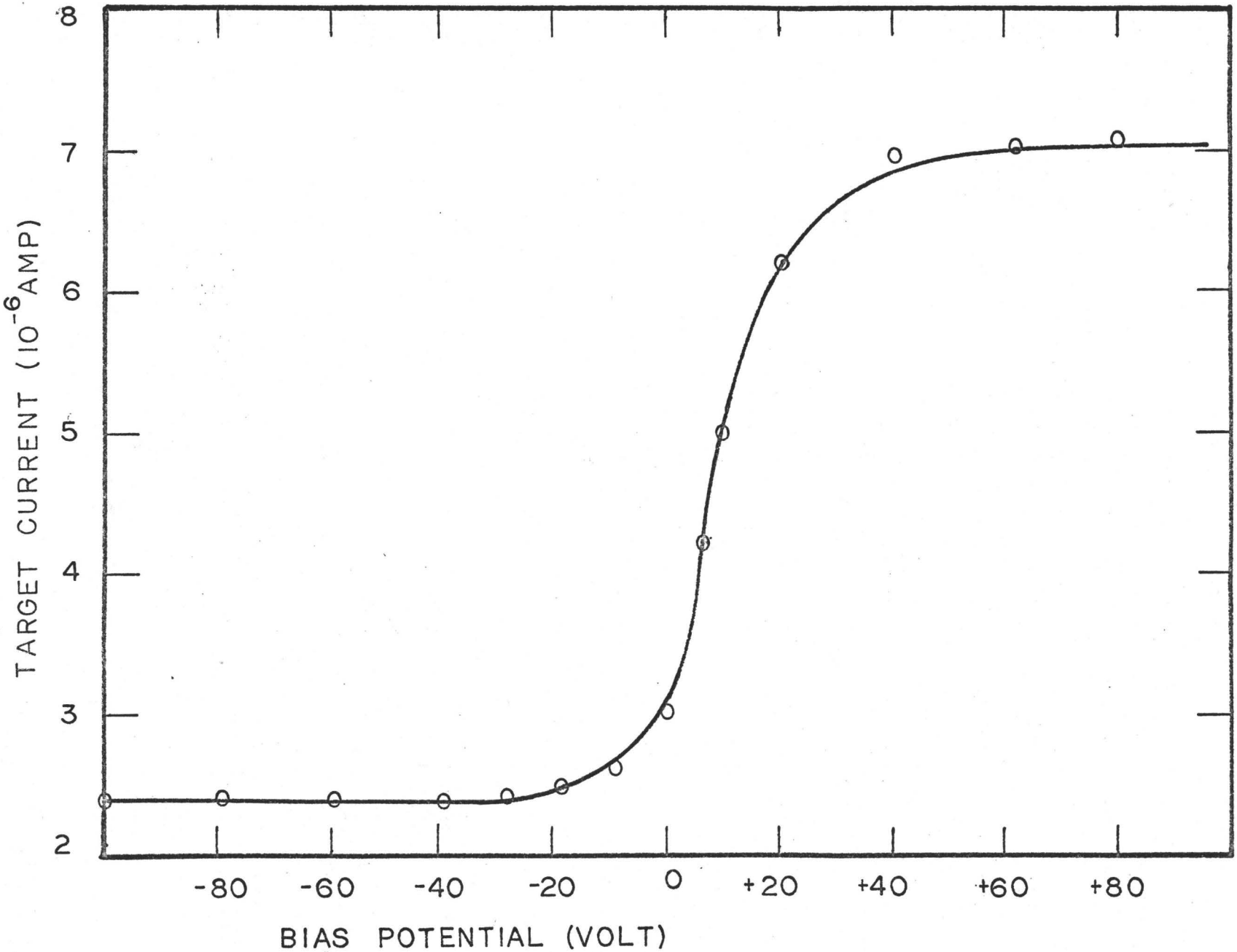

Figure 25
Variation of Faraday cup current with bias voltage

CHAPTER 5

INVESTIGATION OF SHORT-LIVED MOLECULES AND IONS

Experimental:

The apparatus used for the production and analysis of neutral molecules is shown in Figure 1. A beam of ions was produced from the source, mass analysed and passed through the neutralizing chamber containing lithium vapour. The resulting neutrals were allowed to continue undeflected while the ions remaining in the beam were removed by applying a potential to the deflector plates. Immediately following the neutralizing chamber, a fraction of the neutral beam was reionized by electron bombardment, and the beam composition determined by mass analysis.

Since there was no accelerating potential associated with the second mass analyser, only ions produced from neutrals, which themselves originated from the primary beam, could be focused in the second mass analyser. This means that only atoms or molecules which were neutral for the time of transit of the electrostatic field could become available for reionization and subsequent detection in the second mass analyser. The electrostatic field was approximately 3 cm. in length, and the velocity of a 5000 ev. beam of mass 5 ions is of the order 5×10^{7} cm. sec^{-1}, so that the time of transit of such an ion would be approximately 6×10^{-8} seconds.

In order to calibrate the apparatus and establish the feasibility of studying short-lived molecules, the behaviour of a number of well known monatomic and diatomic species was first investigated. The results obtained with these molecules were then compared with the results obtained with molecules whose lifetimes were unknown.

Results and Discussion:

1) Monatomic Systems.

The simplest systems and those first studied were He^+, H^+, and D^+ ions. The mass spectrum of a beam of He^+ ions, having undergone no neutralization or reionization, was obtained by scanning the magnetic field of the second mass analyser. This spectrum is shown in Figure 26a. This may be termed the primary He^+ beam. The intensity was $1x10^{-6}$ amperes. With charges up to 5000 volts on the deflector plates, and the introduction of gas into the neutralizing chamber, the spectrum shown in Figure 26b was obtained by reionizing a fraction of the neutrals and scanning the second mass analyser. This may be termed the secondary He^+ beam. The secondary peak appeared at the same position as the primary He^+ ions, but the intensity was reduced to $2x10^{-10}$ amperes. Thus approximately 1 in 10,000 of the primary ions underwent both charge-changing processes and appeared as a secondary beam. This factor may be termed the transmission through the apparatus.

Although the secondary peak was somewhat broader than the primary peak, showing that an energy spread had been introduced, the spread was relatively small and did not interfere with the assignment of the peak to mass 4. It was clear therefore, that the secondary peak corresponded to He^+ ions resulting from the neutralization and reionization processes, and that the majority of these ions underwent both processes

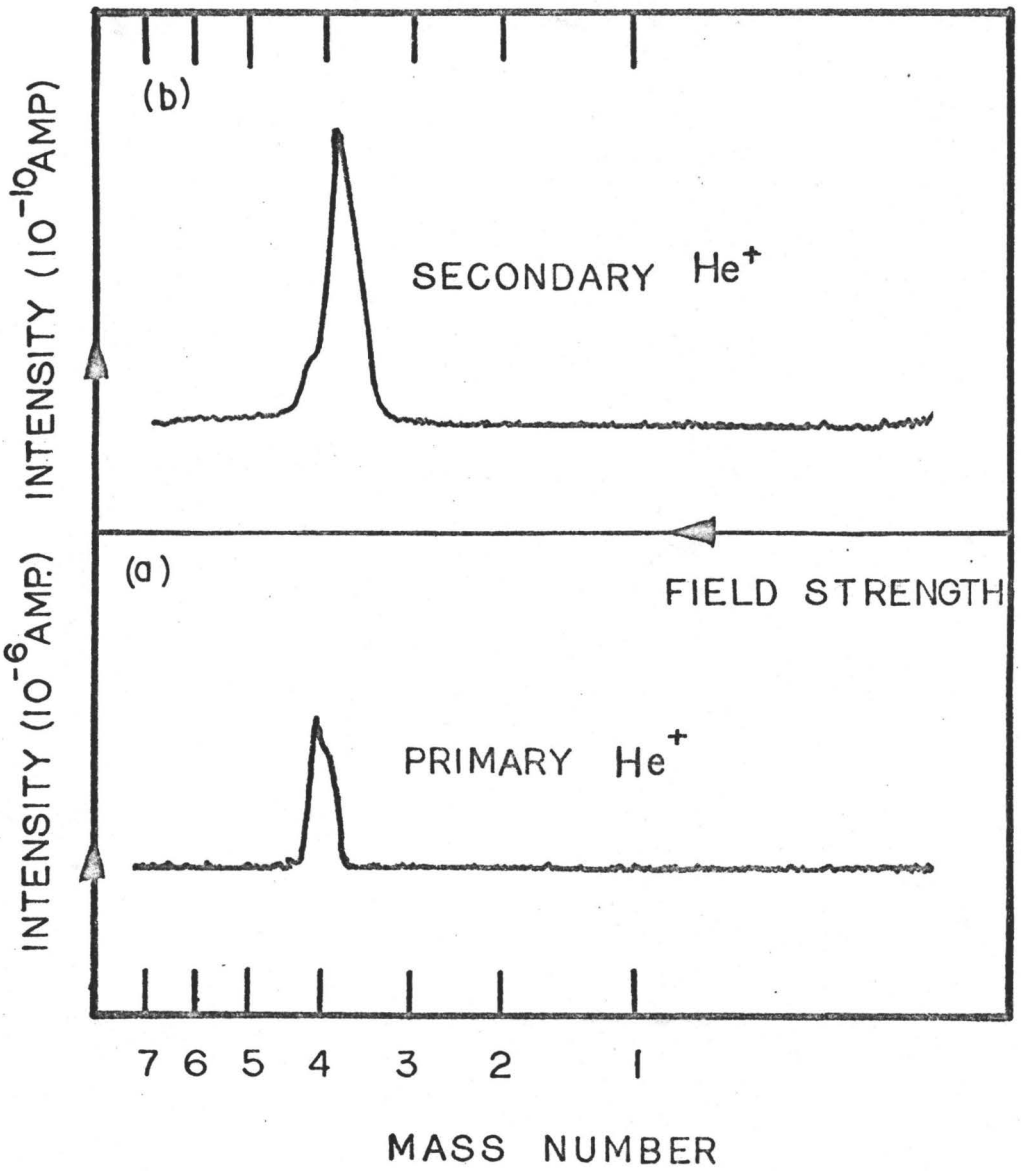

Figure 26

Primary and secondary spectra from a beam of He^+ ions

with little change in kinetic energy.

Similar experiments with beams of H^+ and D^+ ions resulted in the spectra shown in Figure 27. In both cases, the beam intensities were approximately $1x10^{-5}$ amperes of primary beam, and $2x10^{-8}$ amperes of secondary beam, indicating that approximately 1 in 1000 of the primary ions underwent both charge-changing processes and appeared as a secondary beam. This suggests that the charge-changing reactions in the H^+ - H systems were approximately 10 times more efficient than those in the He^+ - He system. Assuming similar pressure conditions for the helium and hydrogen experiments, this difference should be reflected in the cross sections for the two processes. The appropriate cross sections at 5000 ev. kinetic energy are shown in Table XIV [30].

An indication of the overall efficiency of the neutralization and ionization processes may be obtained from the product of the cross sections for these reactions, ${}_1q_0$ and ${}_0q_1$. For helium, this product has a value of $4.9x10^{-33}$ and for hydrogen, a value of $8.0x10^{-32}$. The ratio of these is approximately 17. In view of possible variations in the pressure of charge-transfer gas in the two experiments, this ratio agrees reasonably well with the 10 fold difference found experimentally.

The relative ease of production of neutral beams may be understood in terms of the cross sections shown in Table XIV. The ratio of neutralization to ionization cross section for the hydrogen system, ${}_1q_0/{}_0q_1$, is 12.5. Thus a beam of particles

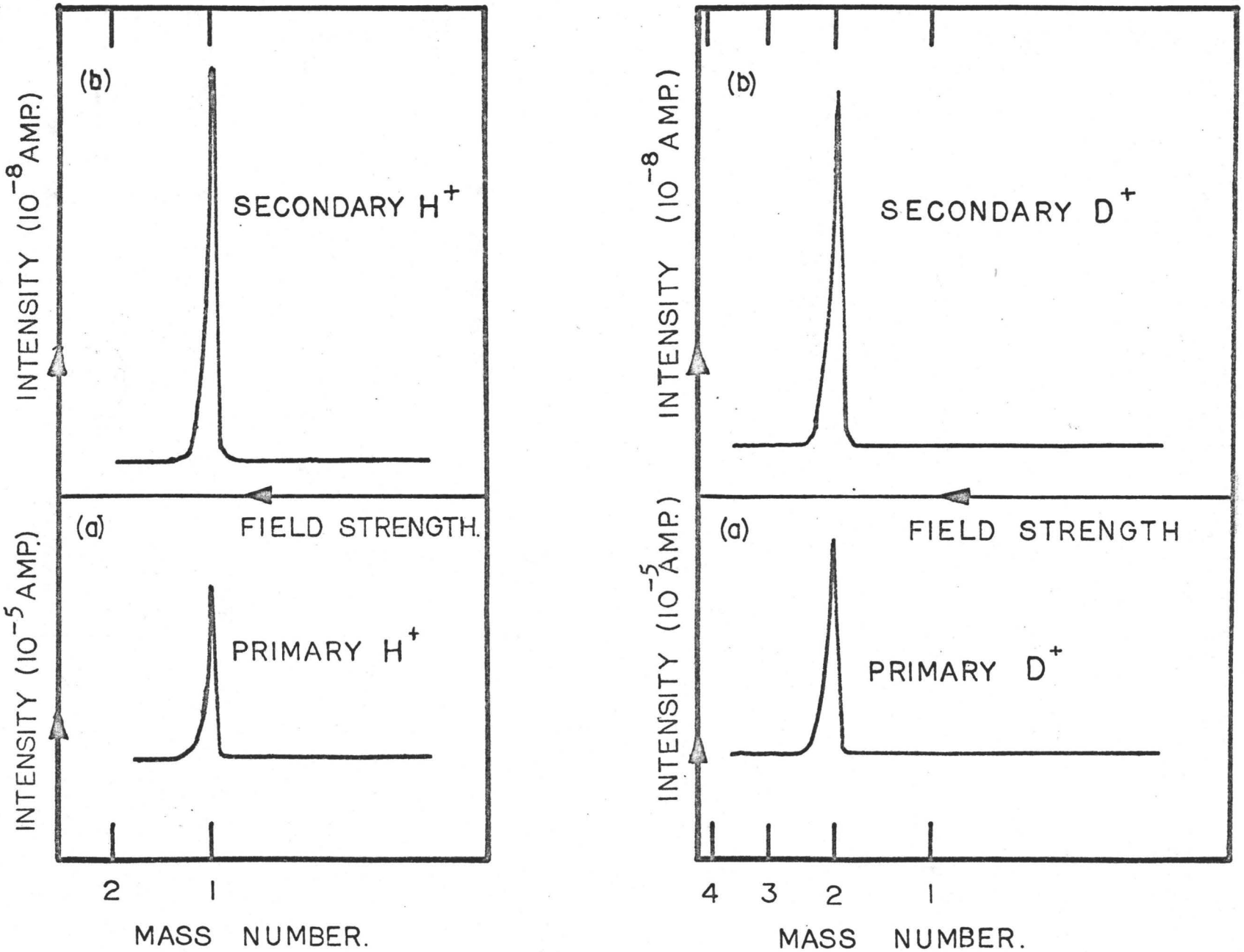

Figure 27

Primary and secondary spectra from beams of H^+ and D^+ ions

Table XIV

Charge-changing Cross Sections

at 5000 ev.

Process	Cross Section	Value $cm.^2$ per atom or mol.
$He^+ + He \longrightarrow He + He^+$	${}_1q_0(He)$	7×10^{-16}
$He + He \longrightarrow He^+ + He + e$	${}_0q_1(He)$	7×10^{-18}
$H^+ + H_2 \longrightarrow H + H_2^+$	${}_1q_0(H)$	1×10^{-15}
$H + H_2 \longrightarrow H^+ + H_2 + e$	${}_0q_1(H)$	8×10^{-17}

reaching charge equilibrium while passing through a charge-transfer gas would be expected to produce a large percentage of neutrals. The competing process of scattering by momentum-transferring collisions would be expected to be unimportant, since generally the cross section for momentum transfer is considerably less than that for charge transfer. Further, momentum-transferring collisions tend to occur at large scattering angles and result in considerable changes in the kinetic energy of the collision partners. The cross section for momentum transfer is given by:

$$q_{mt} = 2\pi \int_0^{\pi} I_s(\theta)(1 - \cos\theta)\sin\theta d\theta$$

where θ is the centre-of-mass scattering angle and $I_s(\theta)$ the differential microscopic scattering cross section. q is then a measure of the average forward momentum lost by a particle during a collision. Scattering at small angles produces only a small contribution to q since the quantity $(1-\cos\theta)$ goes to zero as θ^2 for small deflections. Thus appreciable momentum scattering will occur only at large angles and will result in the particles being lost from the beam. Further, in a collision between a projectile of mass m and a target molecule of mass M, the mean fractional energy lost per collision ΔE, is given by:

$$\Delta E = \frac{2mM}{(m + M)^2}$$

so that in a collision between an H^+ ion and an H_2 molecule e.g. $\Delta E = 4/9$. Thus the probability of an ion undergoing a collision

of this type and still being detected as a peak in the secondary spectrum is minimal.

The results shown for monatomic systems demonstrated that it was possible to carry out the two charge-changing processes and still detect the final product as a relatively sharp peak at the expected position in the mass spectrum.

2) Diatomic Systems

Using the same procedure as for monatomic systems, a number of diatomic molecules were investigated. Figure 28 shows the spectrum obtained from a beam of H_2^+ ions together with the secondary spectrum obtained after neutralization. Two peaks were found in the secondary spectrum, one at the same position in the magnetic field as the primary H_2^+ peak, the other occurring at one half this magnetic field. The positions in the mass spectrum corresponded to mass-to-charge ratios of 2 and $\frac{1}{2}$. The peak at half field may be identified by considering the energetics of the dissociation of H_2^+ ions during charge-transfer reactions.

Disregarding for the present, contributions from binding energies, the products of the dissociation of H_2^+ ions will have the same velocity (and half the energy) as the parent H_2^+ ions. The equation governing the motion of an ion of mass m and charge e, moving in a magnetic field H, with trajectory of radius r, is:

$$H = \frac{mv}{er}$$

For e, r and velocity v, constant, the magnetic field is directly proportional to mass. Thus the peak at half the field of the

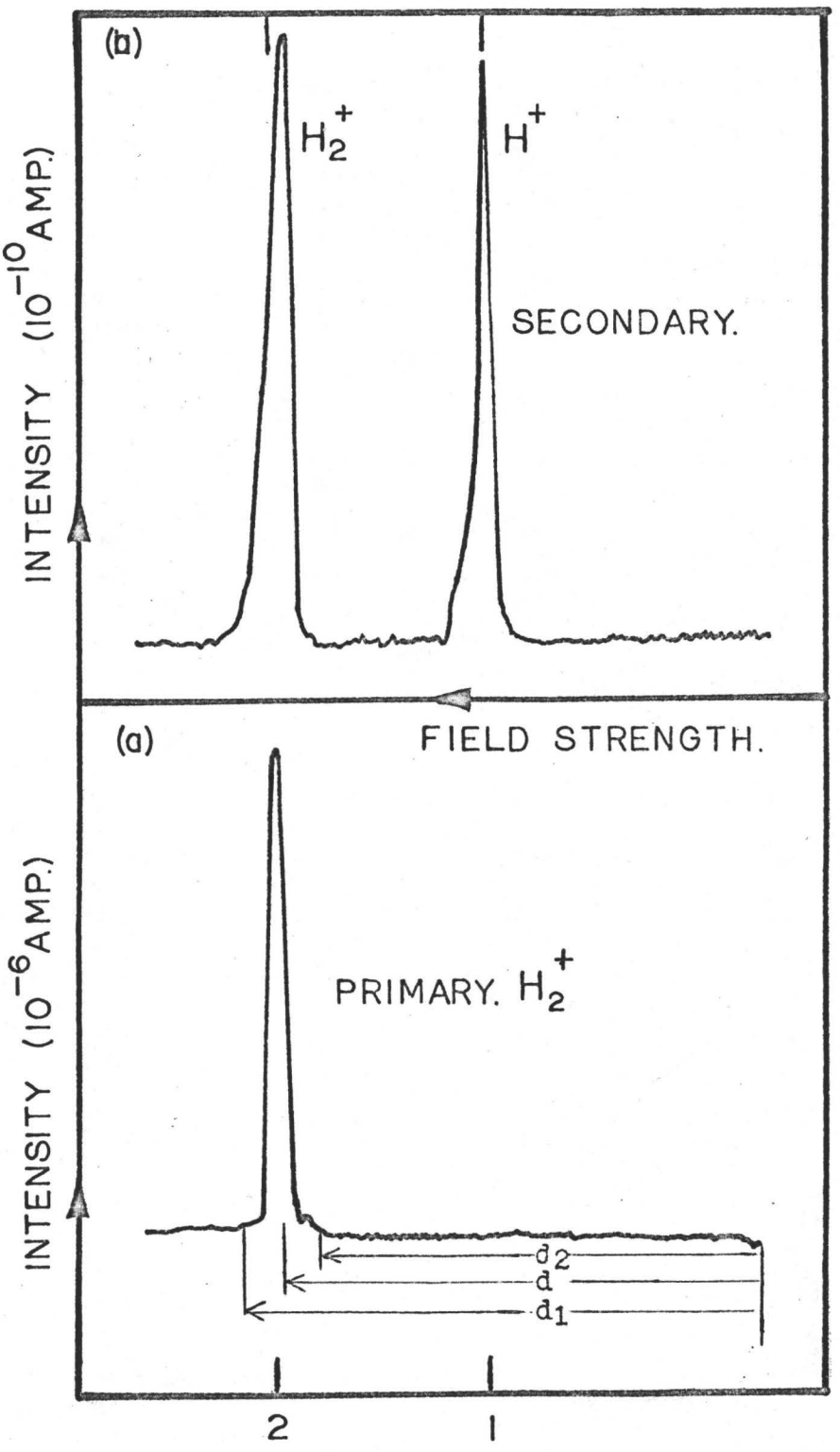

Figure 28

Primary and secondary spectra from a beam of H_2^+ ions

primary H_2^+ ion may be assigned to H^+ ions produced by dissociation of H_2^+ ions. This may be considered from a different viewpoint. The appearance of a peak with a mass-to-charge ratio $\frac{1}{2}$ may be understood in terms of a well-known mass spectrometric phenomenon. Ions undergoing dissociation after acceleration but prior to analysis in a magnetic field, are focused at an apparent mass-to-charge ratio given by:

$$\frac{m^*}{q} = \frac{(m_f/q_f)^2}{m_i/q_i}$$

where m_f/q_f, and m_i/q_i are the mass-to-charge ratios of the final and initial ions.(86-88)

Thus H^+ ions and reionized H atoms resulting from the dissociation of H_2^+ ions, will be focused at an apparent mass-to-charge ratio of $\frac{1}{2}$. The results may thus be interpreted in terms of the primary H_2^+ ions undergoing dissociation to give H^+ ions and H atoms, in addition to normal charge transfer producing H_2 molecules. These reactions may be written:

$H_2^+ + e(Li) \longrightarrow H_2$ Charge Transfer

$H_2^+ + e(Li) \longrightarrow H^+ + H + e$ Excitation and Dissociation

$H_2^+ + e(Li) \longrightarrow H + H$ Dissociative Charge Transfer

The final products in the secondary beam are the result of ionizing the neutral products of these reactions:

$H_2 + e \longrightarrow H_2^+ + 2e$

$H + e \longrightarrow H^+ + 2e$

The separation of the peaks in the secondary spectrum caused by their difference in energy, improves the ability of

the mass analyser to resolve the secondary beam. In the spectra showing dissociation products, the mass number for a given peak is written to show the identity of that peak, and does not correspond to the position expected for that mass in the primary spectrum.

Using the same techniques, spectra were obtained from beams of D_2^+ and HD^+ molecular ions. These are shown in Figures 29 and 30. Both spectra are analogous to those obtained with the H_2^+ ion beam. The secondary spectrum of the D_2^+ ion beam shows peaks at mass positions 1 and 4, which are assigned to D^+ and D_2^+ ions. The secondary spectrum of the HD^+ ions shows peaks at mass positions 1/3, 4/3 and 3, which are assigned to H^+, D^+, and HD^+ ions. Although the velocities of 5000 ev. beams of H_2^+, HD^+ and D_2^+ ions differ by a small factor, it may be expected that the neutralization and ionization cross sections should be approximately constant for all three systems. This is shown to be so experimentally since the transmission through the charge-changing processes was approximately 1 in 10^4 in all three systems.

The maximum energy spread in a 5000 ev. beam produced from a radio-frequency ion source of the type used in this work has been found to be about 100 ev.[106] From Figure 28 it is possible to estimate the apparent energy spread in the primary beam of H_2^+ ions using the equation relating magnetic field H, kinetic energy E and mass m,

$$H^2 = \frac{2mE}{(er)^2}$$

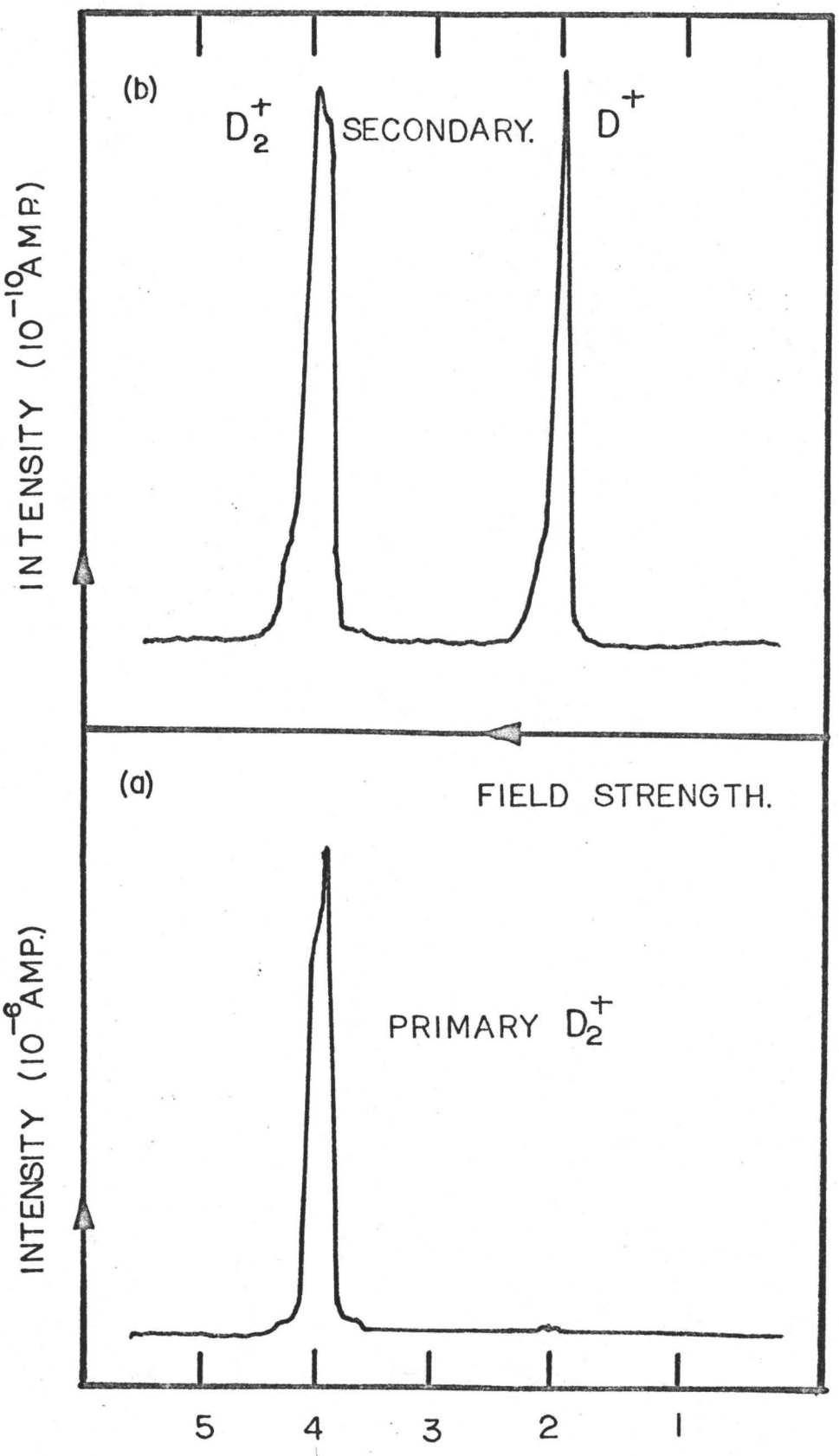

Figure 29

Primary and secondary spectra from a beam of D_2^+ ions

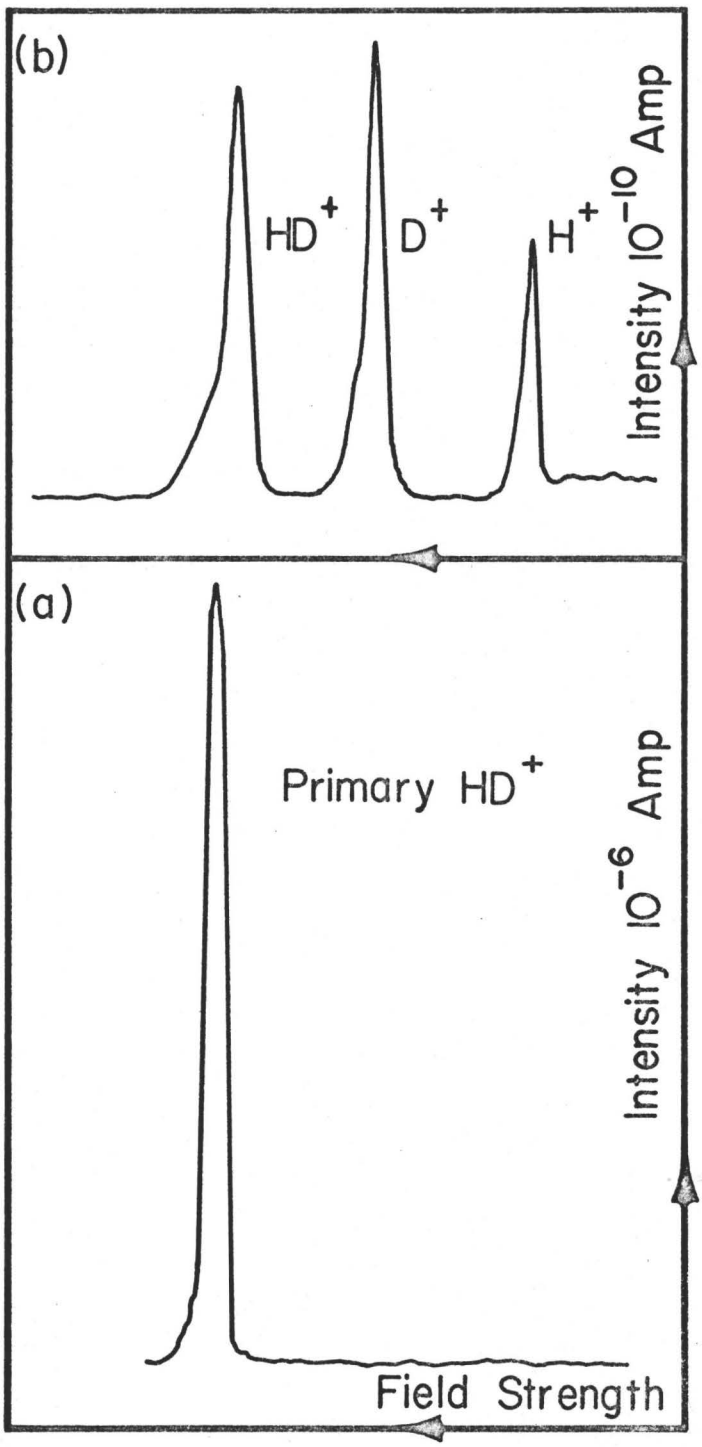

Figure 30

Primary and secondary spectra
from a beam of HD^+ ions

Since in obtaining the spectrum in Figure 28, the magnet current and chart drive were varied linearly with time and since at the low magnetic fields used, the magnetic field was linearly related to the magnet current, the field H is approximately proportional to d, the distance of the peak from the origin of the spectrum. (Fig. 28). Thus the equation may be written:

$$d^2 = \frac{mE}{K}$$

where K is a constant of proportionality. For primary H_2^+ ions m=2, E=5000 ev. and d=68 mm. (Fig 28), so that K=2.16. The energy spread at the base of the H_2^+ peak may then be written

$$\triangle E = \frac{2.16}{m}(d_1^2 - d_2^2)$$

where d_1 and d_2 are the distances from the origin at which the high and low energy ions are respectively focused. From Fig. 28 $d_1 = 70$ and $d_2 = 65$, so that the apparent energy spread of the primary H_2^+ ion beam is 700 ev. This is considerably greater than the expected energy spread of 100 ev. and shows that the peak width is largely characterized by the beam width and to a much lesser extent by the energy spread of the ions.

The process of dissociation may result in the introduction of an energy spread in addition to that already present in the primary beam. For instance, when an H_2^+ ion is dissociated to H^+ ions and H atoms, it is excited from the ground state into one of the repulsive states shown in Figure 31[8,41]. The potential energy of the components at the initial intermolecular spacing is then transformed into kinetic energy as the products move apart. Each component acquires a velocity u,

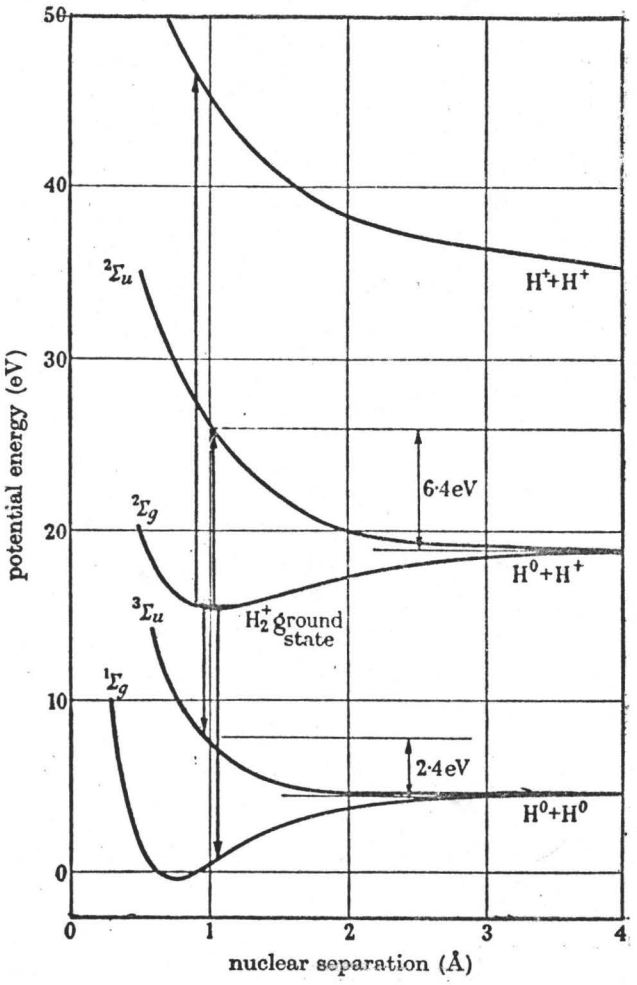

Figure 31

Some of the potential energy curves of the H_2 and H_2^+ systems (from reference 69)

in the centre-of-mass system, which must be added vectorially to the translational velocity v, of the original ion, to obtain the final velocity in the laboratory system. Considering first the molecules which have this dissociation axis at 0^{o} and 180^{o} to the beam direction, the energies E^{+} and E^{-} of the dissociation products will be:

$$E^{\pm} = \tfrac{1}{2}m(v \pm u)^{2}$$

where m, is the mass of the H atom. The spread in energy between the two groups is:

$$\Delta E = E^{+} - E^{-} = 4(E_{o}E_{1})^{\frac{1}{2}}$$

where $E_{o}=\frac{1}{2}mv^{2}$ and $E_{1}=\frac{1}{2}mu^{2}$.

For the excitation reaction

$$H_{2}^{+} \longrightarrow H + H^{+}$$

E_{o} is 2500 ev. for a primary beam energy of 5000 ev. and application of the Franck-Condon principle gives the most probable value of E_{1} as 3.2 ev. for each component. (Fig. 31). The energy spread ΔE is then calculated to be 358 ev.

For the charge-transfer reaction

$$H_{2}^{+} + e \longrightarrow H + H$$

E_{o} is 2500 ev. and E_{1} is 1.2 ev. so that ΔE is 218 ev.

Thus the energy spread introduced in this way may be appreciable, although, because of the poorly characterized peak shapes and the large beam width, an additional energy spread of this order would not be detectable in the secondary peak corresponding to H^{+} ions in Figure 28. The introduction of

a defining slit system in the mass analyser would enable this effect to be observed. Purser et al.[41] have observed an energy spread of approximately 500 ev. in H^+ ions produced by dissociation of 10 kev. H_2^+ ion beams.

When the dissociating molecule does not lie along the beam axis, the velocity u, will produce an angular spread in the beam, in addition to the energy spread discussed. This angular spread will be greatest when the dissociating molecule has its axis perpendicular to the beam axis. However, the initial component of velocity in this direction is zero, so that the final velocity component will be due to the dissociation energy only. Thus for double neutral production from H_2^+ ions, an energy component of only 1.2 ev. will be introduced at right-angles to the beam. For the 5 kev. beam used in this work, this will produce a spread in the beam which is small in relation to the width of the primary beam, since the distance travelled by the ions before analysis and detection is short.

The experiments carried out with diatomics demonstrated that peaks in the secondary spectra, resulting from dissociation reactions, were sufficiently well defined to enable them to be identified. They indicated however, that if molecules having high molecular weights were to be studied, the introduction of a slit system would be necessary.

3) The He_2 Molecule

The mass 8 component of the beam produced from a helium discharge, was selected at the first mass analyser and the primary and secondary spectra obtained by scanning the second mass analyser. The results are shown in Figure 32. Beam intensities were approximately $3x10^{-8}$ amperes of primary and $1x10^{-12}$ amperes of secondary. The transmission was therefore 1 in 10^4, which is of the same order as found for the He^+ system. Two peaks appeared in the secondary spectrum, one corresponding to the same position as the primary He_2^+ peak, the second at an apparent mass-to-charge ratio of 2. Using the reasoning described above, this was assigned to He^+ ions having half the kinetic energy of the parent He_2^+ ion. Thus the spectrum obtained is qualitatively similar to those found with stable diatomics, and the results suggest that the He_2 molecule was stable for at least the time of transit of the electrostatic field.

A possible complication arises in that the primary mass 8 beam may have contained O^{2+} ions. The presence of mass 8 peaks in both the hydrogen and helium primary spectra (Figures 19 and 21) suggested that this was possible. However, in order that O^{2+} ions be responsible for the peak assigned to secondary He_2^+ ions, the O^{2+} ions must undergo two charge-transfer collisions to produce O atoms. This in itself is improbable. Further, the O atoms having traversed the electrostatic field, must then

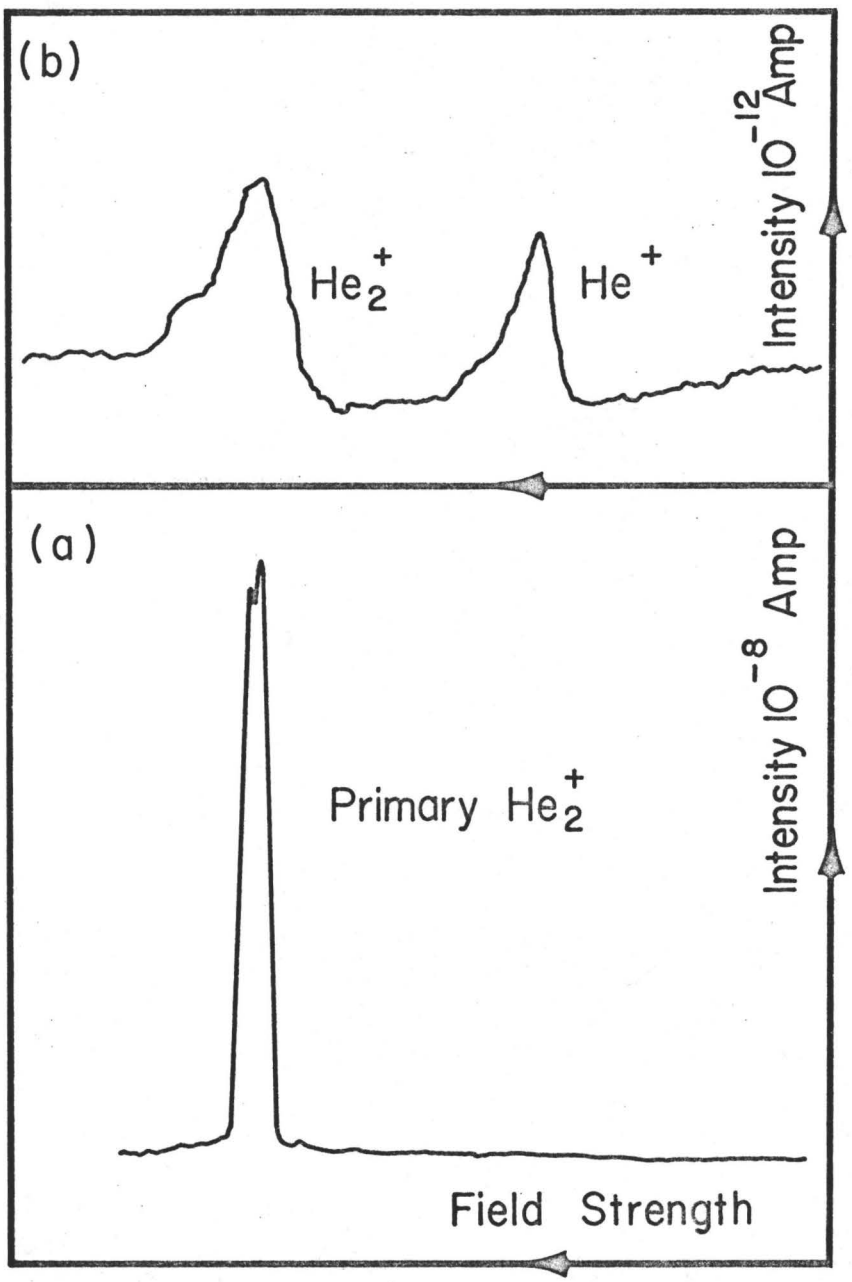

Figure 32

Primary and secondary spectra

from a beam of He_2^+ ions

undergo two ionizing collisions to give back O^{2+} ions, and produce a secondary peak at mass 8. The probability of this occurring in the short distance between the reionizer and the mass analyser is extremely small. However, to eliminate this possibility entirely, a secondary spectrum of the He_2^+ ion beam was obtained and the magnetic field scanned up to the peak position expected for an ion with mass-to-charge ratio 16. A peak at this position would be expected due to the formation of O^+ ions in the reionization of O atoms to O^{2+} ions. No peak was found with mass-to-charge ratio greater than 8. Thus O^{2+} ions could not be responsible for the secondary mass 8 peak.

To eliminate the possibility of primary ions in some way passing through the deflector plates, and being detected as a secondary beam, a number of experiments were carried out. A beam of He_2^+ ions was obtained, passed through the charge-transfer cell containing lithium vapour, reionized and detected in the second mass analyser. The deflector plate voltage was set at zero so that the current measured at the Faraday cup was the sum of the primary and secondary He_2^+ ion currents. On increasing the deflector plate potential to 500 volts, the beam intensity fell from 10^{-8} to 10^{-12} amperes. If some or all of the remaining 10^{-12} amperes of He_2^+ were due to primary ions passing through the deflector plates, it would be expected that a higher deflector plate potential would reduce the beam current still further. Increasing the potential from 500 to 5000 volts was found to have no effect on the beam intensity. This showed

that the secondary He_2^+ current was the result of reionizing neutrals which were unaffected by the electrostatic field.

In a second experiment, a primary beam of He_2^+ ions was scanned with the second mass analyser. The 5000 volt electrostatic field was then applied with the reionizer in operation but no gas was fed into the charge transfer cell. No secondary peaks were detected even with the electrometer measuring 10^{-14} amperes. When lithium vapour was introduced into the cell however, secondary peaks were found at intensities of 10^{-12} amperes, demonstrating that the secondary peaks resulted from the production of neutrals in the charge transfer cell.

A third experiment could be envisaged in which the primary beam was passed through the neutralizing gas without the reionizer in operation,and all the ions removed by the electrostatic field. There should then be no beam current at the detector. With the reionizer then turned on secondary peaks would be expected to appear. This experiment could not be carried out however, since ionization of the beam by background gas would result in a secondary spectrum even without the use of the reionizer.

The mass 8 peak in the secondary spectrum of He_2^+ ions must therefore be interpreted as the result of reionizing neutral He_2 molecules produced by charge transfer of He_2^+ ions. These ions are known to exist as stable species in mass spectrometers and gas discharges[89]. The earliest spectrometric work on the He_2^+ ion was reported in 1929 by Weizel and Pestel[90]. Phelps

and Brown[91] showed mass-spectrometrically that He_2^+ ions were present in high-pressure helium discharges. They accounted for the formation of the ion by a three-body collision process:

$$He^+ + 2He \longrightarrow He_2^+ + He$$

Experiments carried out by Dalgarno et al.[129] on the mobility of ions in gases confirmed the existence of the He_2^+ ion. Later work[92] showed the presence of He_2^+ ions in low-pressure discharges (10^{-3} mm. Hg) where the probability of three-body collisions taking place was small. Results from mass-spectrometric investigations[93-95] have established the mechanizm of formation as:

$$He + e \longrightarrow He^* + e$$

$$He^* + He \longrightarrow He_2^+ + e$$

where He^* is some excited state of the atom. Comes[95] reports a minimum value of 1.5 ± 0.3 ev. for the dissociation energy of the $^2\sum_u^+$ state of He_2^+. Calculations by Reagan et al.[96,128] yield a minimum value of 2.04 ev. The calculated $^2\sum_u^+$ ground-state potential curve is shown in Figure 33[96], together with some of the predicted triplet state potential curves of the He_2 molecule[130].

The He_2 molecule has been identified spectroscopically and details of its various states summarized by Herzberg[131] and Ginter[132]. Calculations have shown that some of the excited states of the molecule are expected to be bound[133], whereas the ground state has been found to be repulsive at all internuclear distances except for weak van der Waal interactions[134].

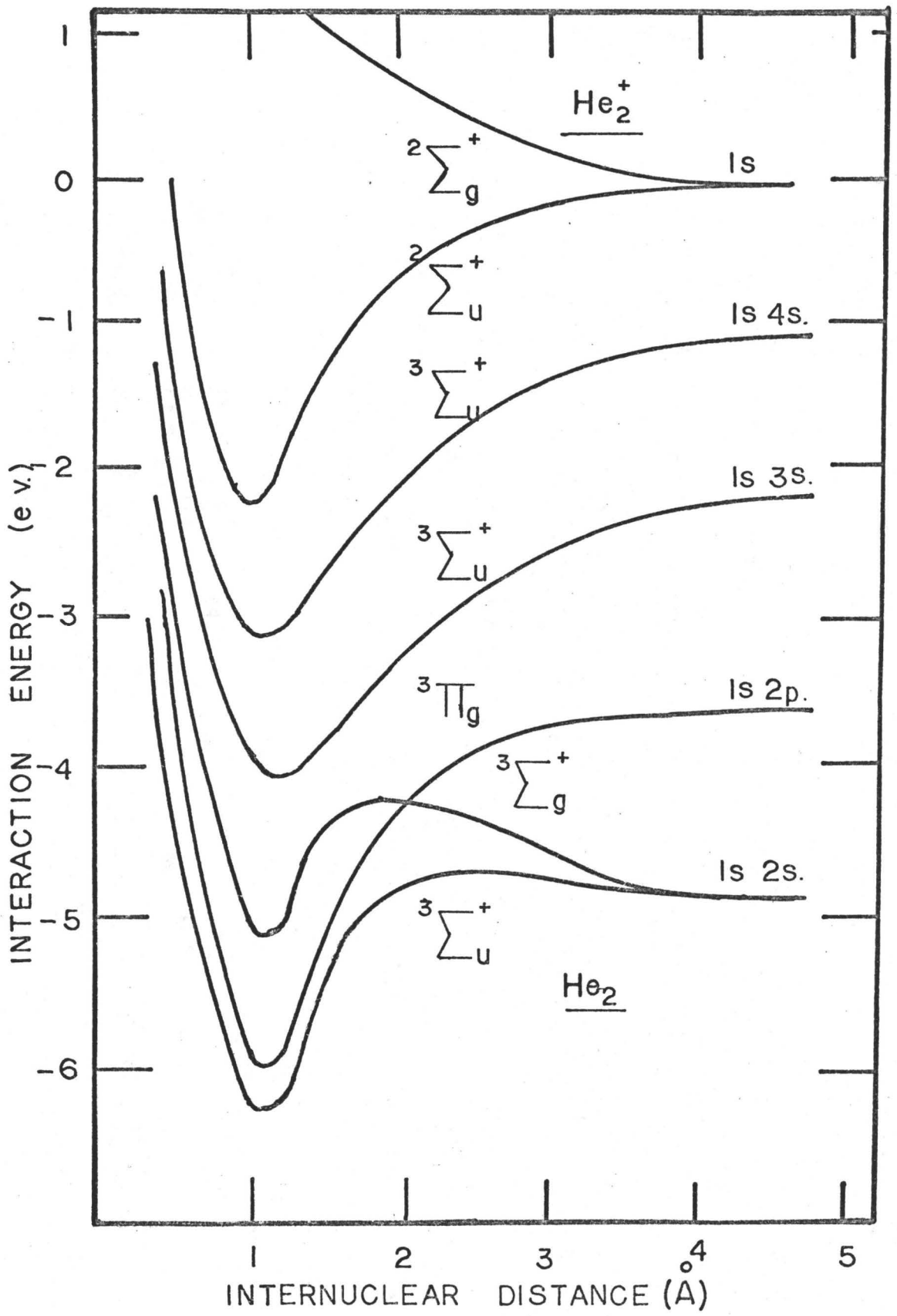

Some of the potential energy curves of the He_2 and He_2^+ systems

The spectroscopic dissociation energy of the He_2 $^3\sum_u^+$ state is 2.6 ev.(131) The dissociative ground state of the He_2 molecule is a $^1\sum_g$ state, so that the excited triplet states are metastable with respect to transitions to the ground state.

The mean lifetime of excited states may be discussed in terms of the equation:

$$N_n^t = N_n^o \, e^{-Anmt}$$

where $A_{nm}dt$, is the probability that a molecule in state n, will decay spontaneously to a lower state m, in time dt. N_n^o and N_n^t are the numbers of molecules in state n, initially and after time t. This equation may be written:

$$N_n^t = N_n^o \, e^{-t/\tau n}$$

where $\tau_n = 1/A_{nm}$ is the mean lifetime of an excited state n. For allowed transitions, (electric dipole), τ_n is of the order 10^{-8} seconds. If no allowed transitions can occur from the state n to any lower states, the mean lifetime may be of the order of 10^{-3} seconds if magnetic dipole transitions can occur, and of the order of 1 second if only quadrupole transitions can occur.

The He_2^+ ions produced from the r.f. source would all be in the doublet ground state on entering the charge-transfer cell, since approximately 10^{-4} seconds had elapsed before the ions reached this point. On neutralization of the ion, the molecule may be formed in singlet or triplet states. The singlet states are unstable relative to the ground state and molecules formed in these states would be expected to decay to the ground

state and dissociate into two He atoms

$$He_2^+\left|^2\sum_u^+\right| + e(Li) \longrightarrow He_2 \text{ (Singlet States)} \longrightarrow 2He$$

If however, the molecule is formed in one or more of the bound triplet states, these will decay to the $^3\sum_u^+$ which is metastable relative to the ground state and may be expected to have a mean lifetime of 10^{-3} seconds or longer.

$$He_2^+\left|^2\sum_u^+\right| + e(Li) \longrightarrow He_2 \text{ (Triplet States)}$$

There would be essentially no decay of the $^3\sum_u^+$ state of the He_2 molecule in the time between formation of the molecule and subsequent reionization (10^{-7} secs.). The reionization reactions may be written:

$$He_2\left|^3\sum_u^+\right| + e \longrightarrow He_2^+\left|^2\sum_u^+\right| + 2e$$

$$He + e \longrightarrow He^+ + 2e$$

The observations are therefore consistent with the assumed existence of a metastable beam of He_2 molecules in the bound $^3\sum_u^+$ state, having a lifetime which is long in relation to the 10^{-7} seconds necessary for their detection in the apparatus.

4) The Helium Hydride Molecule

A beam of HeH^+ ions was produced from an r.f. discharge containing a mixture of hydrogen and helium. The primary and secondary spectra were obtained using the method described and are shown in Figure 34a&b. The beam intensities were 1.5×10^{-9} amperes of primary and 5×10^{-13} amperes of secondary HeH^+ ions. Three peaks were observed in the secondary spectrum and from

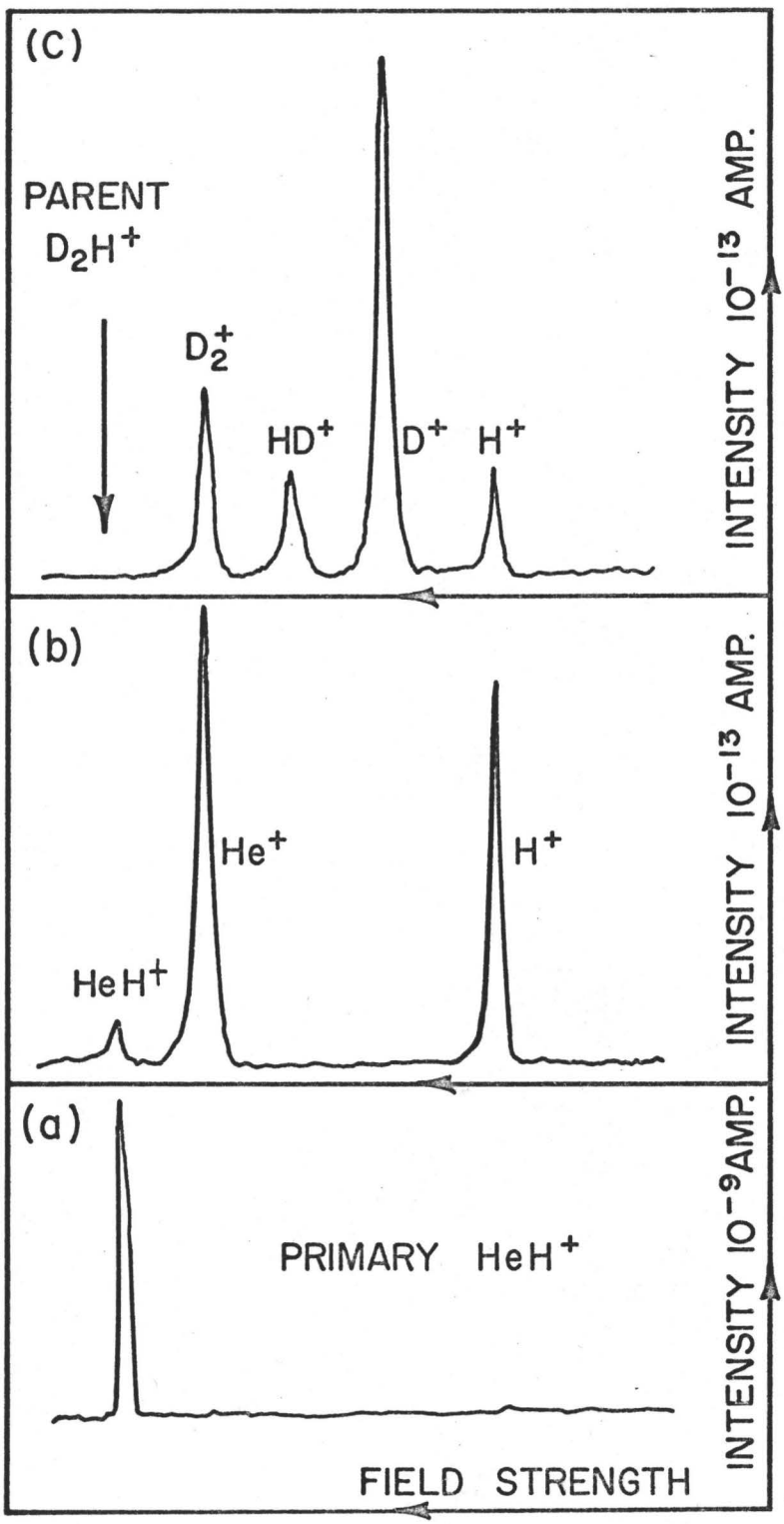

Figure 34 a and b: Primary and secondary spectra from a beam of HeH^+ ions

c: Secondary spectrum from a beam of D_2H^+ ions

their positions in the magnetic field, these were assigned to H^+, He^+ and HeH^+. The appearance of a peak at mass 5 indicates the existence of HeH molecules with lifetimes sufficiently long for the molecule to traverse the electrostatic field.

To ensure that the relatively small mass 5 peak was not the result of spreading or "tailing" of the larger mass 4 (He^+) peak, the analogous spectra were obtained from a beam of HeD^+ ions. These are shown in Figures 35a and b. Again three peaks were observed which were assigned to D^+, He^+ and HeD^+ ions. The increased separation between the secondary He^+ and HeD^+ peaks enabled the possibility of "tailing" to be ruled out. The beam intensities were $1x10^{-8}$ and approximately $5x10^{-13}$ amperes of primary and secondary ions respectively.

A complication which arose in these spectra was the possible interference from D_2H^+ and D_3^+ ions (masses 5 and 6). These ions are produced in relatively high abundances in the discharges used, and in particular, the mass 6 beam produced from a helium-deuterium discharge may contain appreciable amounts of D_3^+ ions along with the HeD^+ ions. It was therefore necessary to investigate the D_2H^+ and D_3^+ systems under the same experimental conditions as were used for the HeH^+ and HeD^+ systems. These experiments will be discussed in the next section but for comparison purposes, the secondary spectra obtained are shown in Figures 34c and 35c. The position of the parent ion has been shown in each spectrum. In neither case was it possible to detect a signal corresponding to secondary D_2H^+ or

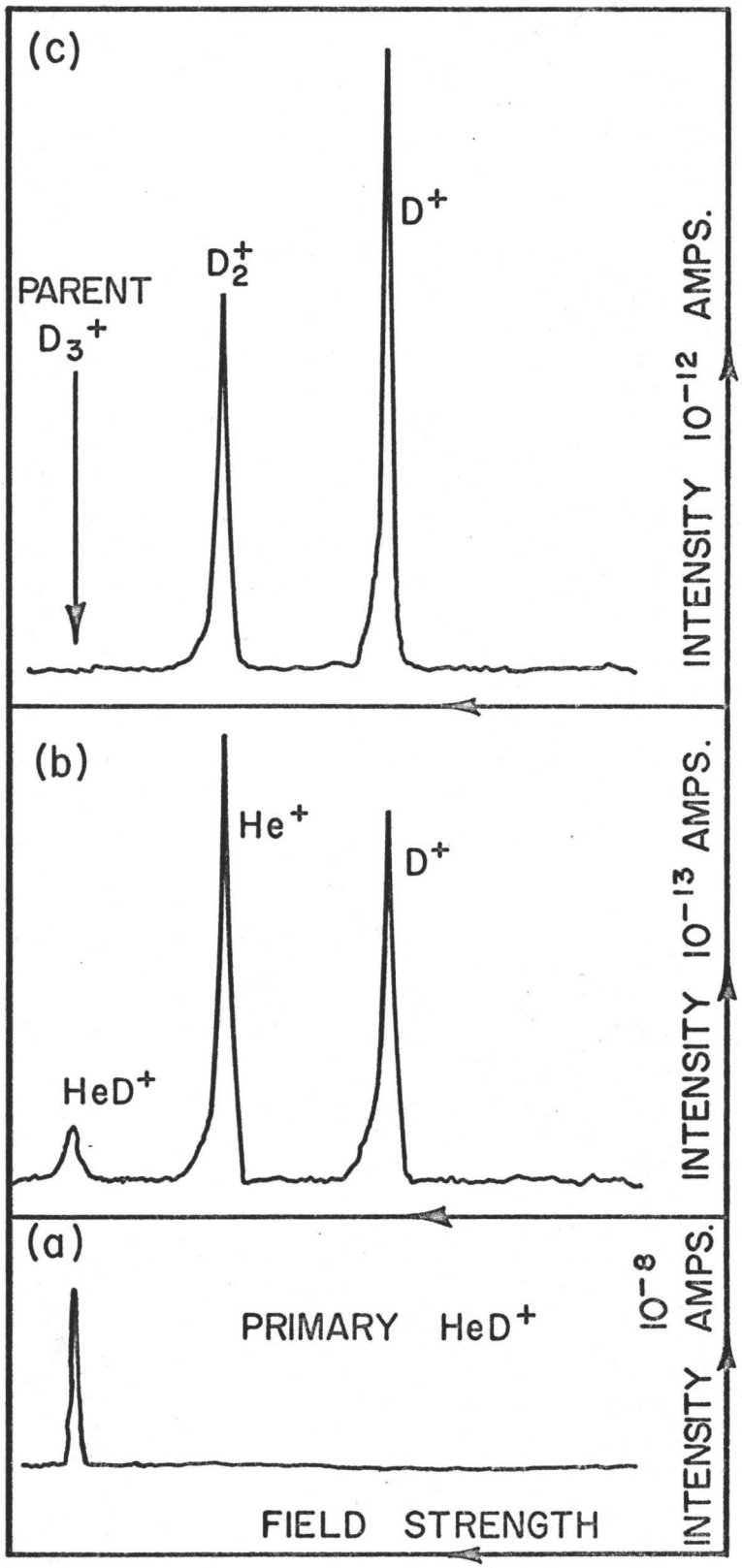

Figure 35 a and b: Primary and secondary spectra from a beam of HeD^+ ions
c: Secondary spectrum from a beam of D_3^+ ions

D_3^+ ions. It was clear therefore, that these ions could not interfere with the HeH^+ and HeD^+ spectra.

A further possible complication arose in that the HeH^+ peak in the secondary spectrum may have been the result of an ion-molecule reaction between He^+ ions and background hydrogen, taking place in the region between the deflector plates and the mass analyser.

$$He^+ + H_2 \longrightarrow HeH^+ + H$$

Friedman however[135, 136], has shown that, although at thermal energies the cross section for the endothermic reaction

$$H_2^+ + He \longrightarrow HeH^+ + H$$

may be relatively high, the cross section for the exothermic reaction above is negligibly small even at thermal energies. As discussed previously, the cross section for an ion-molecule reaction decreases with increased interaction energy so that interference from this reaction is unlikely. Further, reactions of this kind are accompanied by angular scattering and large changes in kinetic energies of the reactants. Thus the probability of any HeH^+ ions produced in this way being focused at the expected mass position is virtually zero.

These deductions were verified experimentally by passing 4 kev. He^+ ions through the neutralization and reionization stages of the apparatus and allowing the background pressure of hydrogen to increase. No indication of a peak corresponding to HeH^+ ions was found in the spectrum.

The peaks at masses 5 and 6 in the secondary spectra

of HeH^+ and HeD^+ ions respectively, must therefore be interpreted as the result of reionizing neutral HeH and HeD molecules produced by charge transfer of primary HeH^+ and HeD^+ ions.

The HeH^+ ion is well known mass-spectrometrically[137], and many quantum-mechanical calculations have been performed on the $^1\sum$ ground state. These have been summarized by Michels[138] who reports results on the ground and low-lying states of the ion. A dissociation energy of approximately 2.0 ev. for the ground state has been reported by Michels[138], Anex[139] and Wolniewicz[140]. Beam-scattering experiments carried out by Simons et al.[141, 142] on the H^+- He system are in good agreement with this value.

The HeH^+ ion is produced in the r.f. discharge by the reaction:

$$H_2^+ + He \longrightarrow HeH^+ + H$$

Berkowitz has investigated this reaction over an energy range of 0 to 100 ev. and with varying vibrational excitation of the H_2^+ ions.[147] It was found that the cross section depended more strongly on the vibrational energy than on the interaction energy. Peak cross sections at an interaction energy of 2 ev. were found to be 0.1 $\mathring{A}^2$ for the first vibrational level and 2.49 $\mathring{A}^2$ for v = 5.

The ground state of the HeH molecule has been calculated to be repulsive at all internuclear separations[143, 144] and scattering experiments performed by Amdur and Mason have confirmed this[145]. However, there exists a Rydberg series of

excited doublet states up to the ionization limit, which are essentially identical in character to the lowest $^1\Sigma$ state of the HeH^+ ion. Further it has been predicted that with the exception of the ground state, all the doublet states of the HeH molecule are bound[146]. These states are shown schematically in Figure 36.

There has been no previous experimental evidence reported for the existence of neutral HeH molecules, although the possibility of spectroscopic examination exists. Michels has calculated the basic spectroscopic constants of the HeH molecule from a vibrational-rotational analysis of the potential energy curves.

The results of the present work are interpreted as the production of HeH and HeD molecules in bound excited states which are unstable with respect to transitions to a repulsive ground state. In the analogous spectrum obtained from He_2 molecules, the secondary He_2^+ peak is the same order of magnitude as the secondary He^+ peak. (Fig. 32). With the HeH spectrum however, the secondary HeH^+ peak is approximately 10% the intensity of the secondary He^+ and H^+ peaks. Assuming as a rather crude approximation that the cross sections for neutralization and reionization of the HeH system are of the same order as those of the He_2 system, this suggests that only 10% of the HeH molecules produced by charge transfer are travelling through the electrostatic field without undergoing dissociation. Using the equation governing the lifetime of a molecular state

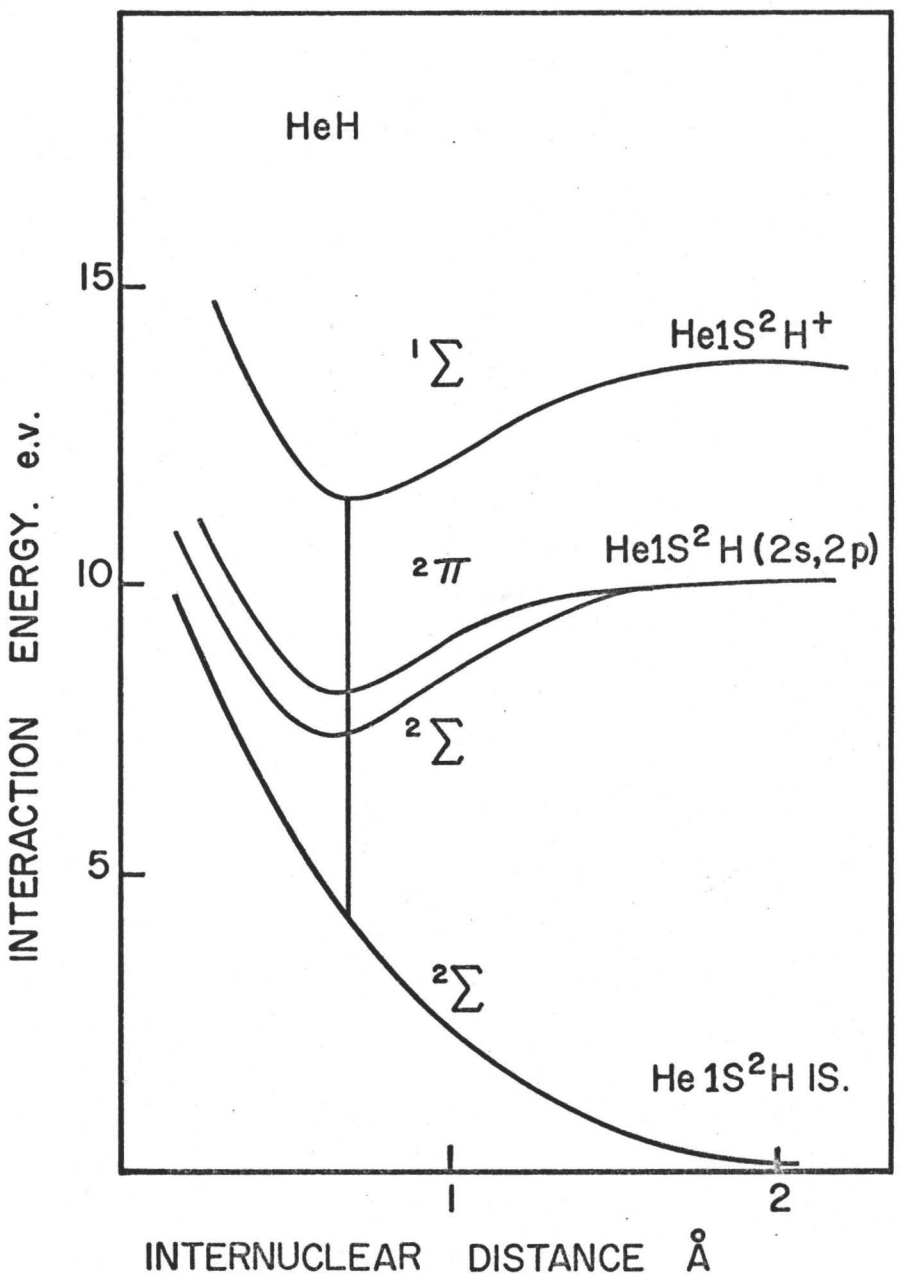

Figure 36

Some of the potential energy curves of the HeH and HeH^+ systems

it can be written that:

$$\frac{N^t}{N^o} = \frac{1}{10} = e^{-\frac{5x10^{-8}}{\tau}}$$

where $5x10^{-8}$ seconds is the time to traverse the electrostatic field. τ is then approximately $2x10^{-8}$ seconds. Thus in view of the assumptions made, the value for the mean lifetime is reasonable for molecules in bound non-metastable states.

The neutralization reactions are believed to be:

$$HeH^+(^1\Sigma) + e(Li) \longrightarrow HeH \text{ (excited doublet states)}$$

$$HeH^+(^1\Sigma) + e(Li) \longrightarrow He + H \text{ (dissociative recombination)}$$

It was not possible to obtain a peak corresponding to HeH molecules when hydrogen or helium was used in the charge-transfer cell. The states in which the HeH molecules are formed depend upon the energy defect of the charge-transfer process[56]. The cross section for charge transfer is large when the energy defect is small[54] and when the ionization energy of the atoms is small[54]. For these reasons, lithium was chosen as the atom from which a HeH^+ ion could gain an electron , since a) the energy defect for the process

$$HeH^+ + Li \longrightarrow HeH\ (^2\Sigma \text{ bound}) + Li^+$$

is approximately 1.5 ev. in contrast to 12 ev. for the process

$$HeH^+ + H_2 \longrightarrow HeH\ (^2\Sigma \text{ bound}) + H_2^+$$

and b) the ionization energy of lithium is only 5.36 ev. in contrast to 15.44 ev. for H_2. An even better choice would be cesium (ionization energy 3.87 ev.) but problems of chemical handling made lithium more desirable.

The HeH^+ ion has been produced by the β decay of HT in experiments performed separately by Snell[148] and Wexler[149] who both report that the $(^3HeH)^+$ daughter product remains bound and accounts for over 90% of the positively charged fragments. Michels has postulated[138] that an explanation for this may be found in that transitions occur not only to the ground state of the $(^3HeH)^+$ ion, but also to the bound Rydberg states of the HeH molecule. A subsequent collision may then cause ionization into the lowest $^1\Sigma$ state of $^3HeH^+$. However, in the experimental arrangement used by Wexler, the reactions take place at a pressure of 10^{-6} mm. Hg and at room temperature. The time between collisions would then be of the order 10^{-3} seconds. This experiment suggests no evidence for HeH molecules having lifetimes of this order so that ionization by collision would be unlikely.

5) The H_3, D_2H and D_3 systems

A beam of D_2H^+ ions was produced from the ion source containing hydrogen and deuterium and the primary and secondary spectra obtained. These are shown in Figure 37. The intensities of the primary and secondary beams were approximately 2×10^{-9} and 5×10^{-12} amperes respectively. The four peaks appearing in the secondary spectrum were assigned to H^+, D^+, HD^+ and D_2^+ ions. No peak was found in the secondary spectrum corresponding to mass 5. The analogous spectra obtained from a beam of D_3^+ ions are shown in Figure 38. Secondary peaks corresponding to

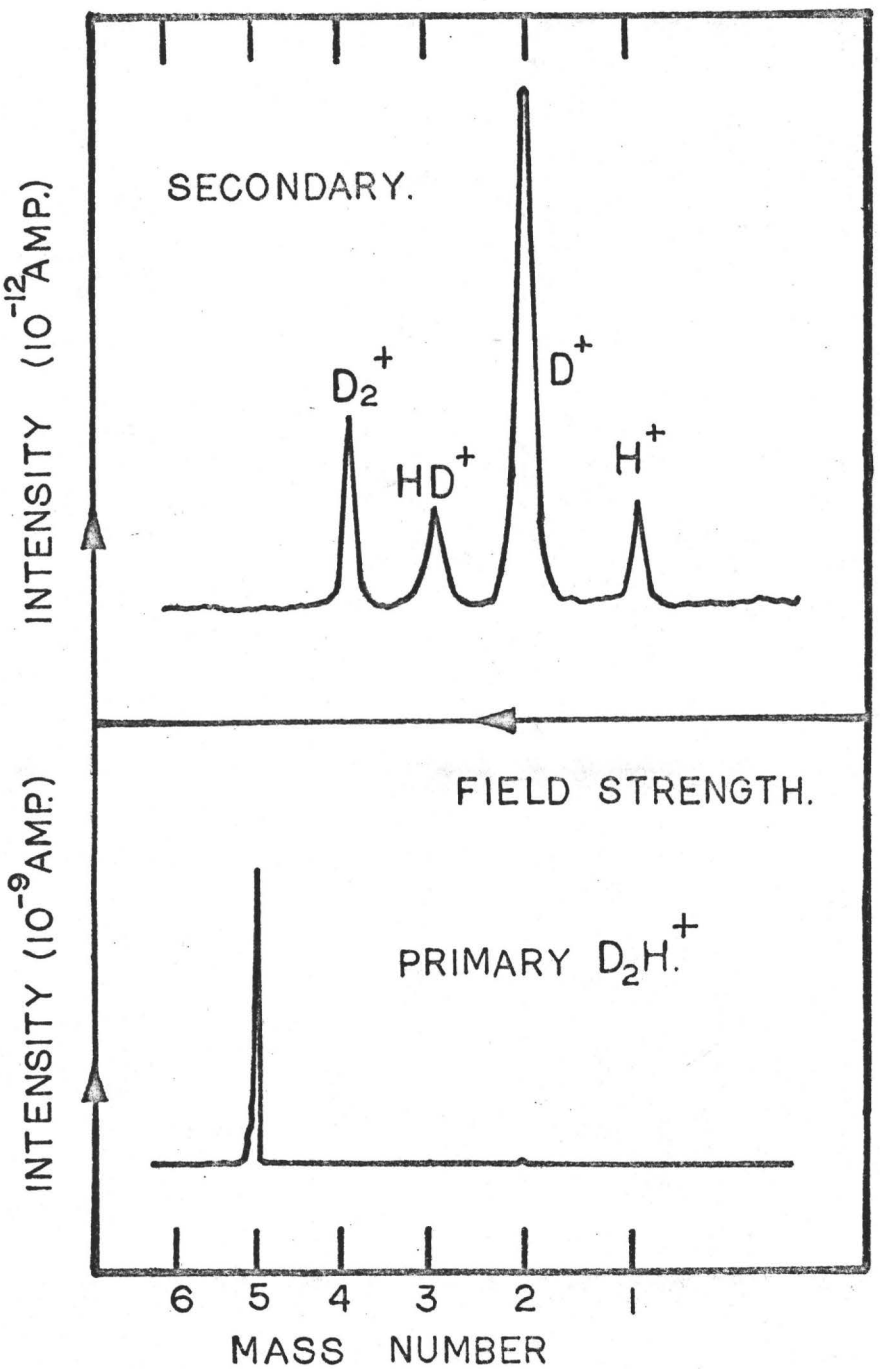

Figure 37

Primary and secondary spectra from a beam of D_2H^+ ions

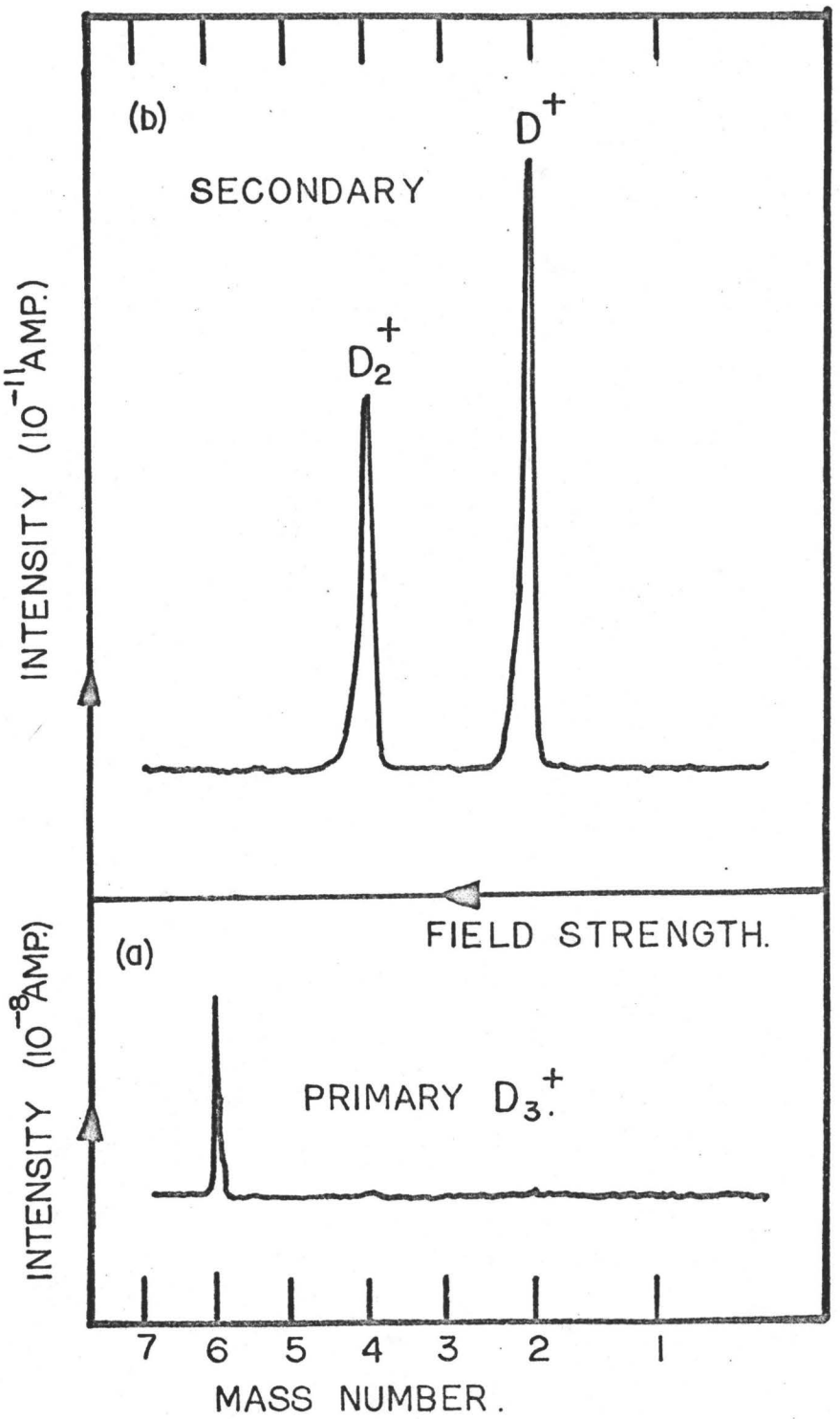

Figure 38

Primary and secondary spectra from a beam of D_3^+ ions

D^+ and D_2^+ ions were obtained but no signal corresponding to the primary peak position was detected.

A complication arises in the spectra obtained from H_3^+ ions shown in Figure 39. A peak was detected in the secondary spectrum which corresponded to the primary peak position, suggesting the presence of neutral H_3 molecules within the apparatus. However, in view of the lack of evidence for D_2H and D_3 molecules, it is believed that this peak is caused by the presence of HD^+ ions in the primary mass 3 beam. The isotopic abundance of deuterium in hydrogen is approximately 1 in 10^4. Data obtained from hydrogen discharges (Chapter 4) show that a beam intensity of 1×10^{-6} amperes of H_2^+ ions is typical when the H_3^+ beam intensity is 3×10^{-7} amperes as in Figure 39. Thus from the isotopic abundance of deuterium, an HD^+ ion beam of 1×10^{-10} amperes will be produced. This would appear in the mass 3 beam and since the masses of the dissociation products of H_3^+ and HD^+ ions are the same, they will be indistinguishable. Thus approximately 0.1% of the primary mass 3 beam in Figure 39 is due to HD^+ rather than H_3^+ ions. On neutralization and reionization, the HD^+ will appear in the secondary spectrum at mass 3. The transmission of HD^+ ions through the apparatus has been found to be 1 in 10^3 so that a secondary HD^+ beam of approximately 10^{-13} amperes would be expected. In Figure 39, the intensity of the secondary mass 3 peak is 4×10^{-13} amperes.

Supporting evidence for the presence of HD^+ ions in the primary mass 3 beam from a hydrogen discharge is found in

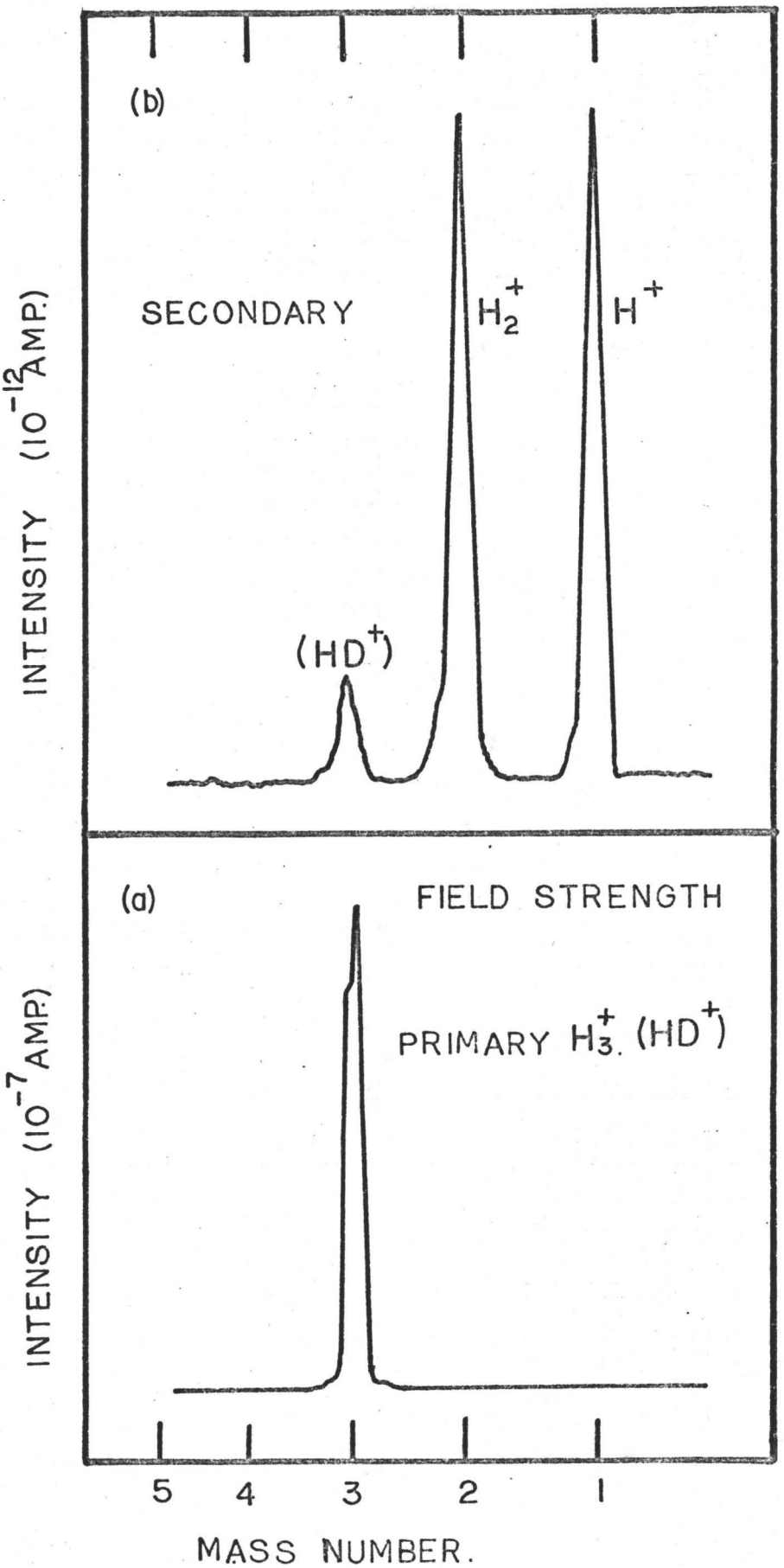

Figure 39 Primary and secondary spectra from a beam of H_3^+ ions

the appearance of a trace peak at mass 4 in the mass spectrum of a hydrogen discharge (Fig. 19), which may be assigned to D_2^+ ions. The concentration of HD is about 10^4 times that of D_2 in hydrogen, so it is reasonable to assume that HD^+ ions constitute an appreciable fraction of the mass 3 beam.

Thus no evidence was found for the existence of neutral D_3, D_2H or H_3 molecules capable of being detected in this apparatus. By the same arguments as used with the HeH system, the mean lifetime of the H_3 molecular system must be less than 2×10^{-8} seconds in order that no secondary H_3^+ peak be detected. Such a lifetime would in fact be very long in relation to the vibrational and rotational times expected with an H_3 molecule having reasonable bond lengths and binding energy.

The H_3^+ ion produced in the r.f. discharge is well known mass spectrometrically and hydrogen glow discharges have been found to contain a large fraction of H_3^+ ions at high pressure. The process of formation is thought to be:

$$H_2^+ + H_2 \longrightarrow H_3^+ + H$$

Eyring and Weingartschofer have calculated a cross section for this reaction which is in good agreement with experimental values. (150, 151)

The existence of the H_3 molecule has long been debated with reference to a "long-lived" transition complex in the reaction:

$$H + H_2 \longrightarrow H_2 + H$$

or the isotopic variation:

$$D + H_2 \longrightarrow HD + H$$

Kinematic calculations performed by Wall[153] and Karplus[154] show no evidence for a long-lived transition complex and suggest an interaction time of the order 10^{-14} seconds which is approximately the time for the hydrogen atom to pass unimpeded by the molecule. The validity of these calculations, however, depends to a large extent on the accuracy and applicability of the potential energy surfaces used.

A matter of discussion for many years has been the question of the existence of a relative minimum , or "well" in the saddle-point region of the H_3 potential energy surface. The original potential surfaces calculated by Eyring and Polanyi showed a very broad and pronounced "well" at the saddle-point[155, 156]. However, semi-empirical calculations performed by Sato[157], Herschbach[158] and Porter and Karplus[159], show no such minimum. The a-priori treatments [160-165], together with the calculations carried out by Shavitt et al.[166] are in agreement concerning the absence of a "well", and calculations by Michels and Harris [167] suggest that although the potential energy surface is relatively flat at the saddle-point, there is no evidence for a minimum. McCullough and Wyatt[168] have recently reported calculations on the collinear (H,H_2) reaction which suggest an interaction time of less than $2x10^{-14}$ seconds, in good agreement with the results of Karplus et al.[154]

The only experimental evidence for the existence of H_3 molecules has been reported by Devienne[152] who performed

experiments in which beams of H_3^+ were neutralized by charge-transfer, and the neutral products detected on a photo-scintillator device. A second experiment measured the accomodation coefficients of the neutral molecules on silver. The presence of H_3 molecules in the beam was inferred from the presence of molecules which produced "different" results to those from H and H_2 in the two experiments. However, no mass analysis was used and no indication given of beam intensities, so that interpretation of the results is difficult. The results obtained in the present work however, suggest that the "different" molecules found by these authors were in fact HD and not H_3 as suggested.

6) The He_3^+ ion

The existence of the He_3^+ molecular ion was first suggested by Fite et al.[169] and Starodubtsev et al.[170], in experiments involving mass analysis of the ions in helium discharges. A beam with a mass-to-charge ratio of 12 was assigned to He_3^+ ions. Unfortunately, C^+, a well known ion in mass spectrometry also has a mass-to-charge ratio of 12. Subsequent ion-mobility studies carried out by Patterson[171], showed that at gas temperatures below 170 ^oK a third ion, different from He^+ and He_2^+, was present in helium discharges. This was believed to be He_3^+. Shortly afterwards, Ferguson et al.[172] reported the possible existence of He_3^+ ions in flowing helium discharges at 82 ^oK.

The presence of He_3^+ ions in the r.f. helium discharge used in the present work was investigated with the apparatus shown in Figure 1. The discharge was cooled by surrounding the ion-bottle with a Styrofoam sheath, into which, liquid nitrogen was continually passed. The primary mass 12 beam was selected with the first mass analyser and passed through lithium vapour in the charge-transfer canal and subsequently reionized. The ions in the beam were mass analysed in the second magnetic field. No ion-removal was employed so that all the ions in the beam were available for detection.

The problem of distinguishing between C^+ and He_3^+ ions was overcome by causing a fraction of the beam to dissociate in the charge-transfer cell. On dissociating, He_3^+ ions will produce He^+ and He_2^+ ions so that a mass spectrum of the beam would be expected to show three peaks equally spaced in the magnetic field. On the other hand, only a peak at mass 12 would be expected with a beam of C^+ ions. Figure 40 shows the spectrum obtained at room temperature compared with the low-temperature spectrum.

At room temperatures, the spectrum shows a peak at mass 12 only, whereas the low-temperature spectrum contains peaks corresponding to mass-to-charge ratios of 4 (He^+) and 8 (He_2^+). On the other hand, the intensity of the mass 12 beam was observed to decrease as the temperature was lowered. Since the He_3^+ ion is expected to increase in stability as the temperature is reduced, the mass 12 beam cannot be considered as being

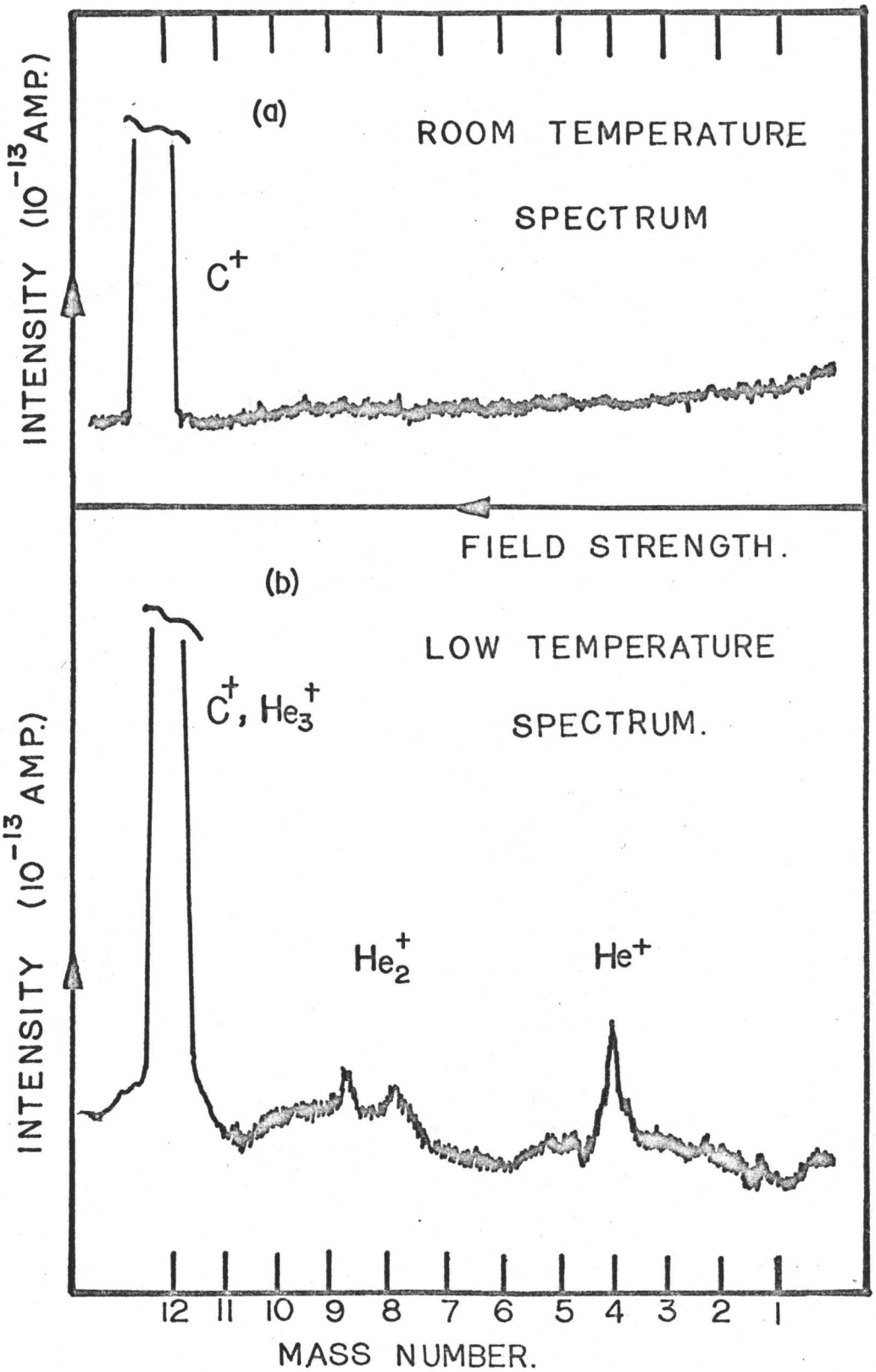

Figure 40

a: Spectrum from a mass 12 beam at room-temperature

b: Spectrum from a mass 12 beam at low-temperature

primarily He_3^+ ions, but must be largely C^+ ions. The decrease in intensity of the beam being caused by a reduction in the vapour pressure of the carbon compounds in the ion source as the temperature was reduced. The appearance of the peaks at masses 4 (He^+) and 8 (He_2^+) in the low-temperature spectrum of the mass 12 beam is interpreted as establishing that part of the beam consists of He_3^+ ions.

Before these results could be reported, de Vries and Oskum[173] published mass analysis data on low-temperature discharges containing a mixture of ^3He and ^4He. The presence of peaks at masses 9 $(^3He_3)^+$, 10 $(^3He_2{}^4He)^+$ and 11 $(^3He^4He_2)^+$ demonstrated the existence of the He_3^+ ion. The work reported here substantiates these findings.

The possibility exists of investigating lifetimes for the neutral He_3 system using the neutralization-ionization techniques developed in this work. Interference caused by the large C^+ component of the mass 12 beam would necessitate the use of the ^3He isotope. At the present time, however, it has not been possible to obtain sufficiently intense beams of primary He_3^+ to undertake this experiment.

Conclusions

An experimental technique has been developed which permits the identification of ions in beams by analysis of the products formed in charge transfer and dissociation reactions. For instance, primary mass 4 beams of D_2^+ and He^+ may be distinguished by the presence of secondary peaks corresponding to masses 2 and 4 in the D_2^+ spectrum and to mass 4 only, in the He^+ spectrum. Similarly, secondary peaks corresponding to beams of H^+, D^+, HD^+ and D_2^+ identify D_2H^+ ions in the primary spectrum.

A neutralization-reionization procedure has been devised to show the existence of He_2, HeH and HeD molecules. The He_2 molecules are believed to be formed in bound triplet states which are metastable with respect to a repulsive ground state and may have lifetimes of the order 10^{-3} seconds. The HeH and HeD molecules are believed to be produced in bound doublet states which are not metastable with respect to a repulsive ground state. Experimental results suggest a mean lifetime of the order 2×10^{-8} seconds.

The same procedure has produced no evidence for the existence of H_3, D_2H or D_3 molecules with lifetimes as long as 2×10^{-8} seconds. The results of these investigations suggest that the neutralization-ionization technique may be of considerable value in the experimental investigation of short-lived molecules, particularly those which are amenable to quantum-mechanical calculation.

BIBLIOGRAPHY

1. Ramsay, N.F., Molecular Beams. Methuen and Co.Ltd., London (1955).
2. Eldridge, J.A., Phys. Rev., 30, 931 (1927).
3. Hostettler, H.U., and Bernstein, R.B., Rev. Sci. Instr., 31, 872 (1960).
4. Trujillo, S.M., Rol, P.K., and Rothe, E.W., Rev. Sci. Instr., 33, 841 (1962).
5. Amdur, I., Glick, C.F., and Pearlman, H.,Proc. Am. Acad. Arts and Sci., 76, 101 (1948).
6. Utterback, N.G., and Miller, G.H., Phys. Rev., 124, 1477 (1961).
7. Devienne, F.M., Souquet, J. and Clapier, R. Comptes. Rendus, 256, 233 (1963).
8. Massey, H.S.W., and Burhop, E.H.S., Electronic and Ionic Impact Phenomena. Oxford University Press, Oxford (1952).
9. Hasted, J.B., Recent Measurements on Charge Transfer. in Advances in Atomic and Molecular Physics V.4. Ed. Bates, D.R., Academic N.Y. (1968).
10. Abuaf, N., Anderson, J.B., Andres, R.P., Fenn, J.B., and Marsden, D.G.H., Science 997 (1967).
11. Becker, E.W., and Bier, K., Z. Naturforsch., 9a 975 (1954).
12. Anderson, J.B., Andres, R.P., and Fenn, J.B., Supersonic Nozzle Beams. in Advances in Chemical Physics Vol X. Ed. Ross, J., Wiley N.Y. (1966).
13. Valleau, J.P., and Deckers, J.M., Can. J. Chem., 42, 225 (1964).
14. Leroy, R.L., and Deckers, J.M. Can. J. Chem., 47, 2161 (1968).
15. Becker, E.W., Z. Physik., 62, 290 (1961).

16. Skinner, G.T., Phys. Fluids, 4, 1172 (1961).

17. Zapata, R.M., and Parker, H.M., Proc. Atomic Mol. Beam Conf., University of Denver, (1960).

18. Schlier, C., Proc. German Phys. Soc., (Spring 1967).

19. Toennies, J.P., Disc. Farad. Soc., 33, 96 (1962).

20. Foner, S.N., and Hudson, R.L., J. Chem. Phys., 21, 1374 (1953).

21. Trujillo, S.M., Neynaber, R.H., and Rothe, E.W., Rev. Sci. Inst., 37, 1655 (1966).

22. Dunoyer, L., Comptes Rendus, 152, 594 (1911).
Le Radium, 8, 142 (1911).

23. Stern, O., Z. Phys., 2, 49 (1920).
Z. Phys., 3, 417 (1920).

24. Stern, O., Z. Phys., 7, 249 (1921).

25. Gerlach, W., and Stern, O., Z. Phys., 8, 110 (1921); 9, 349 (1922); 9, 353 (1922).

26. Estermann, I., Frisch, O., and Stern, O., Zeitschrift fur Physik, V. 73, 348 (1931).

27. Fraser, R.G.J., Molecular Rays. Cambridge University Press, London (1931).

28. Smith, K.F., Molecular Beams, Methuen and Co. Ltd., London (1955).

29. Estermann, I., Ed., Recent Research in Molecular Beams, Academic Press, New York (1959).

30. McDaniel, E.W., Collision Phenomena in Ionized Gases, Wiley, New York (1964).

31. Fite, W., and Datz, S., Ann. Phys. Chem., 14, 61 (1963).

32. Zorn, J.C., Resource Letter MB-1, Experiments with Molecular Beams. Am. J. Phys., 32, 721 (1964).

33. Livingstone, M.S., and Blewett, J.P., Particle Accelerators. McGraw Hill N.Y. (1962).

34. Henchman, M.J., Chem. Soc. Ann. Rep. LXII, 39 (1965).

35. Blythe, A.R., Fluendy, M.A.D., and Lawley, K.P., Quarterly Reviews 465 (1965).

36. Herman, Z., Lee, A., and Wolfgang, R., J. Chem. Phys., 51, 452 (1969).

37. Menzinger, M., and Wolfgang, R., J. Chem. Phys., 50, 2991 (1969).

38. Paulus, J.M., and Adloff, J.P., Rad. Chim. Acta., 4, 146 (1965).

39. Paulus, J.M., Rad. Chim. Acta., 7, 141 (1967).

40. Jaffe, S.B., and Anderson, J.B., Chem. Phys., 51, 1057 (1969).

41. Purser, K.H., Rose, P.H., Brooks, N.B., Bastide, R.P., and Wittkower, A.B., Physics Letters, 6, 176 (1963).

42. Schopman, J., Barua, A.K., and Los, J., Physics Letters, 29A, 112 (1969).

43. Champion, R.L., Doverspike, L.D., and Bailey, T.L., J. Chem. Phys., 45, 4377 (1966).

44. Cramer, W.H., and Simons, J.H., J. Chem. Phys., 26, 1272 (1957).

45. Cramer, W.H., J. Chem. Phys., 28, 688 (1958).

46. Doverspike, L.D., Champion, R.L., and Bailey, T.L., J. Chem. Phys., 45, 4385 (1966).

47. Fink, R.D., and King, J.S., J. Chem. Phys., 47, 1857 (1967).

48. Rothe, E.W., and Neynaber, R.H., J. Chem. Phys., 42, 3306 (1965).

49. Gillen, K.T., Riley, C., and Bernstein, R.B., J. Chem. Phys., 50, 4019 (1969).

50. Brooks, P.R., J. Chem. Phys., 50, 5031 (1969).

51. Helbing, R.K.B., and Rothe, E.W., J. Chem. Phys. 51, 1607 (1969).

52. Gray, J., and Tomlinson, R.H., Chem. Phys. Letters, 3, 523 (1969).

53. Gray, J., and Tomlinson, R.H., Chem. Phys. Letters, 4, 251 (1969).

54. Hasted, J.B., Adv. Electronics and Electron Physics, 13, 1 (1960).

55. Hasted, J.B., Physics of Atomic Collisions, Butterworths, London (1964).

56. Massey, H.S.W., Rept. Prog. Phys., 12, 248 (1949).

57. Allison, S.K., Rev. Mod. Phys., 30, 1137 (1958).

58. McClure, G.W., Phys. Rev., 130, 1852 (1963); 132, 1636 (1963).

59. Bates, D.R., and Dalgarno, A., in "The Airglow and the Aurorea", (edited by Armstrong, E.B., and Dalgarno, A.) Pergamon, London (1956).

60. Allison, S.K., and Garcia-Munoz, M., Electron Capture and Loss at high Energies, in Atomic and Molecular Processes,

(Edited by Bates, D.R.), Academic N.Y. (1962).

61. Wittkower, A.B., Rose, P.H., Bastide, R.P., and Hopwood, L., Physics Letters, 13, 134 (1964).

62. Wittkower, A.B., Rose, P.H., Bastide, R.P., Brooks, N.B., Rev. Sci. Instr., 35, 1 (1964).

63. Massey, H.S.W., Handbuch der Physik, Vol. XXXVI, Springer-Verlag, Berlin, 307 (1956).

64. Burke, P.G., and Smith, K., Rev. Mod. Phys., 34, 458 (1962).

65. Burke, P.G., Schey, H.M.. and Smith, K., Phys. Rev., 129, 1258 (1963).

66. von Engel, A., Handbook of Physics, 21, Springer (1956).

67. Thomson, J.J., and Thomson, G.P., Conduction of Electricity through Gases, 3rd. Ed., Cambridge U. Press, Cambridge (1933).

68. Hooper, J.W., Harmer, D.S., Martin, D.W.. and McDaniel, E.W., Phys. Rev., 125, 2000 (1962).

69. Sweetman, D.R., Proc. Roy. Soc., (London.) A256, 416 (1960).

70. Fodorenko, N.V., Afrosimov, V.V., Ilin, R.I., and Kaminkev, D.M., J. Exp. Phys., 36, 385 (1959).

71. Wilmenius, P., and Lindholm, E., Arkiv Fys., 21, 97 (1962),

72. von Koch, H., and Lindholm, E., 19, 123 (1961).

73. Melton, C.E., and Wells, G.F., J. Chem. Phys., 27, 1132 (1957).

74. McGowan, J.W., and Kerwin, L., Can. J. Phys., 38, 642 (1960).

75. Riviere, A.C., and Sweetman, D.R., Proc. Phys. Soc., (London), 78, 1215 (1961).

76. Talrose, V.L., and Lyubimova, A.K., Dokl. Acad. Nauk S.S.S.R., 86, 909 (1952).

77. Stevenson, D.P., and Schissler, D.O., J. Chem. Phys., 23, 1353 (1955); 24, 926 (1956); 29, 282, 294 (1958).

78. Field, F.H., Franklin, J.L., and Lampe, F.W., J. Amer. Chem. Soc., 78, 5967 (1957); 79, 2419, 2665, 6132 (1957).

79. Henglein, A., Ion-Molecule Reactions in the gas phase, Advances in Chemistry, series 58, Chapter 5, (Ed. Gould, R.F.), American chemical Soc. Publications (1966).

80. Futrell, J.H., and Abramson, F.P., Ion-Molecule Reactions in the gas phase, Advances in Chemistry, series 58, Chapter 8, Amer. Chem. Soc. Publications (1966).

81. Firsov, O., Soviet Phys.- JETP 21, 1001 (1951).

82. Fetisov, I.K., and Firsov, O., Soviet Phys.- JETP 10, 67 (1960).

83. Papoular, R., Electrical Phenomena in Gases, American Elsevier Pub. Co. New York (1965).

84. Shakin, M.A., Ion-Molecule Reactions in the Gas Phase, Advances in Chemistry Series 58, Ch. 18, (Ed. Gould,R.F.) Amer. Chem. Soc. Publications (1966).

85. Varney, R.N., Phys. Rev. Letters, 5, 559 (1960).

86. McGowan, W., and Kerwin, L., Can. J. Phys., 41, 316 (1963).

87. Field, F.H., and Franklin, J.L., Electronic Impact Phenomena and the Properties of Gaseous Ions. (Academic Press) New York (1957).

88. Harris H.H., and Russel M.E., J. Chem. Phys., 47, 2267, 2270 (1967).

89. Tuxen, O., Z. Physik, 103, 463 (1936).

90. Weizel, W., and Pestel, E., Z. Physik, 56, 197 (1929).

91. Phelps, A.V., and Brown, S.C., Phys. Rev., 86, 102 (1952).

92. Yeung, T.H.Y., and Sayers, J., J. Proc. Phys. Soc. London, 70B, 663 (1957).

93. Arnot, F.L., and McEwan, M.B., Proc. Roy. Soc. London, A 177, 106 (1939).

94. Hornbeck, J.A., and Molnar, J.P., Phys. Rev., 84, 621 (1951).

95. Comes, F.J., Z. Naturforsch, 17a, 1032 (1962).

96. Reagan, P.N., Brown, J.C., and Matsen, F.A., Phys. Rev., 132, 304 (1963).

97. Livingstone, M.S., Blewett, J.P.; Particle Accelerators, McGraw Hill Book Co., N.Y. (1962).

98. Rose, P.H., Nuclear Inst. and Methods, 28, 146 (1964).

99. von Ardenne, M., Tabellen der Elektronenphysik und Ubermikroskopie, Deutscher Verlag der Wissenschaften, (1956).

100. Moak, C.D., Banta, H.E., Thurston, J.W., and King, R.F., Rev. Sci. Instr., 30, 694 (1959).

101. Morgan, O.B., Kelley, G.G., and Davis, R.C., Rev. Sci. Instr., 38, 467 (1967).

102. Thoneman, P.C., Nature, 158, 61 (1946).

103. Rutherglen, J.C., and Cole, J.F.I., Nature, 160, 545 (1947).

104. Bayly, A.J., and Ward, A.G., Can. J. Res., A26, 69 (1948)

105. Moak, C.D., Rees, H., Jr., and Good, W.M., Nucleonics

9, (3), 18 (1951).

106. Thoneman, P., Moffatt, J., Roaf,O., and Sanders, J., Proc. Phys. Soc. (London), 61, 483 (1948).

107. Hall, R.N., Rev. Sci. Instr., 19, 905 (1948).

108. Inghram, M.G., Hayden, R.J., Mass Spectrometry, Nuclear Science Series, Rep. no. 14, Nat. Acad. Sci., Nat. Res. Council, Washington D.C. (1954).

109. Geise, C.F., Rev. Sci. Instr., 30, 260 (1959).

110. Kinzer, E.T., and Carr, H., Rev. Sci. Instr., 30, 1132 (1959).

111. Courant, E.D., Livingstone, M.S., and Snyder, H.S., Phys. Rev., 88, 1190 (1952).

112. Blewett, J.P., Phys. Rev., 88, 1197 (1952).

113. Teng, L.C., Rev. Sci. Instr., 25, 264 (1954).

114. Chih-Shun Lu, and Carr, H.E., Rev. Sci. Instr., 33, 823 (1962).

115. Barber, N.F., Proc. Leeds Phil. Soc., 2, 427 (1933).

116. Stephens, W.E., and Hughes, A.L., Phys. Rev., 45, 123 (1934).

117. Stephens, W.E., Phys. Rev., 45, 513 (1934).

118. Donnally, B.L., Clapp, T., Sawyer, W., and Schultz, M., Phys. Rev. Letters, 12, 502 (1964).

119. Donnally, B.L., and Sawyer, W., Phys. Rev. Letters, 15, 439 (1965).

120. Middleton, R., and Adams, C.T., Preliminary Notes on the Penn Negative helium and lithium Ion sources, Internal

Publication, Dept. of Physics, U. of Pennsylvania, Philadelphia, Pa.

121. Bleakney, W., Phys. Rev. 34, 157 (1929).

122. Bleakney, W., Phys. Rev., 35, 139 (1930).

123. Nier, A.O., Rev. Sci. Instr., 11, 212 (1940).

124. Nier, A.O., Ney, E.P., and Inghram, M.G., Rev. Sci. Instr., 18, 191 (1947).

125. Nier, A.O., Ney, E.P., and Inghram, M.G., Rev. Sci. Instr., 18, 294 (1947).

126. Nier, A.O., Rev. Sci. Instr., 18, 398 (1947).

127. Phillips, L.F., Electronics for Experimenters in Chemistry, Physics, Biology., John Wiley & Sons Inc., N.Y. (1966).

128. Reagan, P.C., Brown, J.C., and Matsen, F.A., J. Am. Chem. Soc., 84, 2650 (1962).

129. Dalgarno, A., McDowell, M.R.C., and Williams, A., Phil. Trans., A250 (1958).

130. Mulliken, R.S., Phys. Rev., 136, 962 (1964).

131. Herzberg, G., Spectra of Diatomic Molecules, Van Nostrand Pub. Co., Princeton, N.J., 535 (1957).

132. Ginter, M.L., J. Chem. Phys., 45, 248 (1966).

133. Peat, F.D., Can. J. Chem., 45, 847 (1967).

134. Beck, D.E., Mol. Phys., 14, 311 (1968).

135. Klein, F.S., Friedman, L., J. Chem. Phys., 41, 1789 (1964).

136. Moran, T.F., Friedman, L., J. Chem. Phys., 42, 2391 (1965).

137. Hogness, T.R., and Lunn, E.C., Phys. Rev., 26, 44 (1925).

138. Michels, H.H., J. Chem. Phys., 44, 3834 (1966).

139. Anex, B.G., J. Chem. Phys., 38, 1651 (1963).

140. Wolniewicz, L., J. Chem. Phys., 43, 1087 (1965).

141. Muschlitz, Bailey, and Simons, J. Chem. Phys., 24, 1202 (1956).

142. Mason, A.E., and Vanderslice, J.J., J. Chem. Phys., 27, 917 (1957).

143. Gentile, G., Z. Physik, 63, 795 (1930).

144. Mason, E.A., Ross, J., and Schatz, P.N., J. Chem. Phys., 25, 626 (1956).

145. Amdur, I., and Mason, E.A., J. Chem. Phys., 25, 630 (1956).

146. Michels, H.H., and Harris, F.E., J. Chem. Phys., 39, 6 (1963).

147. Chupka, W.A., Berkowitz, J., and Russel, M.E., Seventh Annual Conf. on Mass Spec. and Allied Topics, Dallas Texas, May 1969.

148. Snell, A.H., Pleasonton, F., and Leming, H.E., J. Inorg. Nucl. Chem., 5, 112 (1957).

149. Wexler, S., J. Inorg. Nucl. Chem., 10, 8 (1959).

150. Ree, T.S., Ree, T., Eyring, H., and Fueno, T., J. Chem. Phys., 36, 281 (1965).

151. Weingartscholer, A., and Clarke, E.M., Phys. Rev. Letters, 12, 591 (1964).

152. Devienne, F.M., and Roustan, J.C., C.R. Acad. Sc., Paris 263B, 1389 (1966).

153. Wall, F.T., Hiller, Jr., L.A., and Mazur, J., J. Chem. Phys., 29, 255 (1959).

154. Karplus, M., Porter, R.N., and Sharma, R.D., J. Chem. Phys., 43, 3259 (1965).

155. Glasstone, S., Laidler, K.J., and Eyring, H., The Theory of Rate Processes, McGraw Hill Book Co., New York 1941.

156. Eyring, H., and Polanyi, M., Z. Physik Chem. B12, 279 (1931).

157. Sato, S., J. Chem. Phys., 23, 2465 (1955).

158. Cashion, J.K., and Herschbach, D.R., J. Chem. Phys., 40, 2358 (1964).

159. Porter, R.N., and Karplus, M., J. Chem. Phys., 40, 1105 (1964).

160. Hirschfelder, J.O., Eyring, H., and Rosen, N., J. Chem. Phys., 4, 121 (1936).

161. Hirschfelder, J.O., J. Chem. Phys., 6, 795 (1938)

162. Snow, R., and Eyring, H., J. Phys. Chem., 61, 1 (1957).

163. Ransill, B.J., J. Chem. Phys., 26, 971 (1957).

164. Kimball, G.E., and Trulio, J.G., J. Chem. Phys., 28, 493 (1958).

165. Boys, S.F., and Shavitt, I., University of Wisconsin, Naval Research Laboratory, Tech Rept. WIS-AF-13 (1959).

166. Shavitt, I., Stevens, R.M., Minn, F.L., and Karplus, M., J. Chem. Phys., 48, 2700 (1968).

167. Michels, H.H., and Harris, F.E., J. Chem. Phys., 48, 2371 (1968).

168. McCullough, E.A., Jr., and Wyatt, R.E., J. Chem. Phys., 51, 1253 (1969).

169. Fite, W.L., Rutherford, J.A., Snow, W.R., and van Lint, V.A.J., Disc. Farad. Soc., 33, 264 (1962).

170. Starodubtsev, S.V., Pozkarov, S.L., Chernov, I.G., and Knopov, V.M., Soviet Physics-Dolad, 11, 432 (1966).

171. Patterson, P.L., J. Chem. Phys., 48, 3625 (1968).

172. Ferguson, E.E., Dunkin, D.B., Fehsenfeld, F.C., and Schmeltekopf, A.L., Bull. Am. Phys. Soc., 13, 212 (1968).

173. de Vries, C.P., and Oskum, H.J., Phys. Letters, 29A, 299 (1969).